SynDIG4 is an auxiliary protein which regulates trafficking, gating, and synaptic plasticity of AMPA-type receptors

By

KRISTOPHER ERNEST PLAMBECK

DISSERTATION

Submitted in partial satisfaction of the requirements for the degree of

DOCTOR OF PHILOSOPHY

in

Biochemistry, Molecular, Cellular, and Developmental Biology

in the

OFFICE OF GRADUATE STUDIES

of the

UNIVERSITY OF CALIFORNIA

DAVIS

Approved:

_____

Elva D. Díaz, Chair

_____

Johannes W. Hell

_____

Karen Zito

_____

John Gray

Committee in Charge

2022

Abstract

Trafficking, localization, and biophysical properties of AMPA-type glutamate receptors (AMPARs) at synapses are predominant mechanisms for regulating synaptic strength underlying learning and memory. AMPARs are highly regulated by a number of auxiliary proteins such as TARPs, cornichons, and CKAMPs, as well as the members of the SynDIG/Prrt family, which will be the focus of this study. Previous studies of the transmembrane protein Synapse Differentiation Induced Gene 1 (SD1; SD1) as an AMPAR interacting protein that regulates excitatory synaptic strength and AMPAR number both *in vitro* and *in vivo*. The SynDIG family is defined by a family of four genes, SD1-4, which are expressed in distinct locations within the brain. SynDIG4 (SD4/Prrt1) is primarily expressed within the hippocampus, the main site of memory formation in both mice and humans. SD4 was identified in several independent proteomic screens in complex with AMPARs, suggesting it may also function as an AMPAR auxiliary factor. We previously observed that long-term potentiation (LTP) is abolished by single tetanus stimulation of hippocampal slices from SD4 knockout (KO) mice. In this study we demonstrate that only specific protein domains are necessary for clustering of AMPARs and SD4. Furthermore, we observed that some SD4 co-localizes with extra-synaptic GluA1-containing AMPARs in primary neurons, while loss of SD4 results in reduced extra-synaptic AMPARs, implying a role of SD4 outside the synapse. We hypothesize that SD4 regulates AMPARs through maintenance of an extra-synaptic pool of GluA1-containing AMPARs required for trafficking and LTP.

Acknowledgements

I would like to thank my mentor Dr. Elva Diaz for her incredible patience, understanding, encouragement, advice, and undying support. Additionally, I would like to thank our collaborator Dr. Yael Stern-Bach, as well as my committee members, Dr. Karen Zito, Dr. Johannes Hell, and Dr. John Gray, for all their help, advice, and contributions to this project. To my lab members, Dr. Lindsey Kirk and Dr. Tin Ngo for their additional mentorship and help with experimental design, as well as numerous undergraduate and graduate student mentees for their help in analysis and experimental procedures. Lastly, I would like to thank my parents, Mrs. Kathleen Thornton-Trump Plambeck Lindstrom, and Mr. Gary Plambeck, as well as additional family and friends for supporting me in this endeavor; I appreciate the patience, understanding, and encouragement I received.

Table of Contents

Chapter 1:

Introduction

This chapter serves as a review of the function of the hippocampus regarding hippocampal dependent learning and memory formation. These studies focus on the interaction of α-amino-3-hydroxy-5-methyl-4-isoxazolepropionic acid receptors (AMPARs) and previously characterized AMPAR interacting and auxiliary proteins. Furthermore, this chapter describes the importance of the role of AMPARs and AMPAR auxiliary proteins in activity dependent regulation, trafficking, and function during long term potentiation (LTP).

Introduction Outline

I. **The Hippocampus and Hippocampal Dependent Learning and Memory**

II. **Ionotropic Glutamate Receptors**

   a. N-methyl-D-aspartate (NMDA) receptors

   b. Kainate receptors

   c. α-amino-3-hydroxy-5-methyl-4-isoxazolepropionic acid (AMPA) receptors

III. **AMPAR interacting proteins**

   a. Post-synaptic density protein 95kD (PSD-95)

   b. Neuronal activity-regulated pentraxin receptor (NARP; NP2)

   c. Leucine-rich repeat transmembrane protein (LRRTM)

   d. Glutamate receptor-interacting protein (GRIP) and Protein interacting with C-kinase (PICK)

   e. Calcium/calmodulin dependent kinase II (CaMKII)

IV. **AMPAR auxiliary proteins**

   a. Transmembrane AMPAR regulatory proteins (TARPs)

   b. Cornichons (CNIHs)

   c. Cysteine-knot AMPAR modulating proteins (CKAMPs)

   d. Synapse Differentiation Induced Gene (SynDIGs)

V. **Synaptic Plasticity**

   a. Long Term Depression (LTD)

   b. Long Term Potentiation (LTP)

I. The Hippocampus and Hippocampal Dependent Learning and Memory

Neuronal communication is carried out through electrochemical signals transmitted through projections from the cell body, called the axon terminals[1]. These axon terminals form connections, or synapses, with the dendrites of other neurons to transfer information. The ability of mature neurons to form synapses remains the traditional method by which neurons are able to communicate within the brain[1]. Specifically, the hippocampus, one of the brain regions identified as a prominent regulator of cognitive functions, has been widely implicated as the main site of learning and memory in both mice and humans[2,3]. Importantly, the ability of the hippocampus to change over time has been regarded as a key characteristic underlying cognitive function, including memory formation[4,5].

Within the hippocampus lies the sub-granular zone of the dentate gyrus (DG), a site of active neural stem cell activity[2-4]. Neural stem cells within the SGZ can differentiate and migrate outwards to the granule cell layer (GCL) of the DG where they are able to integrate into the tri-synaptic circuit[4,5]. This neural circuit within the hippocampus consists of the DG, CA3, and CA1 regions and is critical for cognitive functions[5,6].

The hippocampus remains the main site of interest underlying cognitive functions, including learning and memory in both mice and humans[2,4]. Here, they are able to integrate into the tri-synaptic circuit where new memories are formed and consolidated by strengthening a new neoural circuit[4,5]. This neural circuit within the hippocampus consists of the DG, CA3, and CA1 regions and is critical for cognitive functions[5,6]. The strengthening of hippocampal connections/circuits is thought to underlie learning and memory formation. Specifically, we are

studying excitatory synapses. At excitatory synapses, glutamate receptors are activated by the release of glutamate from synaptic vesicles of axon terminals in response to stimuli, resulting in activation of downstream calcium dependent processes.

The ability of neurons to either strengthen or weaken due to patterns of stimulation results in synaptic plasticity. This occurs through regulation of synaptic plasticity at pos-synaptic dendritic spines, with each spine representing a possible site for synapse formation. By identifying the mechanisms that regulate synaptic plasticity between neuronal spines and excitatory synapses, we may further understand the molecular basis of hippocampal dependent learning and memory.

II. Ionotropic Glutamate Receptors

Glutamate receptors predominantly regulate the synaptic communication of excitatory neurons in the brain[35,36]. During synaptic transmission, pre-synaptic axon terminals responsible for export of signaling molecules pair with post-synaptic dendritic spines[7-11]. The pre-synaptic bouton contains hundreds of synaptic vesicles (SVs), which dock at the plasma membrane prior to synaptic activity[7,11,12]. These SVs then fuse with the membrane, allowing the export of cell signaling molecules, such as glutamate, across the synapse. Dendritic spines are densely populated with proteins that include glutamate receptors and ion channels which allow for the binding of molecules during synaptic transmission[7,8,10,11,13-15]. Signals received from pre-synaptic neurons trigger signaling cascades which dictate neuronal activity. There are three types of glutamate receptors located at the synaptic site: N-methyl-D-aspartate (NMDA), AMPA, and kainate

receptors[7-9,13,16-18]. Previous studies have shown that NMDA receptors are first recruited to the dendritic surface[7,9,11,13]. The recruitment of AMPA and kainate receptors stabilize the synapse and represent a mature synaptic structure[11,18]. Together these glutamate receptors represent the most common type of receptor in the central nervous system (CNS), and are responsible for fast synaptic transmission, and have been found to play a crucial role in synaptic plasticity[11,18-22].

During synapse maturation, previous studies have shown that NMDA receptors are first recruited to the dendritic surface[7,9,11,13]. The recruitment of AMPA and kainate receptors stabilize the synapse and represent a mature synaptic structure[11,18]. AMPAR trafficking is highly dynamic[21,23]. The regulation of AMPARs is a predominant mechanism for the regulation of excitatory transmission and have been shown to rapidly traffic between membrane compartments and the plasma membrane[19,21,23]. Receptors move laterally through the extra-synaptic plasma membrane and can enter and exit synapses in an activity dependent manner[21,23]. This is a highly regulated process, but mechanisms are not fully understood. An increase in synaptic AMPARs results in increased synaptic strength. Furthermore, impairment in AMPA receptor trafficking has been linked to several neurological disorders, such as Alzheimer's disease[24,25].

The activation of glutamate receptors occurs immediately after the release of glutamate from synaptic vesicles across the synapse[14,16,26]. Specifically, glutamate binds to glutamate receptors located at the post-synaptic density (PSD), the active site during synaptic transmission located on the tips of dendritic spines directly across from the axon terminal[26]. This results in an influx of calcium (Ca^{+2}) into the dendritic spine[26,27]. Additionally, it has been shown that NMDA receptors are the largest source of this Ca^{+2} influx[27]. Studies had previously shown that this Ca^{+2}

influx triggers a diverse array of downstream signaling cascades responsible for multiple cellular processes[28]. Researchers noticed that there seemed to be a direct correlation to an increase in actin polymerization and recruitment to the PSD[28-30]. Furthermore, it was observed that by directly inhibiting NMDA receptor activation, there was a decrease in actin recruitment and an overall decrease in spine dynamics[28,30]. Therefore, it was concluded that the activation of NMDA receptors directly regulates the upregulation of actin polymerization responsible for spine morphogenesis.

III. AMPAR interacting proteins

As mentioned previously, AMPARs are highly dynamic and can rapidly move in and out of the plasma membrane in an activity dependent manner[19,21,23]. From their assembly onwards a "dimer of dimers" of four highly homologous subunits GluA1-4 AMPARs don't function or travel alone, but are surrounded by a wide-array of proteins which guide their subcellular localization[31]. The role of AMPAR interacting proteins has become of significant interest since it be came clear that these auxiliary proteins play a significant role in regulating AMPAR trafficking and function[32,33]. The gating properties of AMPARs (i.e. activation time, inactivation time, latency) are another way to measure surface AMPAR activity. Researchers noticed that surface AMPAR number and AMPAR activity was significantly different in heterologous cells when compared to the activity of AMPARs in wildtype (WT) neurons. Therefore, it was concluded that there must be additional AMPAR interacting proteins present that must have an effect on both the trafficking and gating properties of AMPARs[33].

AMPARs are widely distributed throughout the brain and consist of four glutamate receptor subunits GluA1-4[33]. Within the hippocampus, the AMPAR subunits GluA1 and GluA2 are highly expressed and have shown to be necessary for LTP[34,35]. Furthermore, it was observed that when either AMPAR subunit GluA1 or GluA2 are co-expressed in the presence of specific AMPAR interacting proteins, there is a significant difference in the gating properties compared to GluA1 and GluA2 alone[36,37]. These AMPAR interacting proteins will further be classified as AMPAR auxiliary proteins. Additionally, there was a significant increase in the number of surface AMPARs when GluA1 or GluA2 were co-expressed with AMPAR auxiliary proteins when compared to GluA1 or GluA2 alone[38,39]. AMPAR auxiliary proteins have been shown to increase surface expression of AMPARs and alter gating proprerties[38,40]. Interestingly, STG/Tarp-γto induce the clustering of GluA1 and GluA2-containing AMPARs when co-expressed in heterologous cell, although only in the presence of PSD-95[33,39]. This result was further duplicated in dissociated hippocampal cells where both surface GluA1 and surface GluA2 increased, while there was a significant increase in localization of GluA1 and GluA2 with its potential AMPAR auxiliary binding protein, which is further exacerbated by induction of LTP. This provides evidence that AMPAR auxiliary factors bind GluA1- or GluA2-containing AMPAR, alter their surface trafficking and gating properties, and affect localization of AMPAR and AMPAR auxiliary proteins in an activity dependent manner.

Like many proteins, AMPARs contain sites for post-translational modifications, including phosphorylation and palmitoylation, which also mediate the trafficking and localization of these GluA1 and GluA2-containing AMPARs **(See AMPAR topology map below)**. Although GluA1

and GluA2 are similar in structure, they contain unique phosphorylation and palmitoylation sites. Likewise, GluA1 and GluA2 contain unique binding sites for important AMPAR regulating interacting proteins. Just a few of these proteins of interest include PSD-95, NARP, LRRTM, GRIP, PICK, CaMKII, PKA, and PKC[33,41].

Topology of AMPARs and auxiliary binding sites.

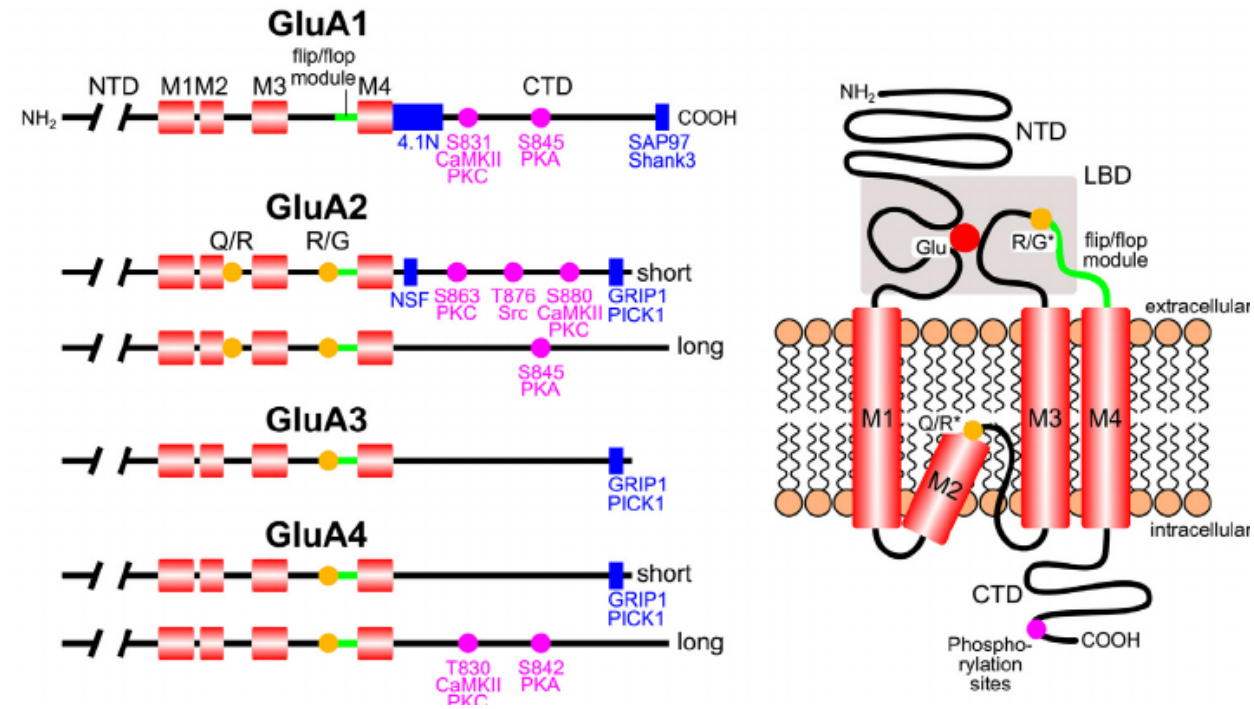

a. Post-synaptic density protein 95 kD (PSD-95)

PSD-95 is a scaffolding protein which binds to actin filaments within dendritic spines and anchors synaptic proteins to the PSD[13,39,42,43]. Proteins that bind to PSD-95 include a PDZ binding motif which has been shown to be highly conserved across multiple PSD binding proteins[42,44].

NMDARs contain a PDZ binding motif which allows receptors to bind to PSD-95 at the PSD[42,44]. This results in NMDARs becoming a mostly fixed component of the PSD[39,44]. Conversely, AMPARs do not contain a PDZ binding motif and are unable to bind to PSD-95 directly[42,44]. AMPARs must bind to the PSD through an intermediate protein interaction whereby AMPARs are bound with an AMPAR interacting or auxiliary protein that allows them to anchor to the PSD[44]. Therefore, AMPARs are able to rapidly enter and exit the plasma membrane in an activity dependent manner and bind to the PSD, increasing the overall number of surface AMPARs[42,44].

b. Neuronal activity-regulated pentraxin receptor (Narp; NP2)

Narp, also known as NP2, has been observed to mediate AMPAR clustering at synaptic contacts[13,45-48]. NP1 and NP2 are secretary proteins which bind to the extra-cellular integral membrane protein Neuronal Pentraxin Receptor (NPR) where it becomes bound, potentially forming a transsynaptic complex[13,47,49]. The formation of this complex results in strengthening and maturation of the synaptic contact[13,49]. It had previously shown that the N-terminal domain (NTD) of GluA4 is necessary for interaction and synaptic recruitment of GluA4-containing AMPARs[13,50]. Another study used a dominant negative form of Narp mutant protein to reduce NP1 and NP2 activity[50]. This resulted in an overall decrease in synaptic clustering of AMPARs and a reduction in the number of excitatory synapses in transfected neurons[50]. Furthermore, NP1/2 knockout neurons result in a reduction of AMPAR mediated synaptic transmission and an increase of silent synapses, suggesting NP1/2 are critical for synaptic recruitment of AMPARs in an activity dependent manner[13,51].

c. Leucine-rich repeat transmembrane protein (LRRTM)

LRRTMs were observed to effect the differentiation of glutamatergic synapses at both pre-synaptic and post-synaptic sites[52,53]. There are four LRRTM genes in mammals, with all four being highly expressed in the brain[52,53]. LRRTM1/2 have been shown to induce primarily pre-synaptic glutamatergic differentiation[52,53]. Furthermore, it was observed that LRRTM2 clusters with multiple types of AMPARs, while LRRTM1 primarily affects synaptic organization, resulting in the formation of a mature synaptic complex, while mutations in either LRRTM1 or LRRTM2 affects formation of a mature trans-synaptic organizing complex resulting in decreased differentiation of glutamatergic synapses[52,54]. Additionally, shRNA-mediated knockdown (KD) of LRRTM1/2 eliminates LTP in hippocampal neurons[55]. Replacement of LRRTM2-KD neurons with the LRRTM2 extra-cellular domain rescues LTP, indicating that this domain is sufficient for expression of LTP[54,55]. Furthermore, the number of surface AMPARs is significantly reduced in LRRTM2-KD neurons, providing evidence that LRRTM2 is required for both LTP and AMPAR trafficking during synaptic development[54-56].

d. Glutamate receptor-interacting protein (GRIP) and Protein interacting with C-kinase (PICK)

The dynamic regulation of AMPAR trafficking to, from, and within the synaptic membrane is a primary component of LTP and synaptic strengthening[32]. In addition to their spatio-temporal localization, the overall strength and stability of the interaction between the auxiliary proteins and AMPARs is highly dynamic[57]. Some interacting proteins were identified in complex with

AMPARs through several repeated proteomics studies and have been classified as parts of a native AMPAR complex. The interacting protein (GRIP1) and protein interacting with C-kinase (PICK1), were identified in several proteomic studies[58-60].

AMPAR subunits GluA2 and GluA3 share a common PDZ binding sequence consisting of four amino acid residues, -SVKI at the C-terminus, allowing interactions with PDZ domain-containing proteins, such as PSD-95[61]. The role of GRIP1 is less understood at synaptic localizations, however, previous studies have shown that GRIP1 is necessary for synaptic insertion of AMPARS[62-64], while other auxiliary proteins have been observed to actively remove synaptic AMPARs[41,65,66]. GRIP1 and PICK1 bind to GluA2 through phosphorylation by protein kinase C (PKC), resulting in a decreased affinity to GluA2, but no effect on PICK1 activity. This could further indicate a mechanism by which the release of GluA2 from GRIP1, opening up potential binding sites for PICK1, which facilitate the insertion and trafficking of synaptic GluA2[65].

Previous studies have proposed a complementary role for GRIP1 and PICK1 in regulating the insertion and trafficking of surface AMPARs[62,64,67]. According to other studies, PICK1 additionally regulates AMPAR recycling as PICK1 knockout neurons displayed an increased recycling rate of surface AMPARs to the surface without effecting internalization[67-70]. LTP is prevented by PICK1 knockdown and occluded by PICK1 overexpression[71]. However, another study found no defective LTP in PICK1 knockout slices[70]. These differing results could be attributed to the experimenter, neuronal isolation, and overall health of the neuronal cultures and slices. Different results could also be due to variable technique, where an acute knockdown or

chronic knockout can present conflicting data. Furthermore, PICK1 induces clustering of AMPA receptors in heterologous cell culture expression systems.

Lastly, GRIP1/2 double KO mice show increased surface GluA2-containing AMPARs, with gain-of-function mutations using transgenic mice display enhanced surface localization, trafficking, and faster recycling of AMPARs[72,73].

e. Calcium/calmodulin dependent kinase II (CaMKII)

NMDAR dependent LTP requires the activation of NMDAR by the activity dependent release of pre-synaptic glutamate[74,75]. This results in the influx of Ca^{+2} through post-synaptic NMDARs[75]. Ca^{+2}-dependent activation and autophosphorylation of Ca^{+2}/calmodulin-dependent protein kinase II (CaMKII) further results in an increase in surface AMPAR at the plasma membrane[74,75]. LTP induction in primary hippocampal neurons found an increase in autophosphorylation and activation of CaMKII, which was blocked by the CaMKII inhibitor KN-62[74-77]. Additionally, the AMPAR subunit GluA1 is preferentially phosphorylated by CaMKII resulting in a significant increase in surface GluA1 after LTP induction[74,77]. Inhibition of CaMKII activity prevents the NMDAR-dependent trafficking of GluA1 to the plasma membrane[74,76]. Therefore, it was concluded that activation of CaMKII through NMDAR-dependent LTP induction is crucial for expression of LTP and trafficking of GluA1-containing AMPARs[74,75].

IV. AMPAR auxiliary proteins

Modulation of AMPARs is a predominant mechanism for the regulation of excitatory transmission[19,20,22,78,79]. Previous studies have attempted to understand the mechanism by which AMPARs are trafficked to the synapse and have identified a diverse group of AMPAR interacting proteins[8,39,80-82]. For example, the AMPAR auxiliary protein Stargazin, a member of the transmembrane AMPAR regulating protein (TARP) family, has been observed to directly modulate trafficking of AMPARs to the cell surface[39,80-83]. Additional AMPAR auxiliary proteins such as the Cornichons (CNIHs), cysteine-knot AMPAR modulating proteins (CKAMPs), and synapse differentiation induced genes (SynDIGs) have also been shown to affect AMPAR trafficking and functional properties of AMPARs, including sensitivity to glutamate[39,46,59], resulting in increased LTP and synaptic strength. Therefore, AMPAR localization and function is regulated by a wide array of mechanisms.

Topology of AMPAR auxiliary proteins[36].

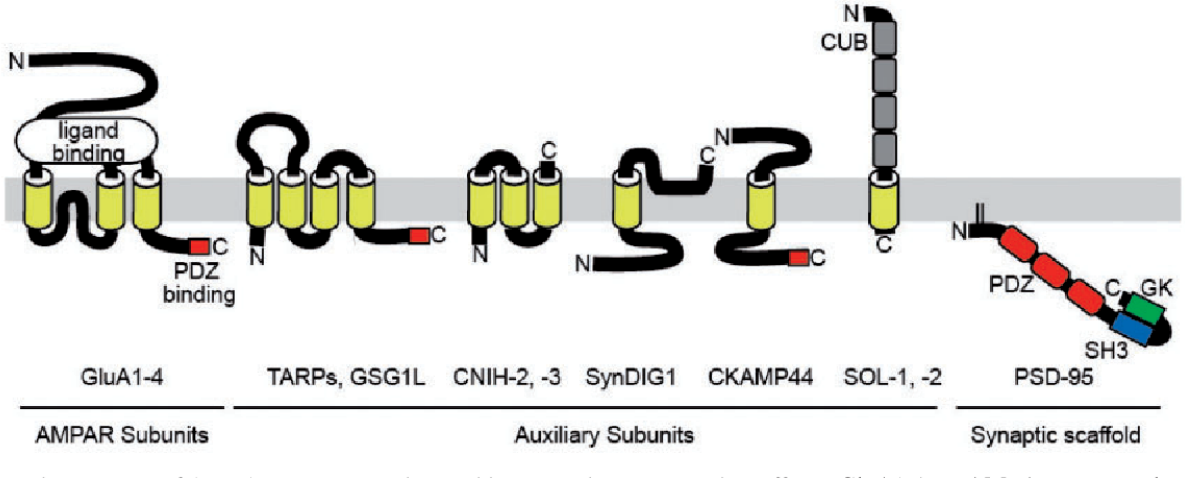

a. Transmembrane AMPAR regulatory proteins (TARPs)

TARPs are a family of eight proteins that consist of an intracellular N-terminus, four transmembrane domains, two extracellular loops, and an intracellular C-terminus. Stargazin (STG; TARP-γ2) has been found to be highly expressed in the cerebellum and has been identified to regulate AMPARs through two distinct domains[83]. STG regulates AMPAR gating kinetics through the extracellular loop domains, while the C-terminus is necessary for the surface trafficking of AMPARs[83]. Furthermore, it has been observed that TARP- γ8 specifically modulates the gating kinetics of AMPARs through extracellular loop 2 and the transmembrane domains 3 and 4 (Ben-Yaacov, Stern-Bach, 2017). While STG is highly expressed in the cerebellum, TARP- γ8 has been identified to be expressed primarily in excitatory hippocampal neurons, making them a candidate regulator of hippocampal AMPARs[84]. Previous studies have shown that TARP- γ8 increases basal levels of surface AMPARs, both synaptic and extra-synaptic, and enhances hippocampal dependent LTP, while a loss of TARP- γ8 negatively regulates these properties[57]. Therefore, TARPs play a critical role in the regulation of AMPARs.

b. Cornichons (CNIHs)

CNIHs were initially identified in a proteomics study used to identify additional AMPAR interacting proteins, with hippocampal AMPARs found to associate mostly with CNIH-2 and CNIH-3[32,58]. CNIH-2/3 bind AMPARs, promote surface trafficking, and slow AMPAR deactivation kinetics, while a loss of CNIH-2/3 results in the reduction of AMPAR synaptic transmission due to the decrease of surface GluA1-containing AMPARs[85,86]. Additionally, it was

observed that CNIHs negatively regulate the binding of TARP- γ8 to AMPARs, indicating that TARPs and CNIHs may work in tandem to create a specific AMPAR complex and affect the number and strength of surface AMPARs[85,86].

c. Cysteine-knot AMPAR modulating proteins (CKAMPs)

An additional proteomics study identified a family of proteins known as CKAMPs, specifically CKAMP44, in complex with AMPARs[87]. This protein family has been further characterized as a novel auxiliary subunit family distinct from other AMPAR interacting proteins[88]. While TARPs and CNIHs are primarily expressed within the CA1 region of the hippocampus, CKAMP44 was found to be primarily expressed within the dentate gyrus[87]. Furthermore, even though the CKAMPS, like AMPARs, are very similar in structure, their ability to modulate gating properties of AMPARs is very diverse. Therefore, CKAMP44 and its family members precisely control AMPAR function[88,89].

d. Synapse Differentiation Induced Genes (SynDIGs)

The Synapse Differentiation Induced Gene (SynDIG) family of transmembrane proteins have been implicated in the regulation of AMPARs. The type-II transmembrane protein SynDIG1 (SD1) was previously identified in a microarray-based approach and found to act as an AMPAR interacting protein responsible for synapse development and localization of AMPARs[15,90]. Specifically, SD1 co-localizes with AMPARs in heterologous COS cells and directly modulates the number of

functional GluA1 and GluA2 containing AMPARs at excitatory synapses[90]. These data provide evidence for the SD1 regulation of development and function of AMPAR containing synapses.

SD1 is a highly conserved transmembrane protein that is expressed throughout the brain with elevated levels localized to the hippocampus and cerebellum[7,9-11,91]. It has been observed that upon loss of SD1, the total AMPA receptor content at synapses is reduced by ~50% resulting in an overall decrease in synapse formation[90]. Conversely, overexpression of SD1 increases excitatory synapse development, as well as the number of AMPA receptors at synapses. Furthermore, SD1 has been shown to affect the distribution of the AMPAR subunits GluA1 and GluA2.

Using heterologous cells, co-expression of SD1 with GluA2 showed a strong clustering phenotype between the two proteins, leading to the clustering of these AMPAR subunits *in vitro*[11]. Additionally, co-expression of GluA2 with a modified form of SD1 containing a C-terminus deletion with the membrane bound regions preserved lead to the inhibition of this clustering behavior. Therefore, it was successfully shown that the C-terminus domain of SD1 is necessary for interaction with the AMPA receptor GluA2 through its C-terminus domain. However, the GluA2 domain responsible for this interaction remains unknown. SD1 has two transmembrane domains with an intracellular N-terminus and extracellular C-terminus[7,11]. GluA2 has four transmembrane domains with the opposite orientation, having an extracellular N-terminus and intracellular C-terminus[18]. Due to the orientation of these two proteins, we postulated that either the C-tail or transmembrane domains of GluA2 were responsible for this interaction with the C-terminus of SD1. However, the C-tail of GluA2 is in the opposite orientation to that of SD1.

Therefore, we hypothesized that the transmembrane domains of GluA2 were responsible for the interaction with SD1.

SynDIG4 (SD4), also known as Proline-rich transmembrane protein 1 (PRRT1), was identified by three independent proteomic studies[58,60,87] and demonstrates sequence similarity to SD1[90]. Therefore, SD4 has been identified as a candidate regulator of AMPARs at excitatory synapses.

Using multiple electrophysiological recording prototocols, we observed that LTP is only affected after single-tetanus LTP induction, indicating the importance of SD4 for functional LTP under specific signal transduction. Acute hippocampal slices were prepared using both wildtype (WT) and SD4 knockout (KO) mice. An electrode was used to stimulate Schaffer collateral axons onto CA1 hippocampal neurons. In WT mice, recordings showed an increase in stable excitatory post-synaptic potentials (EPSPs) after stimulation, indicative of LTP induction. However, in SD4-KO mice, there were deficits in LTP with no stable increase in EPSPs[37]. Interestingly, LTP in SD1-KO neurons appears normal, indicating a specificity for SD4 in mediating LTP.

Importantly, SD4 has been observed in complex with AMPARs, with an affinity for the AMPAR subunit GluA1[58]. SD4 was subsequently identified as another potential regulator of AMPA receptor trafficking. However, little is known regarding the significance of this interaction.

V. Synaptic Plasticity

Synaptic plasticity and LTP was first characterized in a study whereby neurons were repeatedly stimulated within the perforant path of the DG in anesthetized rabbits[92]. This study presented the

conclusion that there were two distinct mechanisms underlying LTP: increased efficiency of synaptic transmission at these synapses, and increased excitability in the GCL[92]. The activity-dependent modulation of synaptic AMPARs is understood to be a mechanism whereby information is stored in neural networks that give rise to higher order cognitive functions. LTP has been widely accepted as the cellular mechanism underlying learning and memory[92,93]. Specifically, high frequency stimulation of a synapse results in an overall increase in the efficacy of synaptic transmission[92,93]. Previous studies have established the importance of AMPARs in LTP, with AMPARs mediating fast excitatory post-synaptic currents[94]. Initially it seemed that the necessity of AMPARs for LTP is subunit specific, with deficits in LTP only seen after a loss of the AMPAR subunit GluA1[94]. However, recent findings suggest that maintenance of an extra-synaptic pool of AMPARs may be more important, independent of subunit specificity[95].

Pioneering studies using confocal and two-photon microscopy has allowed for the visualization of individual neurons and dendritic spines allowed for the manipulation and imaging of these changing neuronal processes[96,97]. By locally releasing glutamate in hippocampal slices researchers can stimulate individual spines, allowing for either an increase or decrease in the overall size of synaptic spines, indicating a potentiated synapse[97]. Furthermore, it has since been shown that treatments involving exercise and caloric restriction can generate pro-youthful factors and pro-aging factors, which can additionally modulate the synaptic density of neurons, ultimately leading to increased learning and memory formation as a mechanism of decreasing cognitive decline[98-101]. These studies have further linked structural and functional plasticity in excitatory synapses[34].

REFERENCES

1 Cohen-Cory, S. The developing synapse: construction and modulation of synaptic structures and circuits. *Science* **298**, 770-776 (2002).

2 Eriksson, P. S. *et al.* Neurogenesis in the adult human hippocampus. *Nat Med* **4**, 1313-1317 (1998). https://doi.org:10.1038/3305

3 Vadodaria, K. C. & Jessberger, S. Functional neurogenesis in the adult hippocampus: then and now. *Front Neurosci* **8**, 55 (2014). https://doi.org:10.3389/fnins.2014.00055

4 Kuhn, H. G., Dickinson-Anson, H. & Gage, F. H. Neurogenesis in the dentate gyrus of the adult rat: age-related decrease of neuronal progenitor proliferation. *The Journal of neuroscience : the official journal of the Society for Neuroscience* **16**, 2027-2033 (1996).

5 Mora, F. Successful brain aging: plasticity, environmental enrichment, and lifestyle. *Dialogues Clin Neurosci* **15**, 45-52 (2013).

6 Kempermann, G. Why New Neurons? Possible Functions for Adult Hippocampal Neurogenesis. *The Journal of Neuroscience* **22**, 635 - 638 (2002).

7 Diaz, E. SynDIG1 regulation of excitatory synapse maturation. *J Physiol* **590**, 33-38 (2012). https://doi.org:10.1113/jphysiol.2011.213884

8 Bats, C., Groc, L. & Choquet, D. The Interaction between Stargazin and PSD-95 Regulates AMPA Receptor Surface Trafficking. *Neuron* **53** (2007).

9 Diaz, E. SynDIG1 regulation of synaptic AMPA receptor targeting. *Communicative & integrative biology* **3**, 347-349 (2010). https://doi.org:10.4161/cib.3.4.11765

10 Diaz, E. Dynamic expression of SynDIG1 mRNA in cerebellar Purkinje neurons. *Current Neurobiology* **1** (2010).

11 Evgenia Kalashnikova, R. A. L. I. K., Gustavo A. Barisone, Bonnie Li, Tatuto Ishimaru, James S. Trimmer, Durga P. Mohapatra, and Elva Diaz. SynDIG1: an activity-regulated AMPA receptor-interacting transmembrane protein that regulates excitatory synapse development. *Neuron* **65** (2010).

12 Guillermo M. Elias, L. F., Valentin Stein, Seth G. Grant, David S. Bredt, and Roger A. Nicoll. Synapse-Specific and Developmentally regulated Targeting of AMPA Receptors by a Family of MAGUK Scaffolding Proteins. *Neuron* **52** (2006).

13 Diaz, S. A. M. a. E. Mechanisms of excitatory synapse maturation by trans-synaptic organizing complexes. *Current Opinion in Neurobiology* **21** (2011).

14 Lissin, D. V. *et al.* Activity differentially regulates the surface expression of synaptic AMPA and NMDA glutamate receptors. *Proc Natl Acad Sci U S A* **95**, 7097-7102 (1998). https://doi.org:10.1073/pnas.95.12.7097

15 Diaz, E. From microarrays to mechanisms of brain development and function. *Biochem Biophys Res Commun* **385**, 129-131 (2009). https://doi.org:10.1016/j.bbrc.2009.05.057

16 Bowie, D. Ionotropic glutamate receptors made crystal clear. *Trends in Neurosciences* **37** (2014).

17 Shanks, N. F. *et al.* Differences of AMPA and kainate receptor interactomes identify a novel AMPA receptor auxiliary subunit, GSG1L. *Cell Rep.* **1** (2012).

18 Nicoll, A. C. J. a. R. A. The Expanding Social Network of Ionotropic Glutamate Receptors: TARPS and Other Transmembrane Auxiliary Subunits. *Neuron* **70** (2011).

19 Sheng, M. & Hyoung Lee, S. AMPA receptor trafficking and synaptic plasticity: major unanswered questions. *Neurosci Res* **46**, 127-134 (2003). https://doi.org:10.1016/s0168-0102(03)00040-3

20 Chen, L., Tracy, T. & Nam, C. I. Dynamics of postsynaptic glutamate receptor targeting. *Curr Opin Neurobiol* **17**, 53-58 (2007). https://doi.org:10.1016/j.conb.2006.11.001

21 Makino, H. & Malinow, R. AMPA receptor incorporation into synapses during LTP: the role of lateral movement and exocytosis. *Neuron* **64**, 381-390 (2009). https://doi.org:10.1016/j.neuron.2009.08.035

22 Barry, M. F. & Ziff, E. B. Receptor trafficking and the plasticity of excitatory synapses. *Curr Opin Neurobiol* **12**, 279-286 (2002). https://doi.org:10.1016/s0959-4388(02)00329-x

23 Huganir, R. L. & Nicoll, R. A. AMPARs and synaptic plasticity: the last 25 years. *Neuron* **80**, 704-717 (2013). https://doi.org:10.1016/j.neuron.2013.10.025

24 Swanson, G. T. Targeting AMPA and kainate receptors in neurological disease: therapies on the horizon? *Neuropsychopharmacology* **34**, 249-250 (2009). https://doi.org:10.1038/npp.2008.158

25 Chang, P. K., Verbich, D. & McKinney, R. A. AMPA receptors as drug targets in neurological disease--advantages, caveats, and future outlook. *The European journal of neuroscience* **35**, 1908-1916 (2012). https://doi.org:10.1111/j.1460-9568.2012.08165.x

26 R. Douglas Fields, C. Y., and Phillip G. Nelson. Calcium, network activity, and the role of NMDA channels in synaptic plasticity in vitro. *The Journal of Neuroscience* **11** (1991).

27 Zucker, R. S. Calcium and activity-dependent synaptic plasticity. *Current Opinion in Neurobiology* **9** (1999).

28 Maria Fischer, S. K., Uta Wagner, Heike Brinkhaus, and Andrew Matus. Glutamate receptors regulate actin-based plasticity in dendritic spines. *Nature Neuroscience* **3** (2000).

29 Maria Fischer, S. K., Darko Knutti, and Andrew Matus. Rapid actin-based plasticity in dendritic spines. *Neuron* **20** (1998).

30 Michael D. Ehlers, S. Z., Jeffrey P. Bernhardt, and Richard L. Huganir. Inactivation of NMDA receptors by direct interaction of calmodulin with the NR1 subunit. *Cell* **84** (1996).

31 Traynelis, S. F. *et al.* Glutamate receptor ion channels: structure, regulation, and function. *Pharmacol Rev* **62**, 405-496 (2010). https://doi.org:10.1124/pr.109.002451

32 Schwenk, J. *et al.* Regional diversity and developmental dynamics of the AMPA-receptor proteome in the mammalian brain. *Neuron* **84**, 41-54 (2014). https://doi.org:10.1016/j.neuron.2014.08.044

33 Bissen, D., Foss, F. & Acker-Palmer, A. AMPA receptors and their minions: auxiliary proteins in AMPA receptor trafficking. *Cell Mol Life Sci* **76**, 2133-2169 (2019). https://doi.org:10.1007/s00018-019-03068-7

34 Kopec, C. D., Real, E., Kessels, H. W. & Malinow, R. GluR1 links structural and functional plasticity at excitatory synapses. *The Journal of neuroscience : the official journal of the Society for Neuroscience* **27**, 13706-13718 (2007). https://doi.org:10.1523/JNEUROSCI.3503-07.2007

35 Molnar, E. Long-term potentiation in cultured hippocampal neurons. *Seminars in cell & developmental biology* **22**, 506-513 (2011). https://doi.org:10.1016/j.semcdb.2011.07.017

36 Sumioka, A. Auxiliary subunits provide new insights into regulation of AMPA receptor trafficking. *J Biochem* **153**, 331-337 (2013). https://doi.org:10.1093/jb/mvt015

37 Matt, L. *et al.* SynDIG4/Prrt1 is required for excitatory synapse development and plasticity underlying cognitive function. *Cell Reports* (2018).

38 Tomita, S. *et al.* Stargazin modulates AMPA receptor gating and trafficking by distinct domains. *Nature* **435**, 1052-1058 (2005). https://doi.org:10.1038/nature03624

39 Chen, L. *et al.* Stargazin regulates synaptic targeting of AMPA receptors by two distinct mechanisms. *Nature* **408**, 936-943 (2000). https://doi.org:10.1038/35050030

40 Ben-Yaacov, A. *et al.* Molecular Mechanism of AMPA Receptor Modulation by TARP/Stargazin. *Neuron* **93**, 1126-1137 e1124 (2017). https://doi.org:10.1016/j.neuron.2017.01.032

41 Sunita DeSouza, J. F., Bradley A. States, and Edward B. Ziff. Differential Palmitoylation Directs the AMPA Receptor-Binding Protein ABP to Spines or to Intracellular Clusters. *The Journal of Neuroscience* (2002).

42 Elias, G. M., Elias, L. A., Apostolides, P. F., Kriegstein, A. R. & Nicoll, R. A. Differential trafficking of AMPA and NMDA receptors by SAP102 and PSD-95 underlies synapse development. *Proc Natl Acad Sci U S A* **105**, 20953-20958 (2008). https://doi.org:10.1073/pnas.0811025106

43 Fregozo, C. S. & Vega, M. I. P. Actin-binding proteins and signalling pathways associated with the formation and maintenance of dendritic spines. *Neurología* (2012).

44 Sheng, N. *et al.* LTP requires postsynaptic PDZ-domain interactions with glutamate receptor/auxiliary protein complexes. *Proc Natl Acad Sci U S A* **115**, 3948-3953 (2018). https://doi.org:10.1073/pnas.1800719115

45 Fong, D. K. & Craig, A. M. The Narp hypothesis? *Neuron* **23**, 195-197 (1999). https://doi.org:10.1016/s0896-6273(00)80768-0

46 Diaz, E. Regulation of AMPA receptors by transmembrane accessory proteins. *The European journal of neuroscience* **32**, 261-268 (2010). https://doi.org:10.1111/j.1460-9568.2010.07357.x

47 Kanehisa, K. *et al.* Neuronal pentraxin 2 is required for facilitating excitatory synaptic inputs onto spinal neurons involved in pruriceptive transmission in a model of chronic itch. *Nat Commun* **13**, 2367 (2022). https://doi.org:10.1038/s41467-022-30089-x

48 O'Brien, R. J. *et al.* Synaptic clustering of AMPA receptors by the extracellular immediate-early gene product Narp. *Neuron* **23**, 309-323 (1999). https://doi.org:10.1016/s0896-6273(00)80782-5

49 Lee, S. J. *et al.* Presynaptic Neuronal Pentraxin Receptor Organizes Excitatory and Inhibitory Synapses. *The Journal of neuroscience : the official journal of the Society for Neuroscience* **37**, 1062-1080 (2017). https://doi.org:10.1523/JNEUROSCI.2768-16.2016

50 O'Brien, R. *et al.* Synaptically targeted narp plays an essential role in the aggregation of AMPA receptors at excitatory synapses in cultured spinal neurons. *The Journal of neuroscience : the official journal of the Society for Neuroscience* **22**, 4487-4498 (2002). https://doi.org:20026354

51 Figueiro-Silva, J. *et al.* Neuronal pentraxin 1 negatively regulates excitatory synapse density and synaptic plasticity. *The Journal of neuroscience : the official journal of the Society for Neuroscience* **35**, 5504-5521 (2015). https://doi.org:10.1523/JNEUROSCI.2548-14.2015

52 Siddiqui, T. J., Pancaroglu, R., Kang, Y., Rooyakkers, A. & Craig, A. M. LRRTMs and neuroligins bind neurexins with a differential code to cooperate in glutamate synapse development. *The Journal of neuroscience : the official journal of the Society for Neuroscience* **30**, 7495-7506 (2010). https://doi.org:10.1523/JNEUROSCI.0470-10.2010

53 Siddiqui, T. J. & Craig, A. M. Synaptic organizing complexes. *Curr Opin Neurobiol* **21**, 132-143 (2011). https://doi.org:10.1016/j.conb.2010.08.016

54 Bhouri, M. *et al.* Deletion of LRRTM1 and LRRTM2 in adult mice impairs basal AMPA receptor transmission and LTP in hippocampal CA1 pyramidal neurons. *Proc Natl Acad Sci U S A* **115**, E5382-E5389 (2018). https://doi.org:10.1073/pnas.1803280115

55 Soler-Llavina, G. J. *et al.* Leucine-rich repeat transmembrane proteins are essential for maintenance of long-term potentiation. *Neuron* **79**, 439-446 (2013). https://doi.org:10.1016/j.neuron.2013.06.007

56 Chamma, I., Sainlos, M. & Thoumine, O. Biophysical mechanisms underlying the membrane trafficking of synaptic adhesion molecules. *Neuropharmacology* **169**, 107555 (2020). https://doi.org:10.1016/j.neuropharm.2019.02.037

57 Rouach, N. *et al.* TARP gamma-8 controls hippocampal AMPA receptor number, distribution and synaptic plasticity. *Nat Neurosci* **8**, 1525-1533 (2005). https://doi.org:10.1038/nn1551

58 Schwenk, J. *et al.* High-resolution proteomics unravel architecture and molecular diversity of native AMPA receptor complexes. *Neuron* **74**, 621-633 (2012). https://doi.org:10.1016/j.neuron.2012.03.034

59 Schwenk, J. *et al.* Functional proteomics identify cornichon proteins as auxiliary subunits of AMPA receptors. *Science* (2009).

60 Shanks, N. F. *et al.* Differences in AMPA and kainate receptor interactomes facilitate identification of AMPA receptor auxiliary subunit GSG1L. *Cell Rep* **1**, 590-598 (2012). https://doi.org:10.1016/j.celrep.2012.05.004

61 Dong, H., O'Brien, R.J., Fung, E.T., Lanahan, A.A., Worley, P.F. and Huganir, R.L. GRIP: A Synaptic PDZ Domain-Containing Protein that Interacts with AMPA Receptors. *Nature* (1997). https://doi.org:http://dx.doi.org/10.1038/386279a0

62 Kim, C. H., Chung, H. J., Lee, H. K. & Huganir, R. L. Interaction of the AMPA receptor subunit GluR2/3 with PDZ domains regulates hippocampal long-term depression. *Proc Natl Acad Sci U S A* **98**, 11725-11730 (2001). https://doi.org:10.1073/pnas.211132798

63 Pavel Osten, L. K., Joey L. Perez, Georg Kohr, Guenter Giese, Christopher Daly, Torsten W. Schulz, Allen Wensky, Laveria M. Lee, and Edward B. Ziff. Mutagenesis Reveals a Role for ABP/GRIP Binding to GluR2 in Synaptic Surface Accumulation of the AMPA Receptor. *Neuron* **27**, 313-325 (2000).

64 Hee Jung Chung, J. X., Robert H. Scannevin, Xiaoqun Zhang, and Richard L. Huganir. Phosphorylation of the AMPA Receptor Subunit GluR2 Differentially Regulates Its Interaction with PDZ Domain-Containing Proteins. *The Journal of Neuroscience* **20**, 7258–7267 (2000).

65 Hirbec, H. *et al.* Rapid and Differential Regulation of AMPA and Kainate Receptors at Hippocampal Mossy Fibre Synapses by PICK1 and GRIP. *Neuron* **37**, 625-638 (2003). https://doi.org:10.1016/s0896-6273(02)01191-1

66 Braithwaite, S. P., Xia, H. & Malenka, R. C. Differential roles for NSF and GRIP/ABP in AMPA receptor cycling. *Proc Natl Acad Sci U S A* **99**, 7096-7101 (2002). https://doi.org:10.1073/pnas.102156099

67 Seidenman, K. J., Steinberg, J. P., Huganir, R. & Malinow, R. Glutamate receptor subunit 2 Serine 880 phosphorylation modulates synaptic transmission and mediates plasticity in CA1 pyramidal cells. *The Journal of neuroscience : the official journal of the Society for Neuroscience* **23**, 9220-9228 (2003).

68 Hanley, D. L. R. a. J. G. PICK1 links AMPA receptor stimulation to Cdc42. *Neuroscience Letters* (2014).

69 Sossa, K. G., Beattie, J. B. & Carroll, R. C. AMPAR exocytosis through NO modulation of PICK1. *Neuropharmacology* **53**, 92-100 (2007). https://doi.org:10.1016/j.neuropharm.2007.04.005

70 Citri, A. *et al.* Calcium binding to PICK1 is essential for the intracellular retention of AMPA receptors underlying long-term depression. *The Journal of neuroscience : the official journal of the Society for Neuroscience* **30**, 16437-16452 (2010). https://doi.org:10.1523/JNEUROSCI.4478-10.2010

71 Terashima, A. *et al.* An essential role for PICK1 in NMDA receptor-dependent bidirectional synaptic plasticity. *Neuron* **57**, 872-882 (2008). https://doi.org:10.1016/j.neuron.2008.01.028

72 Mejias, R. *et al.* Gain-of-function glutamate receptor interacting protein 1 variants alter GluA2 recycling and surface distribution in patients with autism. *Proc Natl Acad Sci U S A* **108**, 4920-4925 (2011). https://doi.org:10.1073/pnas.1102233108

73 Han, M. *et al.* Mice lacking GRIP1/2 show increased social interactions and enhanced phosphorylation at GluA2-S880. *Behav Brain Res* **321**, 176-184 (2017). https://doi.org:10.1016/j.bbr.2016.12.042

74 Appleby, V. J. *et al.* LTP in hippocampal neurons is associated with a CaMKII-mediated increase in GluA1 surface expression. *J Neurochem* **116**, 530-543 (2011). https://doi.org:10.1111/j.1471-4159.2010.07133.x

75 Herring, B. E. & Nicoll, R. A. Long-Term Potentiation: From CaMKII to AMPA Receptor Trafficking. *Annu Rev Physiol* **78**, 351-365 (2016). https://doi.org:10.1146/annurev-physiol-021014-071753

76 Lemieux, M. *et al.* Translocation of CaMKII to dendritic microtubules supports the plasticity of local synapses. *J Cell Biol* **198**, 1055-1073 (2012). https://doi.org:10.1083/jcb.201202058

77 Villers, A., Giese, K. P. & Ris, L. Long-term potentiation can be induced in the CA1 region of hippocampus in the absence of alpha-CaMKII T286-autophosphorylation. *Cold Spring Harbor Laboratory Press* (2014).

78 Yuichi Makino, Richard C. Johnson, Yilin Yu, Kogo Takamiya & Huganir., R. L. Enhanced synaptic plasticity in mice with phosphomimetic mutation of the GluA1 AMPA receptor. *PNAS* (2011).

79 Hey-Kyoung Lee *et al.* Phosphorylation of the AMPA receptor GluR1 subunit is required for synaptic plasticity and retention of spatial memory. *Cell* (2003).

80 Nicoll, A. C. J. a. R. A. The expanding social network of ionotropic glutamate receptors: TARPs and other transmembrane auxiliary subunits. *Neuron* (2011).

81 Anat Ben-Yaacov *et al.* Molecular mechanism of AMPA receptor modulation by TARP/Stargazin. *Neuron* (2017).

82 Edward C. Twomey, Maria V. Yelshanskaya, Robert A. Grassucci, Joachim Frank & Sobolevsky, A. I. Elucidation of AMPA receptor-stargazin complexes by cryo-electron microscopy. *Science* (2016).

83 Susumu Tomita *et al.* Stargazin modulates AMPA receptor gating and trafficking by distinct domains. *Nature* **435** (2005).

84 Fukaya, M. *et al.* Abundant distribution of TARP gamma-8 in synaptic and extrasynaptic surface of hippocampal neurons and its major role in AMPA receptor expression on spines and dendrites. *The European journal of neuroscience* **24**, 2177-2190 (2006). https://doi.org:10.1111/j.1460-9568.2006.05081.x

85 Gill, M. B. *et al.* Cornichon-2 modulates AMPA receptor-transmembrane AMPA receptor regulatory protein assembly to dictate gating and pharmacology. *The Journal of neuroscience : the official journal of the Society for Neuroscience* **31**, 6928-6938 (2011). https://doi.org:10.1523/JNEUROSCI.6271-10.2011

86 Herring, B. E. *et al.* Cornichon proteins determine the subunit composition of synaptic AMPA receptors. *Neuron* **77**, 1083-1096 (2013). https://doi.org:10.1016/j.neuron.2013.01.017

87 von Engelhardt, J. *et al.* CKAMP44: A brain-specific protein attenuating short-term synaptic plasticity in the dentate gyrus. *Science* (2010).

88 Farrow, P. *et al.* Auxiliary subunits of the CKAMP family differentially modulate AMPA receptor properties. *Elife* **4**, e09693 (2015). https://doi.org:10.7554/eLife.09693

89 Schmitz, L. J. M. *et al.* The AMPA receptor-associated protein Shisa7 regulates hippocampal synaptic function and contextual memory. *Elife* **6** (2017). https://doi.org:10.7554/eLife.24192

90 Kalashnikova, E. *et al.* SynDIG1: an activity-regulated, AMPA- receptor-interacting transmembrane protein that regulates excitatory synapse development. *Neuron* **65**, 80-93 (2010). https://doi.org:10.1016/j.neuron.2009.12.021

91 Kathryn L. Lovero, S. M. B., Yun Shi, and Roger A. Nicoll. SynDIG1 Promotes Excitatory Syaptogenesis Independent of AMPA Receptor Trafficking and Biophysical Regulation. *PLOS One* (2013).

92 Bliss, T. V. & Lomo, T. Long-lasting potentiation of synaptic transmission in the dentate area of the anaesthetized rabbit following stimulation of the perforant path. *J Physiol* **232**, 331-356 (1973). https://doi.org:10.1113/jphysiol.1973.sp010273

93 Selcher, J. C., Xu, W., Hanson, J. E., Malenka, R. C. & Madison, D. V. Glutamate receptor subunit GluA1 is necessary for long-term potentiation and synapse unsilencing, but not long-term depression in mouse hippocampus. *Brain Research* (2012).

94 Zamanillo, D. *et al.* Importance of AMPA receptors for hippocampal synaptic plasticity but not for spatial learning. *Science* (1999).

95 Granger, A. J., Shi, Y., Lu, W., Cerpas, M. & Nicoll, R. A. LTP requires a reserve pool of glutamate receptors independent of subunit type. *Nature* **493**, 495-500 (2013). https://doi.org:10.1038/nature11775

96 Geinisman, Y. Structural synaptic modifications associated with hippocampal LTP and behavioral learning. *Cereb Cortex* **10**, 952-962 (2000). https://doi.org:10.1093/cercor/10.10.952

97 Matsuzaki, M., Honkura, N., Ellis-Davies, G. C. & Kasai, H. Structural basis of long-term potentiation in single dendritic spines. *Nature* **429**, 761-766 (2004). https://doi.org:10.1038/nature02617

98 Villeda, S. A. *et al.* The ageing systemic milieu negatively regulates neurogenesis and cognitive function. *Nature* **477**, 90-94 (2011). https://doi.org:10.1038/nature10357

99 Villeda, S. A. *et al.* Young blood reverses age-related impairments in cognitive function and synaptic plasticity in mice. *Nat Med* **20**, 659-663 (2014). https://doi.org:10.1038/nm.3569

100 Smith, L. K. *et al.* β2-Microglobulin is a systemic pro-aging factor that impairs cognitive function and neurogenesis. *Nature Medicine* (2015).

101 Horowitz, A. M. *et al.* Blood factors transfer beneficial effects of exercise on neurogenesis and cognition to the aged brain. *Science* **369**, 167-173 (2020). https://doi.org:10.1126/science.aaw2622

Chapter 2

Bi-directional clustering of SynDIG4/PRRT1 and AMPA receptor subunits GluA1 and GluA2 in heterologous cells

Preface:

In this chapter, I performed most biochemistry and immunochemistry experiments, as well as data analysis. Chun-Wei (Jay) He performed additional immunochemistry replicate experiments of Figure 7. Both Chun-Wei (Jay) He and Hector H. Navarro were instrumental in blinding confocal images and performing data analysis.

This chapter was published in the journal "**Frontiers in Molecular Neuroscience"** on April 8, 2022. For the purpose of this dissertation **Figure 8** from **Plambeck et al. 2022.** has been been replaced with a working model, and moved to **Chapter 3, Figure 2** to separate heterologous cells and neuronal data.

Bi-directional clustering of SynDIG4/PRRT1 and AMPA receptor subunits GluA1 and GluA2 in heterologous cells and primary neurons

Kristopher E. Plambeck[1], Chun-Wei He[1], Hector H. Navarro[1], and Elva Díaz[1*]

[1]Department of Pharmacology, UC Davis School of Medicine, Davis, CA 95616, USA

*Correspondence: Elva Díaz; email: ediaz@ucdavis.edu

ABSTRACT

Regulation of AMPA-type glutamate receptors (AMPARs) at synapses is a predominant mechanism for regulating synaptic strength. We identified the transmembrane protein Synapse Differentiation Induced Gene 1 (SD1; SD1) as an AMPAR interacting protein that regulates excitatory synaptic strength and AMPAR number both *in vitro* and *in vivo*. The related protein SynDIG4 (SD4; also known as PRRT1) was identified in several independent proteomic screens in complex with AMPARs, suggesting it may function as an AMPAR auxiliary factor. Here, we show that co-expression of SD4 with GluA1 or GluA2 homomeric AMPARs in COS cells leads to a 50% or 33% increase in the mean area of AMPAR puncta, respectively. This effect is accentuated when AMPAR puncta are stratified for co-localization with SD4, resulting in a 100% and 65% increase in GluA1 and GluA2 puncta, respectively. Chimeric proteins expressing only the membrane bound domain of SD4 co-expressed with full-length GluA1 or GluA2 recapitulated the effects of wild-type SD4. Additionally, the mean puncta area of GluA1 or GluA2 chimeras expressing the membrane and C-terminal domains increased significantly when co-localized with wild-type SD4. Similarly, co-expression of GluA1 or GluA2 with SD4 results in a significant increase in the mean area of SD4 puncta co-localized with GluA1 or GluA2, respectively. These data indicate bi-clustering of SD4 and AMPAR subunits both in COS cells, suggesting a mechanism for SD4 regulation of AMPARs that may play a role in regulation of synaptic strength.

INTRODUCTION

Neurons form precise connections known as synapses that are necessary for cell-cell communication. During excitatory synapse development, pre-synaptic axon terminals responsible for export of signaling molecules pair with post-synaptic dendritic spines that contain glutamate receptors, scaffolding molecules and cytoskeletal elements[1]. At excitatory synapses, there are two types of glutamate receptors which are recruited to the synaptic site via different mechanisms[2]: N-methyl-D-aspartate receptors (NMDARs) and α-amino-3-hydroxy-5-methyl-4-isoxazolepropionic acid receptors (AMPARs). NMDARs are first recruited to the dendritic surface during early maturation of excitatory synapses while the later recruitment of AMPARs stabilize the synapse and represent a mature synaptic structure[3]. AMPARs are necessary for fast synaptic transmission, and changes in the number of synaptic AMPARs directly reflect changes in synaptic strength[4]. Previous studies have identified a diverse group of AMPAR interacting proteins necessary for modulation of AMPAR biophysical properties and trafficking to the synapse[5-7]. For example, the AMPAR auxiliary protein Stargazin, a member of the transmembrane AMPAR regulating protein (TARP) family TARP-γ2, has been observed to decrease the deactivation and desensitization rates of AMPARs, as well as traffic AMPARs to the cell surface[8]. Stargazin/TARP-γ2 influences AMPARs through interaction with two distinct protein domains[9,10], of which the transmembrane (TM) domains TM3 and TM4 and extracellular loop 2 of Stargazin/TARP-γ2 have been found to be critically important[11]. Additional AMPAR auxiliary proteins such as the Cornichons (CNIHs)[12] and cysteine-knot AMPAR modulating proteins (CKAMPs)[13] have also been shown to affect functional properties of AMPARs. Therefore, AMPAR localization and channel properties are regulated by a wide array of distinct molecules.

The brain-specific type II transmembrane protein Synapse Differentiation Induced Gene 1 (SD1; SD1) was previously identified as an AMPAR interacting protein which regulates excitatory synapse development[14]. Specifically, SD1 clusters with AMPARs in heterologous cells and modulates the number of functional GluA1 and GluA2 containing AMPARs at excitatory synapses. Knockdown of SD1 results in a decrease in the number and strength of excitatory synapses. However, SD1 does not affect the biophysical properties of AMPARs, such as deactivation and desensitization to glutamate[15], indicating SD1 is not a typical auxiliary factor.

SynDIG4 (SD4), also known as Proline-rich transmembrane protein 1 (PRRT1), was identified by three independent proteomic studies[13,16,17] and demonstrates sequence similarity to SD1[14]. Surprisingly, SD4 is de-enriched at the post-synaptic density (PSD) and co-localizes with the AMPAR subunit GluA1 at extra-synaptic sites in primary neurons[18], implying a role of SD4 outside of the PSD. SD4 has been shown to modify AMPAR gating kinetics in a subunit-dependent manner[19]. Specifically, SD4 slows deactivation of GluA1 homomers, as well as GluA1/A2 heteromeric AMPARs. Additionally, SD4 slows desensitization of GluA1 homomers but not GluA1/A2 heteromers. Interestingly, these effects are potentiated when also expressed with TARP-γ8[19], indicating that SD4 may function in AMPAR complexes containing TARP-γ8. In support of this conclusion, a recent cryo-electron microscopy (cryo-EM) study demonstrated that SD4 is associated with native AMPAR complexes that contain both TARP-γ8 and CNIH-2[20].

The primary goal of this study is to further elucidate the role of SD4 in regulating GluA1- and GluA2-containing AMPARs using a structure-function approach. The link between AMPAR subunits and SD4 is necessary to establish a mechanism by which SD4 may affect the localization

and trafficking of AMPARs important for synaptic plasticity in the brain. We hypothesize that SD4 is necessary for establishing a reserve pool of AMPARs important for synaptic plasticity through its ability to cluster AMPARs at extra-synaptic sites. The present study identifies the regions sufficient for clustering of SD4 and the AMPAR subunits GluA1 and GluA2 in heterologous COS cells. As a result, colocalization of SD4 and AMPAR subunits indicates bi-directional clustering of AMPAR subunits and SD4, respectively.

MATERIALS/METHODS

Antibodies

The following antibodies were used: rat IgG1 anti-GluA1 [Neuromab; Cat# 75-327; RRID: AB_2315840; Immunocytochemistry (ICC) 1:200; Immunoblotting (IB) 1:2000]; rat IgG1 anti-GluA2 [Neuromab; Cat# 75-002; RRID: AB_10674575; ICC 1:200; IB 1:2000]; mouse IgG2a anti-SynDIG4 [NeuroMab; Cat# 73-409; RRID: AB_2491106; ICC 1:200; IB 1:2000]; mouse IgG2a anti-SD1 (NeuroMab; Cat# 75-251; RRID: AB_10999753; ICC 1:200); rabbit anti-IFITM3 (ProteinTech; ICC 1:200; IB 1:2000); rat anti-hemagglutinin (HA) (Roche; ICC 1:50; IB 1:1000); Alexa 488-conjugated anti-mouse IgG2a (Molecular Probes; ICC 1:200) and Alexa 594-conjugated anti-rat (Jackson ImmunoResearch; ICC 1:200); mouse anti-beta tubulin (MilliporeSigma; Clone: AA2; IB 1:5000); goat horseradish peroxidase (HRP) conjugated anti-rat (Invitrogen; IB 1:5,000); goat HRP-conjugated anti-mouse (Invitrogen; IB 1:10,000).

Constructs

Full length version of rat SD4 coding sequence was amplified by PCR from pHM6 expression vector and subcloned into pRK5 vector backbone provided by our collaborator Dr. Yael Stern-Bach at the Hebrew University of Jerusalem. Full length version of mouse SD1 was expressed using a previously generated pHM6 construct[14]. pCMV-HA-mIFITM3 was a gift from Howard Hang & Jacob Yount (Addgene plasmid #58389; http://n2t.net/addgene:58389; RRID: Addgene_58389). SD4/IFITM3 chimeras (**Table 1**) were generated by sequential PCR amplification using megaprimers. SD4/IFITM3 chimeras (**Table 1**) were generated by sequential

PCR amplification using megaprimers. Full length wildtype (WT) GluA1 was provided from the Stern-Bach lab and subcloned from the pGEM vector to the pRK5 expression vector. DNA vectors expressing full length GluA2 and GluK2, as well as the GluK2/A1 (**Table 2**, chimera #2-4) and GluK2/A2 (**Table 3**, chimera #1,2) chimeras, were additionally provided by the Stern-Bach lab. Additional GluK2/A1 (**Table 2**, chimeras #1,5,6) and GluK2/A2 (**Table 3**, chimera #3) constructs were generated by sequential PCR amplification using the megaprimer method. All constructs contain an in-frame HA tag at the N-terminus for detection. **Tables 1-3** identify the amino acid (a.a.) sequences of the indicated protein expressed within each chimeric molecule.

Table 1. SD4/IFITM3 chimeras.

HA-IFITM3/SD4	**IFITM3**	**SD4**
1.) HA-IF-NTD/SD4-M	a.a. 1-59	a.a. 224-306
2.) HA-SD4-NTD/IF-M	a.a. 60-137	a.a. 1-223

Table 2. GluK2/GluA1 chimeras.

HA-K2/A1	**GluK2**	**GluA1**
1.) M1-3,S2,M4,CT	a.a. 1-561	a.a. 537-907
2.) M1-3,M4,CT	a.a. 1-561; a.a. 660-819	a.a. 537-631; a.a. 806-907
3.) M1-3, CT	a.a. 1-561; a.a. 660-840	a.a. 537-631; a.a. 827-907
4.) M1-3	a.a. 1-561; a.a. 660-908	a.a. 537-631

5.) S2,M4,CT	a.a. 1-659	a.a. 632-907
6.) M4,CT	a.a. 1-819	a.a. 806-907

Table 3. GluK2/GluA2 chimeras.

HA-K2/A2	**GluK2**	**GluA2**
1.) M1-3,S2,M4,CT	a.a. 1-561	a.a. 543-883
2.) M1-3,S2,M4	a.a. 1-561; a.a. 841-908	a.a. 543-838
3.) M4,CT	a.a. 1-819	a.a. 810-883

Cell culture

The primate cell culture line COS-7 (ATCC CRL-1651) was used for all experiments. COS cells were grown in COS media containing DMEM (Life Technologies) supplemented with 10% Fetal Bovine Serum (Fisher Scientific) and 1% Penicillin/Streptomycin (Life Technologies). Cells were cultured at 37ºC with 5% CO_2.

Immunoblotting

COS cells were seeded in 6-well plates at a density of 300,000 cells per well in COS media. Transfection was performed with 2 µg of DNA using Lipofectamine 2000 (Invitrogen). Cells were lysed for protein extraction 24 hours after transfection using a standard lysis buffer (150 mM NaCl,

50 mM TRIS pH 7.4, 5 mM EDTA, 1% Triton x-100, 1 mM PMSF, and protease inhibitor cocktail). Cells were lifted using a cell scraper and then passed through a 22.5-gauge needle before transferring lysates to 1.5 mL microfuge tubes. Lysates were then transferred to a rotator at 4ºC for 30 minutes. After 30 minutes, lysates were centrifuged at 12,000 rpm for 10 minutes at 4ºC. Supernatant was removed and flash frozen in liquid nitrogen for long term storage. In preparation for immunoblotting, protein samples were thawed on ice. For all blots, 10 µg protein per sample was denatured at 95ºC and loaded onto freshly poured 8% SDS-PAGE. Gels were run for 90 minutes at 120V and transferred to nitrocellulose membrane for one hour at 100V. Membranes were blocked in 5% milk diluted in tris-buffered saline with tween-20 (TBST) for one hour. For testing expression of AMPAR chimeras, membranes were incubated with both rat anti-HA antibodies and mouse anti-tubulin antibodies at 4ºC overnight. For testing expression of SD4/IFITM3 chimeras, membranes were incubated with anti-SD4, anti-IFITM3, and anti-tubulin antibodies at 4ºC overnight. Membranes were washed with TBST and incubated in HRP conjugated goat anti-rat and HRP-conjugated goat anti-mouse secondary antibodies for one hour at room temperature. Luminata Crescendo reagent was added to membrane for direct detection of HRP signal (Azure Biosystems).

Immunocytochemistry

COS cells were plated in 6-well plates containing coverslips coated with poly-L-lysine (Sigma-Aldrich). Cells were plated at a density of 300,000 cells per well and cultured for 24 hours prior

to transfection. All transient transfection experiments contained a total of 2 µg of DNA (1.75 µg receptor and 250 ng of either SD4 or pRK5 empty vector) using Lipofectamine 2000 (Invitrogen) and cells were cultured for an additional 24 hours. For live labeling, cells were first incubated at 4ºC for 10 minutes. Cells were washed once with cold PBS and incubated in rat anti-HA antibody diluted in COS media for 20 minutes at 4ºC. After primary staining, cells were washed three times with cold PBS and incubated in donkey Alexa 594-conjugated anti-rat secondary antibody diluted in COS media for 20 minutes. Cells were washed three times with cold PBS and then with warm COS media. Plates were transferred back to 37ºC incubator for 30 minutes. Cells were washed with PBS and fixed in 4% paraformaldehyde for 10 minutes.

For staining of total SD1 or total SD4, coverslips were incubated in 0.1% Triton-X100 diluted in PBS for 15 minutes. Cells were blocked with 5% milk in PBS for 30 minutes and incubated in primary antibody for 1.5 hours at room temperature. Coverslips were washed three times with PBS and incubated in donkey Alexa 488-conjugated anti-mouse IgG2a for one hour. Coverslips were washed three times with PBS and mounted on slides with Fluoromount G (Southern Biotech).

Image Analysis

For quantitative analyses, images were taken using either an Olympus FluoView 1000 or Zeiss LSM510 confocal microscope with a 63x/1.5 NA oil objective with identical settings for laser

power, photomultiplier gain, and digital offset. Pinhole (1 AU) and resolution (1024 x 1024 pixels) were constant for all images.

Images were analyzed blinded to the experimental condition. Image files were imported into image analysis software (ImageJ) to determine average size of clusters for each condition. Selected cells were cropped from the original pictures and saved, blinded, and subjected to the analysis by an individual not involved in the cell selection and blinding process. The threshold for each independent experiment is determined by averaging the thresholds of at least 25% of images. The average threshold was then applied to all images for analysis. Only clusters within the range of 0.1 – 3.5 μm^2 were measured. After data collection and the unblinding process, the puncta size of all signals was subjected to statistical analysis. For analysis of puncta size based on co-localization with SD4 (stratification analysis), co-localization was defined as overlap of ≥1 pixel. The highlighted colocalized puncta in the image for the receptor with SD4 were then used to select unambiguous single puncta manually in the receptor mask image. XY coordinates were used to confirm the selected puncta in the receptor mask image that corresponded with the highlighted puncta in the receptor with SD4 image. For figure preparation, signals were adjusted for all panels within a figure by using equal linear adjustments of levels in Photoshop (Adobe Systems).

Statistical analysis

Data were collected from at least two independent experiments and a minimum n = 10-15 cells per condition per experiment. All graphs and statistical analyses were generated using GraphPad Prism

software. Graphs depict the data average and the standard error of the mean (SEM). Statistical significance was assessed by either unpaired student's t-test or one-way ANOVA. Significance is defined as *p<0.05; **p<0.01; ***p<0.001; ****p<0.0001.

RESULTS

SD4 clusters GluA1 and GluA2 containing AMPARs

To characterize the relationship between AMPARs and SD4, we used a clustering assay previously established within our lab[14]. The full-length AMPAR subunits GluA1 and GluA2, as well as the kainate receptor subunit GluK2, were expressed in heterologous COS cells either alone or co-expressed with full-length HA-tagged SD4. GluK2 is predicted not to associate with SD4 and served as a negative control. Each receptor subunit contains an N-terminal HA tag for extracellular detection. COS cells were first live-labeled with anti-HA antibodies to examine distribution of surface expressing GluA1, GluA2, or GluK2. The receptors have extracellular N-termini, while SD4 does not, so only surface GluA1, GluA2, or GluK2 were labeled. After fixation and permeabilization, cells were stained with anti-SD4 antibodies for total SD4.

We observed diffuse and even distribution of GluA1, GluA2, and GluK2 when expressed alone. When co-expressed with SD4, a change in the overall distribution of both GluA1 and GluA2 was observed (**Figure 1A)**. No difference was observed when GluK2 was co-expressed with SD4, indicating specificity of SD4 for AMPARs **(Figure 1A)**. Quantification indicates a significant increase in the mean cluster size of GluA1 and GluA2 puncta when co-expressed with SD4 compared to receptor alone **(Figure 1B)**. Although GluK2 puncta are larger at baseline, there was no significant change observed in puncta size when co-expressed with SD4 **(Figure 1B)**.

We noted a distribution of GluA1 or GluA2 cluster sizes in SD4 co-expressing cells. To determine whether cluster size was related to overlap with SD4, which was not captured in the previous analysis, we stratified populations in co-expressing cells into two groups representing

glutamate receptor puncta co-localized with SD4 (w/ SD4) or not co-localized with SD4 (w/o SD4). Stratification of GluA1 puncta co-localized with SD4 showed that the mean cluster size is significantly greater when SD4 and GluA1 are co-localized compared to GluA1 expressed alone **(Figure 1C)**. In contrast, the size of puncta not co-localized with SD4 were not significantly different compared to GluA1 alone **(Figure 1C)**. The mean size of GluA2 clusters is also significantly greater when co-localized with SD4, while non-colocalized clusters are not significantly different compared to GluA2 alone **(Figure 1D)**. No significant differences were observed in the size of GluK2 clusters co-localized with SD4 or not co-localized compared with GluK2 alone **(Figure 1E)**. These results provide evidence that co-expression of SD4 is sufficient to re-distribute and cluster GluA1 and GluA2-containing AMPARs in heterologous cells, and the increased cluster size is dependent on co-localization with SD4.

The proline-rich N-terminus of SD4 is dispensable for clustering with GluA1 and GluA2.

To identify the region of SD4 sufficient for clustering with GluA1 or GluA2, we generated chimeric proteins by swapping domains between SD4 and the distantly related dispanin family[21] member IFITM3 with a similar topology[22,23]. One chimera was generated using the N-terminus of SD4 and the entire membrane associated domain of IFITM3 (SD4-NTD/IF-M), and a second chimera was generated using the N-terminus of IFITM3 and the entire membrane associated domain of SD4 (IF-NTD/SD4-M) **(Figure 2A; Table 1)**. Constructs were first verified by immunoblot with antibodies that only recognize the N-terminus of their respective proteins **(Figure 2B)**. Therefore, signal is only present when the N-terminus is expressed.

GluA1 was expressed in COS cells either alone, or co-expressed with full-length SD4, SD4-NTD/IF-M, or IF-NTD/SD4-M **(Figure 2C).** We observed no difference in mean cluster size of GluA1 populations either co-localized or not co-localized with SD4-NTD/IF-M compared with GluA1 alone **(Figure 2D).** However, stratification of the GluA1 populations indicated a significant increase in the mean size of GluA1 clusters when co-localized with IF-NTD/SD4-M compared with GluA1 alone **(Figure 2E).** Next, GluA2 was expressed in COS cells either alone, or co-expressed with either IF/SD4 chimeras **(Figure 2F)**. Stratification of GluA2 populations co-localized or not co-localized with SD4-NTD/IF-M resulted in no change in the mean size of GluA2 clusters **(Figure 2G**). However, we observed a significant increase in the mean size of GluA2 clusters when co-localized with IF-NTD/SD4-TM compared with GluA2 alone **(Figure 2H)**.

These results indicate that the proline-rich N-terminus of SD4 is dispensable for clustering with GluA1 and GluA2. Furthermore, the membrane domain of SD4 is sufficient for clustering with GluA1- and GluA2-containing AMPARs, and that clustering of AMPARs is dependent on co-localization with SD4.

The N-terminus of GluA1 is dispensable for clustering with SD4.

To identify the region of GluA1 that is sufficient for clustering with SD4, we generated chimeric GluA1 proteins using homologous domains of GluK2 (**Table 2**). Expression of all GluK2/GluA1 chimeras were verified by immunoblot **(Figure 3A)**. The chimeras were then transfected and expressed in COS cells either alone or with full-length SD4 (**Figure 3B-F**). Quantification of mean

area of clusters shows an increase in puncta size when SD4 is co-expressed with GluA1, but no significant difference when co-expressed with the chimera expressing the M1-3, S2, M4, and CT domains of GluA1 **(Figure 3G)**. However, stratification of GluK2/A1/M1-3/S2/M4/CT chimeric puncta (**Figure 3B)** depict a significant increase in puncta size when co-localized with SD4 (**Figure 3H)**. Therefore, we conclude that the N-terminus of GluA1 is dispensable for clustering with SD4, and cluster size is dependent on co-localization with SD4.

The N-terminus of GluA2 is dispensable for clustering with SD4.

We next generated GluA2 chimeras using homologous domains of GluK2 (**Table 3**). Expression of GluA2 chimeras was verified by immunoblot **(Figure 4A)**. All chimeras were transfected in COS cells either alone or with full-length SD4 **(Figure 4B-D)**. We found that only the chimera expressing the M1-3, S2, M4, and CT domains of GluA2 resulted in an altered distribution when co-expressed with SD4 **(Figure 4B)**. Additionally, the GluK2/A2/M1-3/S2/M4 chimera, where the GluA2-CT domain was not present, resulted in a loss of the clustering phenotype **(Figure 4C)**. Therefore, these experiments show the importance of the GluA2 C-terminal domain for clustering with SD4. Quantification of mean area of clusters shows a significant increase in cluster size when SD4 is co-expressed with either full-length GluA2 or the GluK2/A2/M1-3/S2/ M4/CT chimera (**Figure 4E)**. Furthermore, stratification of puncta from **Figure 4B** shows a significant increase in puncta area only when co-localized with SD4 **(Figure 4F)**. Therefore, we conclude that the N-terminus of GluA2 is dispensable for clustering with SD4, and cluster size is dependent on co-localization with SD4.

The M4 and C-terminus of GluA2 is sufficient for clustering with SD1.

For comparison, we sought to identify a region of AMPAR necessary for clustering with the SD4-related family member SD1. Full-length GluA2 had previously been observed to cluster with SD1[14], therefore, GluA2 and GluK2 were used as positive and negative controls, respectively. We observed altered distribution of GluA2, but not GluK2, when co-expressed with SD1 **(Figure 5A)**. Next, we co-expressed two of the key GluA2 chimeras from **Figure 4**. Similar to SD4, we observed clustering when the GluK2/A2/M1-3/S2/M4/CT chimera was co-expressed with SD1. However, in contrast to SD4, we also observed clustering when the GluK2/A2/M4/CT chimera was co-expressed with SD1 (**Figure 5B)**. Quantification depicts a significant increase in mean area of clusters when SD1 is co-expressed with GluK2/A2/M1-3/S2/M4/CT and GluK2/A2/M4/CT, but not with GluK2 **(Figure 5C)**. Lastly, stratification of M4, CT chimera puncta co-localized with SD1 results in a significant increase in the mean area of clusters **(Figure 5D)**. Therefore, the M4 and CT of GluA2 is sufficient for clustering with SD1.

SD4 cluster size increases when colocalized with GluA1 and GluA2.

Next, we were interested in whether co-expression of AMPARs with SD4 results in a reciprocal increase in the cluster size of SD4. For these experiments, SD4 was expressed in COS cells either alone, or co-expressed with either GluA1, GluA2 or GluK2 **(Figure 6A)**. Stratification of SD4 puncta co-localized with GluA1 results in a significant increase in the mean cluster size of SD4 puncta co-localized with GluA1 compared with SD4 alone **(Figure 6B)**. Additionally, the mean

cluster size of SD4 puncta co-localized with GluA2 is also significantly increased **(Figure 6C)**. We observed no difference in the mean cluster size of SD4 puncta whether co-localized or non-colocalized with GluK2 compared with SD4 alone **(Figure 6D)**. We conclude that not only does co-localization of SD4 with AMPARs increase the mean cluster size of the receptor, but colocalization with AMPARs also significantly increase the cluster size of SD4.

SD4 clustering of GluA1 and GluA2 is temperature dependent

Clustering of GluA2 by SD1 requires a 37ºC incubation after the surface labeling at 4ºC[14]. This observation suggests that a biological process such as endocytosis is necessary for clustering by SD1. We were then interested to determine whether SD4 clustering of AMPARs is temperature dependent. For these experiments, duplicate plates of COS cells expressing GluK2, GluA1, or GluA1 either alone or co-expressed with SD4 were prepared. For surface labeling of the receptors, all plates were incubated at 4ºC. Next, one plate was transferred to a 37ºC incubator, while the other plate remained at 4ºC. After incubation, coverslips were fixed and imaged. We observed that incubation at 4ºC does not result in a change of distribution for any of the receptors, either alone or co-expressed with SD4 **(Figure 7A)**. Quantification indicates no significant increase in the mean area of clusters after the 4ºC incubation **(Figure 7B)**. However, incubation at 37ºC resulted in clustering of the receptors as expected **(Figure 7C)**. Quantification shows a significant increase in the mean area of clusters when either GluA1 or GluA2 are co-expressed with SD4, but not

GluK2 **(Figure 7D)**. Therefore, we conclude that endocytosis of surface labeled AMPARs is most likely necessary for clustering with SD4.

Proposed mechanism for SD4 role in AMPAR clustering in heterologous cells.

We propose a mechanism by which SD4 forms a complex with GluA1 or GluA2 AMPAR subunits resulting in readily available pools of AMPARs **(Figure 8)**. SD4 is translated in the nucleus and transported through the secretory pathway where it is exocytosed to the surface of the plasma membrane. However, our studies indicate that, at least in heterologous cells, SD4 remains on the surface only for a brief period, while most SD4 is localized intracellularly. At the plasma membrane, SD4 binds and captures GluA1 and GluA2 AMPAR subunits. The SD4-GluA1/A2 complexes are then endocytosed to early endosomes where they are readily available. After stimulation, these readily available pools are exocytosed to the cell surface to increase the number of surface AMPARs which, in neurons, would then be trafficked to the synapse. These results further indicate a potential role for SD4 in regulating AMPAR trafficking during LTP.

DISCUSSION

Previously, we showed that SD4 alters AMPAR biophysical properties in a subunit-specific manner[19], indicating a direct and specific interaction with AMPARs. Indeed, SD4 has been identified in multiple independent proteomic studies as a component of AMPAR complexes[13,16,17] as well as recent structural studies of native AMPAR complexes from brain[20]. Although present in synaptosomal membranes, SD4 is de-enriched in the PSD[18], suggesting that SD4 associates primarily with extra-synaptic AMPARs. Here we present evidence that SD4 and GluA1 or GluA2 AMPARs bidirectionally increase cluster size of each other in heterologous cells. Distinct regions within SD4, GluA1 and GluA2 are critical for this mutually dependent clustering activity. Intriguingly, the bi-directional clustering requires incubation at 37ºC, suggesting that endocytosis of surface labeled AMPARs is most likely necessary for clustering with SD4. We propose that SD4 establishes a reserve pool of extra-synaptic AMPARs through bidirectional clustering of SD4 and AMPARs necessary for synaptic potentiation.

SD4 is predicted to contain two membrane-bound domains, with only one that spans the membrane, with a large proline-rich intracellular N-terminus and a small extracellular C-terminus[18], confirmed in a recent study[24]. Proline residues have often been linked to protein-protein interactions[25,26]. However, our results indicate that only the membrane bound portion of SD4 is important for clustering with GluA1 or GluA2. Others reported that SD4 is able to co-immunoprecipitate a small amount (2% of input) of GluA1 or GluA2 when co-expressed in HEK293 cells[24]. Furthermore, deletion of the intracellular loop, the transmembrane domain, and the small extracellular tail of SD4 eliminated the observed co-immunoprecipitation[24], consistent

with our results indicating that the proline-rich intracellular N-terminal region is not required for clustering. SD4 does not contain a PDZ binding motif, and it is not enriched in the PSD[18]. The proline-rich domain may be important for interaction with other auxiliary factors or scaffolds necessary for trafficking and anchoring at synapses. Additional experiments will address this possibility.

To identify the GluA1 AMPAR domain sufficient for clustering with SD4, we used GluK2/GluA1 chimeras which swap homologous protein domains between receptors. All GluK2/GluA1 chimeras lacked the NT domain of GluA1. The total mean area of GluA1 puncta was not significantly larger compared to the chimeras when co-expressed with SD4. However, we did observe some clustering with the GluK2/A1/M1-3/S2/M4/CT chimera when expressed alone, which may have occluded any increase in cluster size in this analysis. In support of this possibility, the mean cluster size of GluK2/A1/M1-3/S2/M4/CT chimeric puncta are significantly increased by stratification of puncta co-localized with SD4, while no increase is observed by stratification of other chimeras co-localized with SD4. We observed altered distribution of the receptor only when the entire membrane, S2, and CT domains (GluK2/A1/M1-3/S2/M4/CT) were present and co-localized with SD4 in COS cells. Therefore, we conclude that the NT domain is dispensable, while the entire membrane bound domain of GluA1, in addition to the S2 and CT domains, are necessary for clustering by SD4.

Similar to the GluA1 chimeras, we used GluK2/GluA2 chimeras to identify the region sufficient for clustering with SD4. All GluK2/GluA2 chimeras lacked the NT domains of GluA2. We observed a change in distribution when the entire membrane bound domain, S2 domain, and

CT domain of GluA2 (GluK2/A2/M1-3/S2/M4/CT) was expressed with SD4. In these experiments, we also saw a significant increase in mean puncta size, with no significant differences with any additional chimeras. Interestingly, we observed that clustering was lost when the CT domain was absent, indicating an importance of the CT for clustering with SD4. Additionally, we did not observe clustering when the M1-3 and S2 domains were absent. We conclude that the entire membrane bound domain of GluA2, in addition to the S2 and CT domains, is necessary for clustering by SD4.

Interestingly, we observed that GluA1 and GluA2 also affected cluster size of SD4 when co-expressed in COS cells. These results coincide with an increase in cluster size when stratified for co-localization with GluA1 or GluA2. We conclude that the cluster size of both SD4 and AMPAR puncta is significantly increased only when co-localized in COS cells, indicating a bi-directional interaction mechanism.

We were not able to identify a smaller domain of GluA1 or GluA2 sufficient for clustering with SD4. One possibility is that there are multiple regions within the AMPAR necessary for interacting with SD4. Pioneering work by Ben-Yaacov and colleagues using domain swaps demonstrated AMPAR interaction with Stargazin/TARP-γ2 primarily involves the AMPAR membrane domains M1 and M4 of neighboring subunits, with important contributions by the CT[11]. Structural studies with cryo-EM support these functional results[27-29]. Attempts to express three constructs in COS cells were technically problematic, therefore, we could not pursue this approach. Since SD4 has been shown to affect the biophysical properties of GluA1 and GluA2-contating AMPARS[19], in future experiments we plan to continue the structure-function approach with

electrophysiology to narrow down the critical domain. Moreover, cryo-EM structures of native AMPARs indicates that SD4 is associated with AMPAR complexes that contain TARP-γ8 and CNIH-2[20]. Thus, it will be interesting to determine if SD4-dependent AMPAR clustering is influenced by the presence of TARP-γ8 and/or CNIH-2, or whether SD4 clusters bi-directionally with either of these two auxiliary factors. Furthermore, the co-expression of multiple auxiliary subunits might increase the efficiency of co-immunoprecipitation of AMPAR subunits observed with SD4 alone[24]. It should be noted that clustering of AMPARs required co-expression of Stargazin/TARP-γ2 and PSD-95; Stargazin/TARP-γ2 alone was not sufficient to change the distribution of AMPARs in heterologous cells[8]. Thus, the mutually dependent clustering activity of SD4 with AMPARs might be unique to this auxiliary factor.

Intriguingly, the bi-directional clustering requires incubation at 37°C, suggesting that endocytosis of surface labeled AMPARs is most likely necessary for clustering with SD4. In primary hippocampal neurons at steady-state most of SD4 overlaps with endosomal markers[24], but some protein is available for surface labeling[18,24]. Thus, it is tempting to speculate that SD4 captures AMPARs at the plasma membrane for clustering via transport through an endocytic compartment. Current studies are addressing this possibility. Importantly, the increased cluster size of GluA1 that overlaps with SD4 is observed in primary hippocampal neurons upon chemical-LTP, suggesting that this clustering activity is a mechanism underlying strengthening of synapses during synaptic plasticity. We propose that SD4 establishes a reserve pool of extra-synaptic AMPARs through bidirectional clustering of SD4 and AMPARs necessary for synaptic potentiation.

We were able to identify a minimal domain of GluA2 domain responsible for the interaction with the related protein SD1. SD4 and SD1 share approximately 35% overall amino acid sequence similarity, with higher similarity occurring within the membrane bound domain[14]. However, while SD4 and SD1 share similarity only SD4 has been shown to affect the biophysical properties of GluA1 and GluA2-containing AMPARs[15,19]. Co-expression of GluA2 with SD1 shows significant clustering of GluA2 when compared to GluA2 expression alone, which fits with previously observed results[14]. Conversely, co-expression of GluK2 with SD1 did not exhibit a clustering phenotype. Using the same GluK2/GluA2 chimeras, we observed clustering of the GluK2/A2/M1-3/S2/M4/CT chimera when co-expressed with SD1. In contrast to SD4, we also observed clustering when SD1 was co-expressed with the GluK2/GluA2 chimera expressing only the M4 and CT domain of GluA2. We conclude that the minimal M4/CT domain of GluA2 is sufficient for clustering with SD1, which potentially explains the lack of SD1 effects on biophysical properties.

Most of the excitatory transmission in the brain is mediated by AMPA receptors. Furthermore, many neuropsychiatric and neurological disorders, such as Alzheimer's disease and depression, can be characterized by abnormal AMPA receptor content and trafficking leading to impaired synapse function[30-32]. Therefore, understanding the complete mechanism behind AMPA receptor function is important for understanding disease. Continuing studies utilizing cultured hippocampal neurons and transgenic mouse models will be important to establish the role of SD4 trafficking to the synapse that may yield a better understanding of the underlying mechanism behind neuropsychiatric and neurological disorders.

ACKNOWLEDGEMENTS

The authors thank members of the Diaz, Gray, Hell, and Zito labs at UC Davis for comments and suggestions throughout the project as well as Yael Stern-Bach at the Hebrew University of Jerusalem for constructs and advice. This project was funded by grants to E.D. from the Whitehall Foundation (2015-05-106), the National Science Foundation (1322302) and the National Institute of Mental Health (MH119347).

CONFLICT OF INTEREST

The authors declare no competing financial interests exist.

ROLE OF AUTHORS

Methodology: KEP, ED; *Investigation:* KEP, CWH, ED; *Formal analysis:* KEP, CWH, HHN, ED; *Writing:* KEP, ED; *Funding acquisition:* ED; *Supervision:* ED.

Figure 1. SD4 clusters GluA1 and GluA2-containing AMPARs.

(A) Representative confocal images of COS cells transfected with either receptor alone, or co-transfected with both receptor and SD4. Cells were live labeled with anti-HA antibodies against surface expressing receptors and anti-SD4 antibodies for total SD4. Scale bar = 20 μm. **(B)** Graph depicts mean cluster size of GluA1 alone (n=10), GluA1 + SD4 (n=12), GluA2 alone (n=16), GluA2 + SD4 (n=10), GluK2 alone (n=13), or GluK2 + SD4 (n=11) puncta. **(C-E)** Graphs depict stratification of GluA1 **(C),** GluA2 **(D)**, or GluK2 **(E)** puncta either co-localized or not co-localized with SD4 compared to the average cluster size of receptor alone. Data are represented as mean cluster size +/- SEM; n.s. not significant; **p<0.01; ***p<0.001; ****p<0.0001; one-way ANOVA.

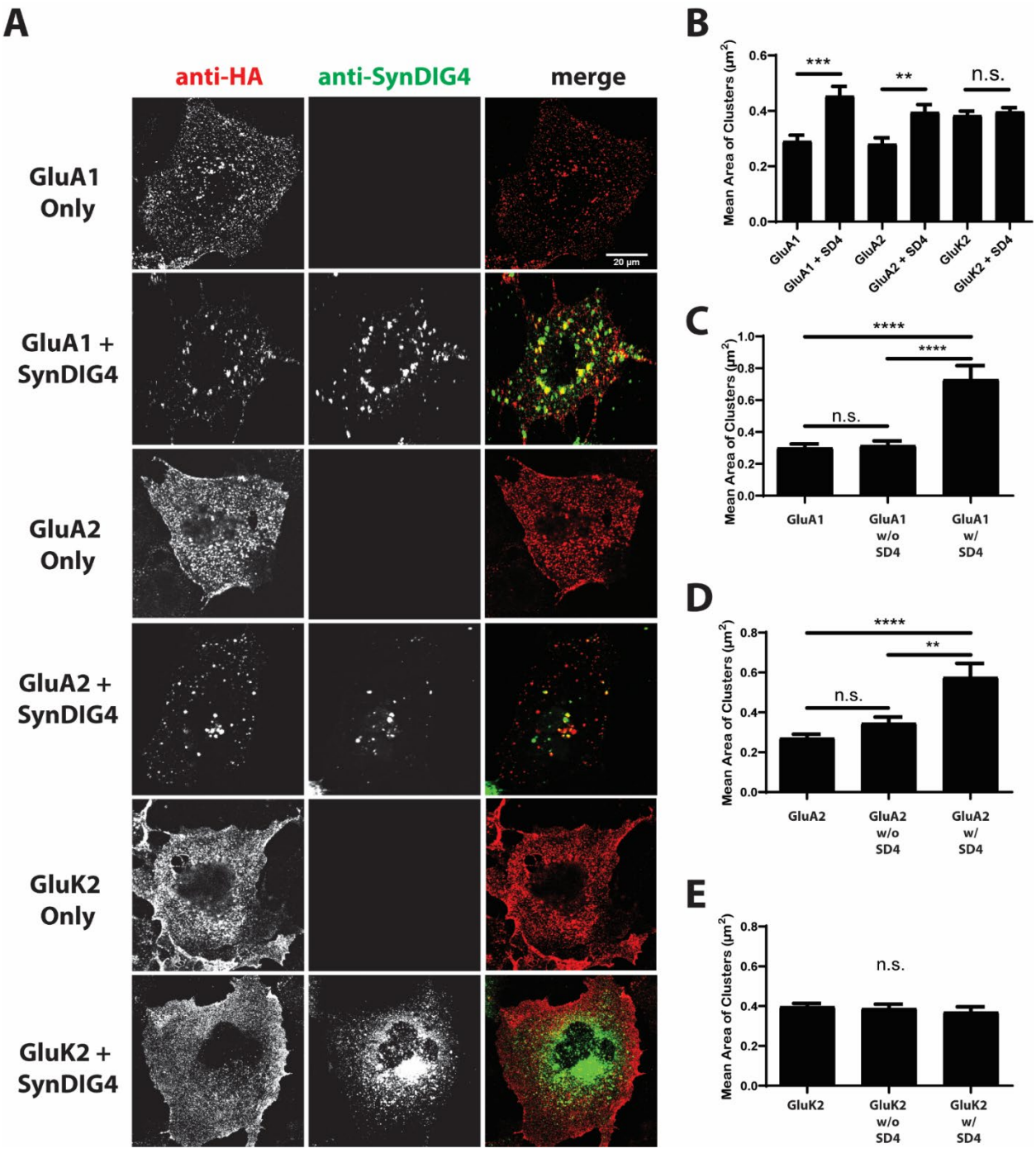
A
anti-HA
anti-SynDIG4
merge
GluA1 Only
GluA1 + SynDIG4
GluA2 Only
GluA2 + SynDIG4
GluK2 Only
GluK2 + SynDIG4
20 µm
B
Mean Area of Clusters (µm²)
0.0
0.2
0.4
0.6
***
**
n.s.
GluA1
GluA1 + SD4
GluA2
GluA2 + SD4
GluK2
GluK2 + SD4
C
Mean Area of Clusters (µm²)
0.0
0.2
0.4
0.6
0.8
1.0
****
****
n.s.
GluA1
GluA1 w/o SD4
GluA1 w/ SD4
D
Mean Area of Clusters (µm²)
0.0
0.2
0.4
0.6
0.8
****
**
n.s.
GluA2
GluA2 w/o SD4
GluA2 w/ SD4
E
Mean Area of Clusters (µm²)
0.0
0.2
0.4
0.6
0.8
n.s.
GluK2
GluK2 w/o SD4
GluK2 w/ SD4

Figure 2. The proline rich N-terminus of SD4 is dispensable for clustering with GluA1 and GluA2.

(A) Schematic depicting the chimeric protein structures. Chimeras were generated expressing either (i) the N-terminus of SD4 and membrane domain of IFITM3 (SD4-NTD/IF-M) or (ii) the N-terminus of IFITM3 and membrane domain of SD4 (IF-NTD/SD4-M) (See Table 1 of Methods). **(B)** Immunoblot of COS cell lysates transfected with SD4 and IFITM3 chimeras. β-Tubulin was used as the loading control. **(C)** Representative confocal images depict either GluA1 expressed alone or co-expressed with either IF/SD4 chimera. Scale bar = 20 μm. **(D, E)** Graph depicts mean cluster size of GluA1 puncta from stratification of GluA1 co-localized or not co-localized with SD4-NTD/IF-M chimeras **(D)** or IF-NTD/SD4-M chimeras **(E)** compared with GluA1 alone. GluA1 alone (n=10), GluA1 + SD4-NTD/IF-M (n=12), and GluA1 + IF-NTD/SD4-M (n=12). **(F)** Representative confocal images of GluA2 alone or co-expressed with IF/SD4 chimeras. Scale bar = 20 μm. **(G, H)** Graph depicts mean cluster size of GluA2 puncta from stratification of GluA2 co-localized or not co-localized with SD4-NTD/IF-M chimeras **(G)** or IF-NTD/SD4-M chimeras **(H)** compared with GluA2 alone. GluA2 alone (n=13), GluA2 + SD4-NTD/IF-M (n=12), and GluA2 + IF-NTD/SD4-M (n=16). Data are represented as mean cluster size +/- SEM; n.s. not significant; *p<0.05; **p<0.01; ****p<0.0001; one-way ANOVA.

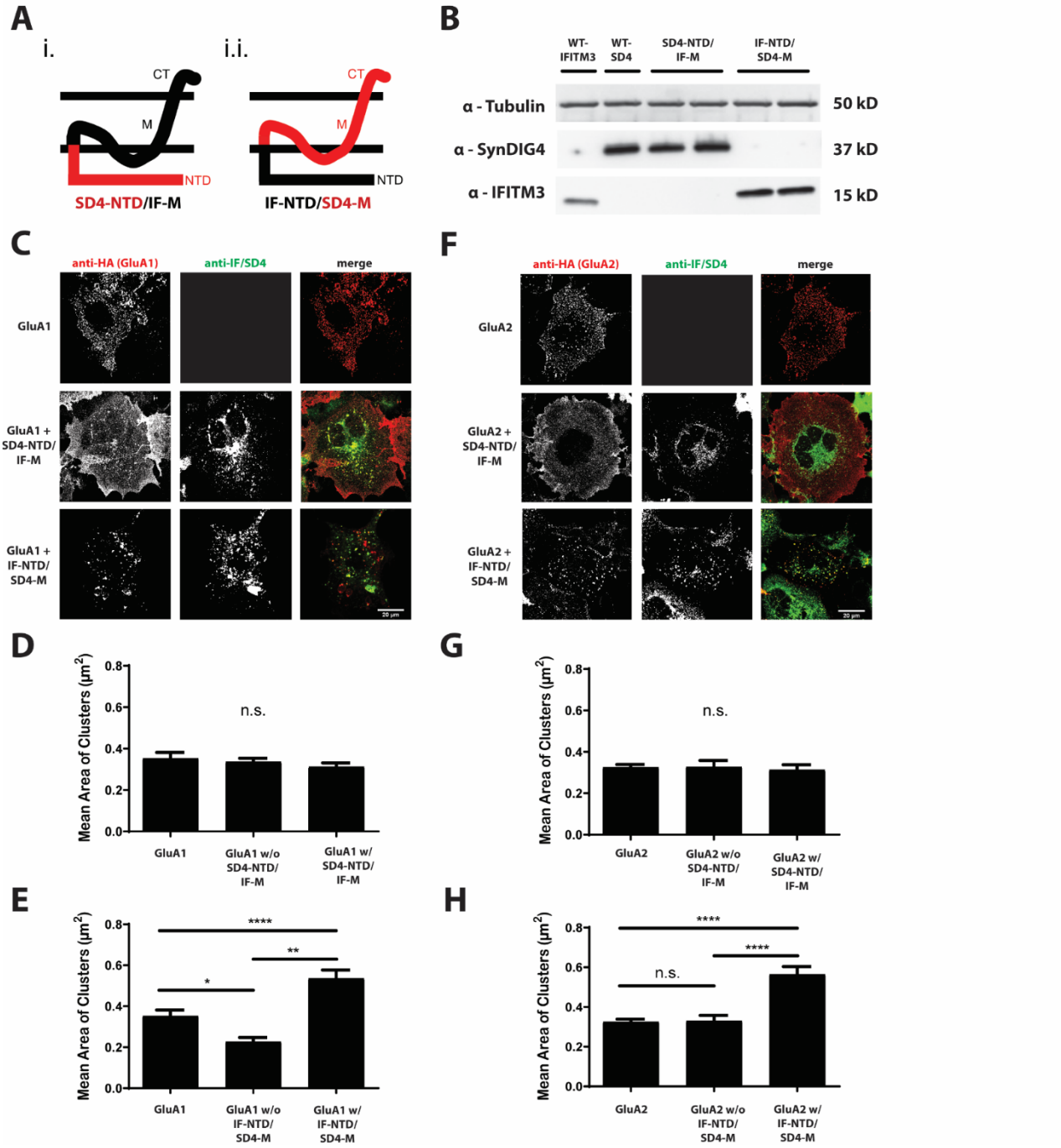
A
i.
i.i.
CT
M
NTD
SD4-NTD/IF-M
IF-NTD/SD4-M
B
WT-IFITM3
WT-SD4
SD4-NTD/IF-M
IF-NTD/SD4-M
α - Tubulin
α - SynDIG4
α - IFITM3
50 kD
37 kD
15 kD
C
anti-HA (GluA1)
anti-IF/SD4
merge
GluA1
GluA1 + SD4-NTD/IF-M
GluA1 + IF-NTD/SD4-M
F
anti-HA (GluA2)
anti-IF/SD4
merge
GluA2
GluA2 + SD4-NTD/IF-M
GluA2 + IF-NTD/SD4-M
D
Mean Area of Clusters (μm²)
n.s.
GluA1
GluA1 w/o SD4-NTD/IF-M
GluA1 w/ SD4-NTD/IF-M
G
n.s.
GluA2
GluA2 w/o SD4-NTD/IF-M
GluA2 w/ SD4-NTD/IF-M
E
****
**
*
GluA1
GluA1 w/o IF-NTD/SD4-M
GluA1 w/ IF-NTD/SD4-M
H
****
****
n.s.
GluA2
GluA2 w/o IF-NTD/SD4-M
GluA2 w/ IF-NTD/SD4-M

Figure 3. The N-terminus of GluA1 is dispensable for clustering with SD4.

(A) Immunoblot depicting expression of GluK2/GluA1 chimeras. Homologous domains of GluA1 were inserted into the backbone of GluK2 (See Table 2 of Methods). β-Tubulin was used as the loading control. **(B-F)** Representative confocal images of COS cells transfected with either a GluK2/A1 chimeric receptor alone, or co-transfected with SD4. Scale bar = 20 μm. **(G)** Graph depicts mean area of clusters when GluK2, GluA1, and each GluK2/A1 chimera is expressed either alone or co-expressed with SD4. **(H)** Graph depicts mean cluster size of M1-3, S2, M4, CT chimera stratified for either co-localized or not co-localized with SD4. M1-3, S2, M4 alone (n=11), M1-3, S2, M4 w/o SD4 (n=13), M1-3, S2, M4 w/ SD4 (n=13). Data are represented as mean +/- SEM; n.s. not significant; *$p<0.05$; ****$p<0.0001$; one-way ANOVA.

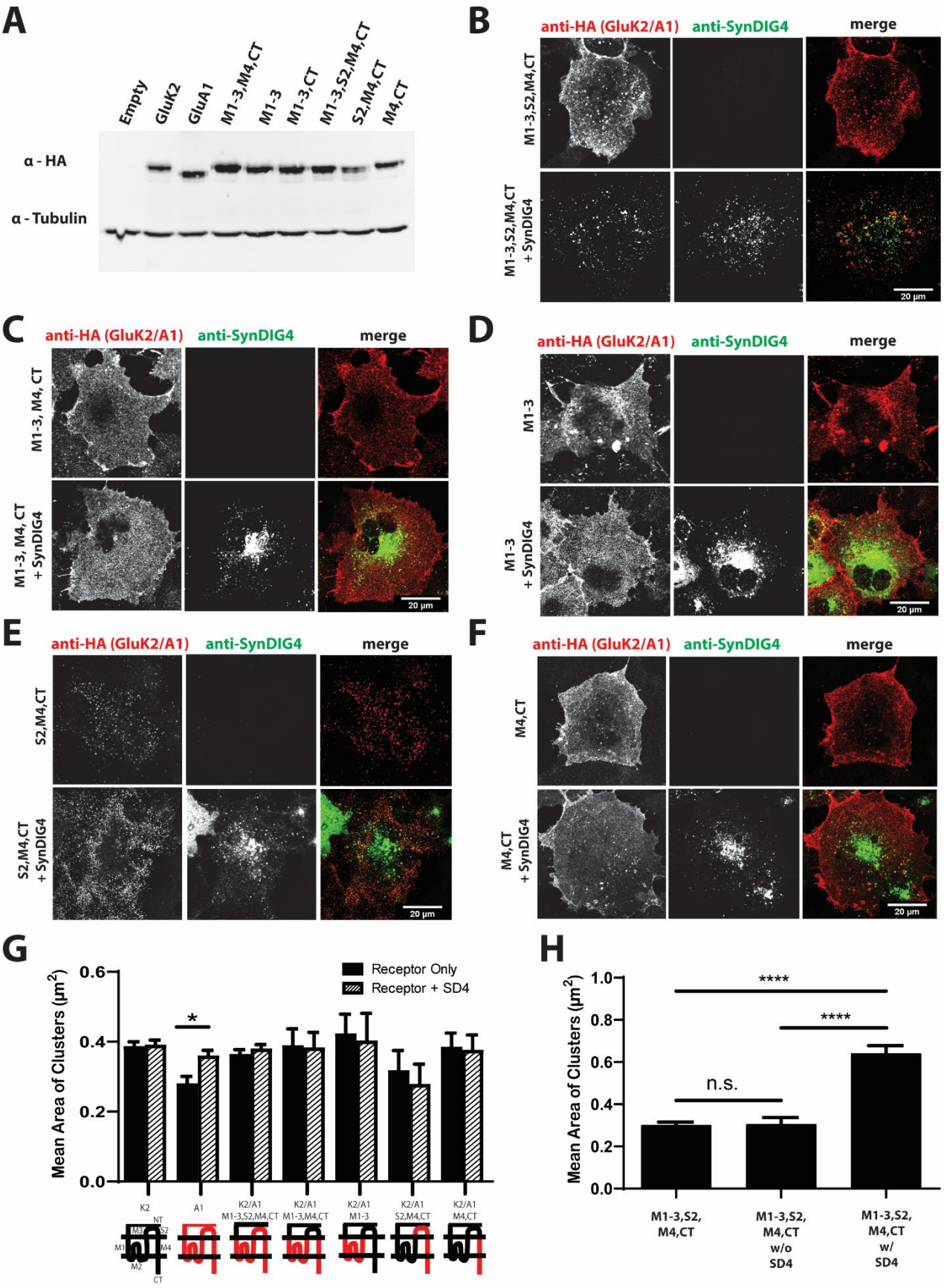
A
Empty
GluK2
GluA1
M1-3,M4,CT
M1-3
M1-3,CT
M1-3,S2,M4,CT
S2,M4,CT
M4,CT
α - HA
α - Tubulin
B
anti-HA (GluK2/A1)
anti-SynDIG4
merge
M1-3,S2,M4,CT
M1-3,S2,M4,CT + SynDIG4
20 μm
C
anti-HA (GluK2/A1)
anti-SynDIG4
merge
M1-3, M4, CT
M1-3, M4, CT + SynDIG4
20 μm
D
anti-HA (GluK2/A1)
anti-SynDIG4
merge
M1-3
M1-3 + SynDIG4
20 μm
E
anti-HA (GluK2/A1)
anti-SynDIG4
merge
S2,M4,CT
S2,M4,CT + SynDIG4
20 μm
F
anti-HA (GluK2/A1)
anti-SynDIG4
merge
M4,CT
M4,CT + SynDIG4
20 μm
G
Receptor Only
Receptor + SD4
Mean Area of Clusters (μm²)
0.6
0.4
0.2
0.0
*
K2
A1
K2/A1 M1-3,S2,M4,CT
K2/A1 M1-3,M4,CT
K2/A1 M1-3
K2/A1 S2,M4,CT
K2/A1 M4,CT
NT
M3
S2
M1
M4
M2
CT
H
Mean Area of Clusters (μm²)
1.0
0.8
0.6
0.4
0.2
0.0
****
****
n.s.
M1-3,S2, M4,CT
M1-3,S2, M4,CT w/o SD4
M1-3,S2, M4,CT w/ SD4

Figure 4. The N-terminus of GluA2 is dispensable for clustering with SD4.

(A) Immunoblot depicting expression of GluK2/GluA2 chimeras. Homologous domains of GluA2 were inserted into the backbone of GluK2 (See Table 3 of Methods). β-Tubulin was used as the loading control. **(B-D)** Representative confocal images of COS cells transfected with either a GluK2/A2 chimeric receptor alone, or co-transfected with SD4. Scale bar = 20 μm. **(E)** Graph depicts mean area of clusters when GluK2, GluA2, and each GluK2/A2 chimera is expressed either alone or co-expressed with SD4. **(F)** Graph depicts mean area of M1-3, S2, M4, CT chimera clusters stratified for either co-localized or non-colocalized with SD4. M1-3, S2, M4, CT alone (n=14), M1-3, S2, M4, CT w/o SD4 (n=11), M1-3, S2, M4, CT w/ SD4 (n=13). Data are represented as mean +/- SEM; n.s. not significant; **p<0.01; one-way ANOVA.

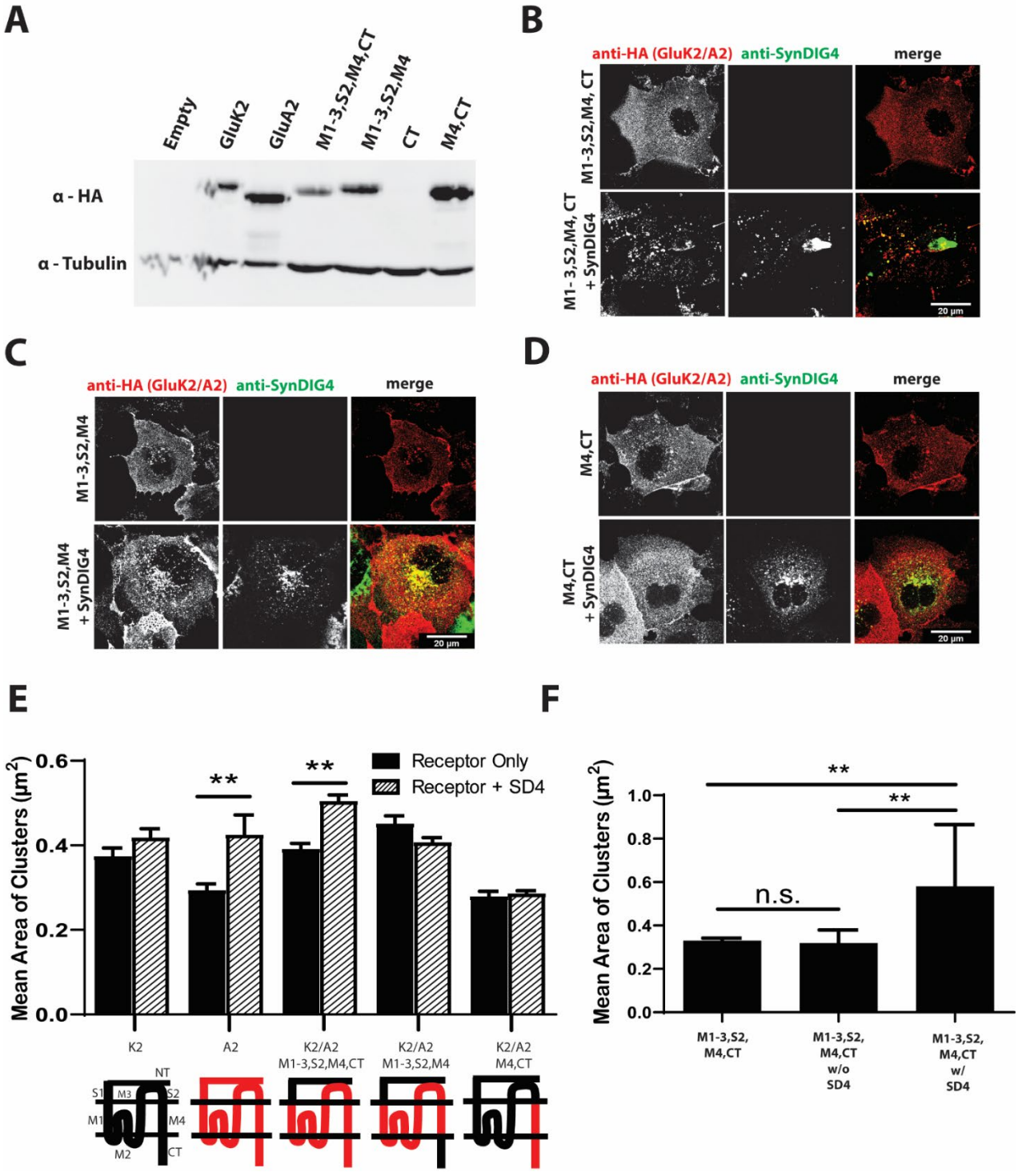
A
Empty
GluK2
GluA2
M1-3,S2,M4,CT
M1-3,S2,M4
CT
M4,CT
α - HA
α - Tubulin
B
anti-HA (GluK2/A2)
anti-SynDIG4
merge
M1-3,S2,M4, CT
M1-3,S2,M4, CT + SynDIG4
20 μm
C
anti-HA (GluK2/A2)
anti-SynDIG4
merge
M1-3,S2,M4
M1-3,S2,M4 + SynDIG4
20 μm
D
anti-HA (GluK2/A2)
anti-SynDIG4
merge
M4,CT
M4,CT + SynDIG4
20 μm
E
Mean Area of Clusters (μm²)
0.6
0.4
0.2
0.0
**
**
Receptor Only
Receptor + SD4
K2
A2
K2/A2 M1-3,S2,M4,CT
K2/A2 M1-3,S2,M4
K2/A2 M4,CT
NT
S1
M3
S2
M1
M4
M2
CT
F
Mean Area of Clusters (μm²)
1.0
0.8
0.6
0.4
0.2
0.0
**
**
n.s.
M1-3,S2, M4,CT
M1-3,S2, M4,CT w/o SD4
M1-3,S2, M4,CT w/ SD4

Figure 5. The M4 and C-terminus of GluA2 is sufficient for clustering with SD1.

(A) Representative confocal images of COS cells transfected with GluA2 alone, GluK2 alone, or co-transfected with GluA2 or GluK2 and SD1. Scale bar = 20 μm. **(B)** Representative confocal images of chimeras expressing the M1-3,S2,M4,CT and M4,CT domains of GluA2 either alone or co-expressed with SD1. Scale bar = 20 μm. **(C)** Graph depicts mean area of clusters when GluK2, GluA2, and each GluK2/A2 chimera is expressed either alone or co-expressed with SD1. **(D)** Graph depicts mean area of M4, CT chimera clusters stratified for either co-localized or non-colocalized with SD1. M4, CT alone (n=13), M4, CT w/o SD1 (n=13), M4, CT w/ SD1 (n=11). Data are represented as mean +/- SEM; n.s. not significant; *p<0.05; **p<0.01; ***p<0.001; ****p<0.0001; one-way ANOVA.

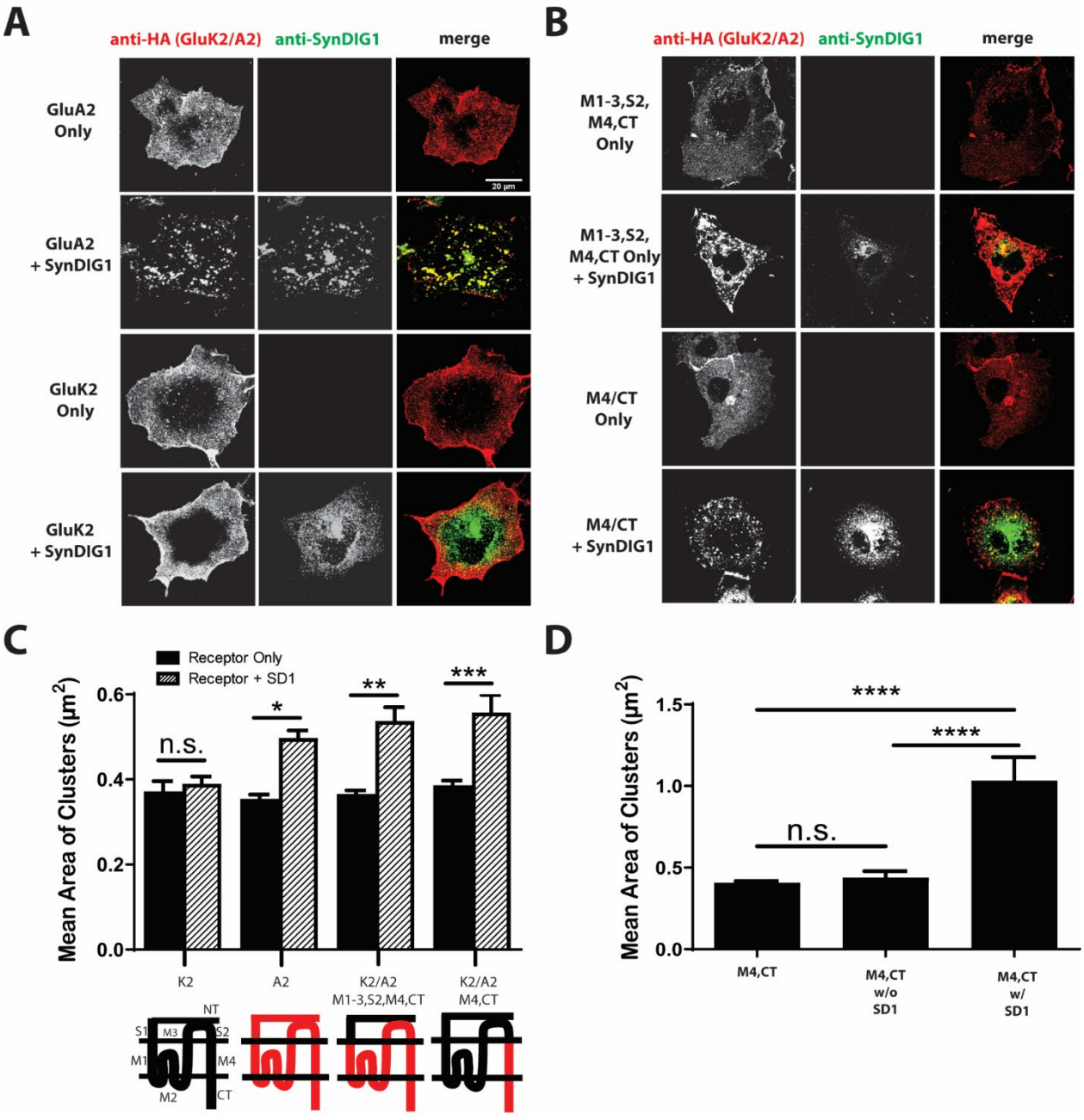
A
anti-HA (GluK2/A2)
anti-SynDIG1
merge
GluA2 Only
GluA2 + SynDIG1
GluK2 Only
GluK2 + SynDIG1
20 µm
B
anti-HA (GluK2/A2)
anti-SynDIG1
merge
M1-3,S2, M4,CT Only
M1-3,S2, M4,CT Only + SynDIG1
M4/CT Only
M4/CT + SynDIG1
C
Receptor Only
Receptor + SD1
Mean Area of Clusters (µm2)
0.6
0.4
0.2
0.0
n.s.
*
**
***
K2
A2
K2/A2 M1-3,S2,M4,CT
K2/A2 M4,CT
NT
S1
M3
S2
M1
M4
M2
CT
D
Mean Area of Clusters (µm2)
1.5
1.0
0.5
0.0
****
****
n.s.
M4,CT
M4,CT w/o SD1
M4,CT w/ SD1

Figure 6. SD4 cluster size increases when colocalized with GluA2.

(A) Representative confocal images of COS cells expressing SD4 alone, or SD4 co-expressed with either GluA1, GluA2 or GluK2. Scale bar = 20 μm. **(B-D)** Graph depicts mean area of SD4 clusters stratified for either co-localized or non-colocalized with GluA1 **(B)**, GluA2 **(C)** or GluK2 **(D)**. **(B)** SD4 alone (n=12), SD4 w/o A1 (n=10), SD4 w/ A1 (n=10). **(C)** SD4 alone (n=12), SD4 w/o A2 (n=10), SD4 w/ A2 (n=10). Data are represented as mean +/- SEM; n.s. not significant; *p<0.05; ****p<0.0001; one-way ANOVA.

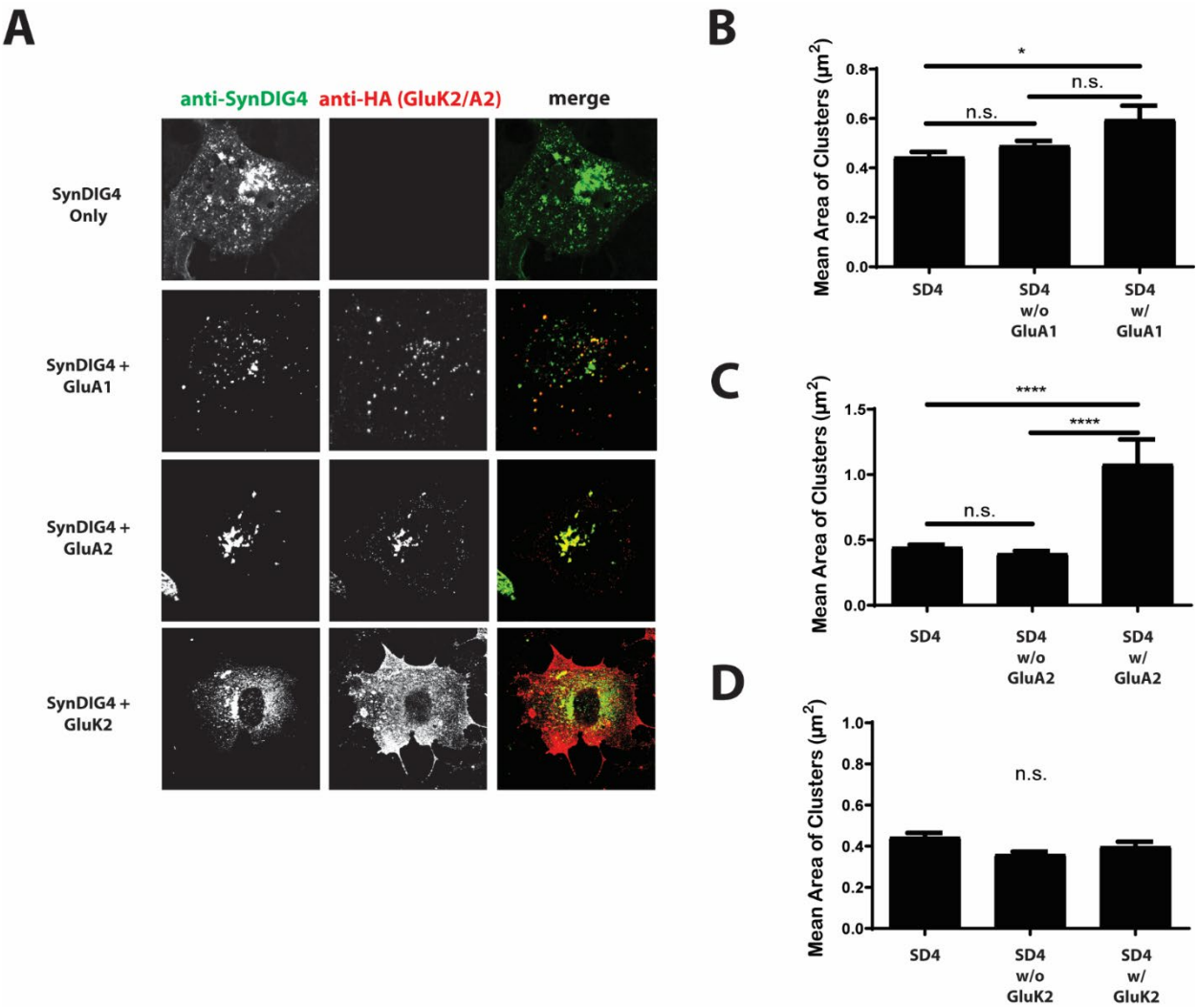
A
anti-SynDIG4
anti-HA (GluK2/A2)
merge
SynDIG4 Only
SynDIG4 + GluA1
SynDIG4 + GluA2
SynDIG4 + GluK2
B
Mean Area of Clusters (μm²)
0.0
0.2
0.4
0.6
0.8
*
n.s.
n.s.
SD4
SD4 w/o GluA1
SD4 w/ GluA1
C
Mean Area of Clusters (μm²)
0.0
0.5
1.0
1.5
****
****
n.s.
SD4
SD4 w/o GluA2
SD4 w/ GluA2
D
Mean Area of Clusters (μm²)
0.0
0.2
0.4
0.6
0.8
1.0
n.s.
SD4
SD4 w/o GluK2
SD4 w/ GluK2

Figure 7. SD4 clustering of GluA1 and GluA2 requires incubation at 37ºC.

(A) Representative confocal images of COS cells expressing either GluK2, GluA1, or GluA2 alone or co-expressed with SD4 after incubation at 4ºC. **(B)** Graph depicts mean area of receptor clusters. GluK2 alone (n=14), GluK2 + SD4 (n=12), GluA1 alone (n=10), GluA1 + SD4 (n=14), GluA2 alone (n=12), GluA2 + SD4 (n=13). **(C)** Representative confocal images of COS cells expressing either GluK2, GluA1, or GluA2 alone or co-expressed with SD4 after incubation at 37ºC. **(D)** Graph depicts mean area of receptor clusters. GluK2 alone (n=11), GluK2 + SD4 (n=16), GluA1 alone (n=10), GluA1 + SD4 (n=10), GluA2 alone (n=10), GluA2 + SD4 (n=10). Data are represented as mean +/- SEM; n.s. not significant; *$p<0.05$; one-way ANOVA.

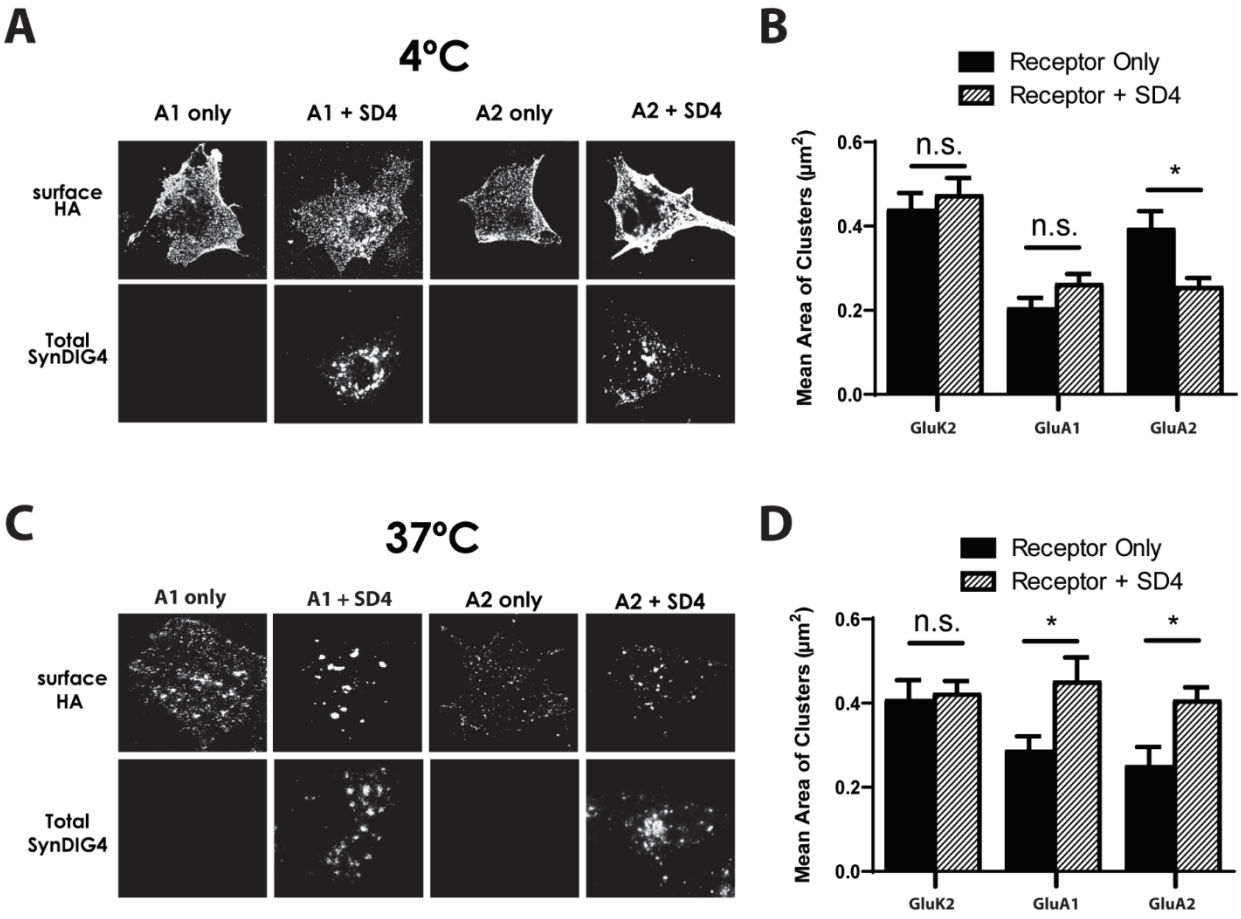
A
4°C
A1 only
A1 + SD4
A2 only
A2 + SD4
surface HA
Total SynDIG4
B
Receptor Only
Receptor + SD4
Mean Area of Clusters (μm²)
0.6
0.4
0.2
0.0
n.s.
n.s.
*
GluK2
GluA1
GluA2
C
37°C
A1 only
A1 + SD4
A2 only
A2 + SD4
surface HA
Total SynDIG4
D
Receptor Only
Receptor + SD4
Mean Area of Clusters (μm²)
0.6
0.4
0.2
0.0
n.s.
*
*
GluK2
GluA1
GluA2

Figure 8. Proposed mechanism for SD4 role in AMPAR clustering in heterologous cells.

SD4 is translated in the nucleus and transported through the secretory pathway where it is exocytosed to the surface of the plasma membrane. Here, SD4 binds and captures GluA1 and GluA2 AMPAR subunits. The SD4-GluA1/A2 complexes are then endocytosed to early endosomes where they are readily available. After stimulation, these readily available pools are exocytosed to the cell surface to increase the number of surface AMPARs which, in neurons, would then be trafficked to the synapse.

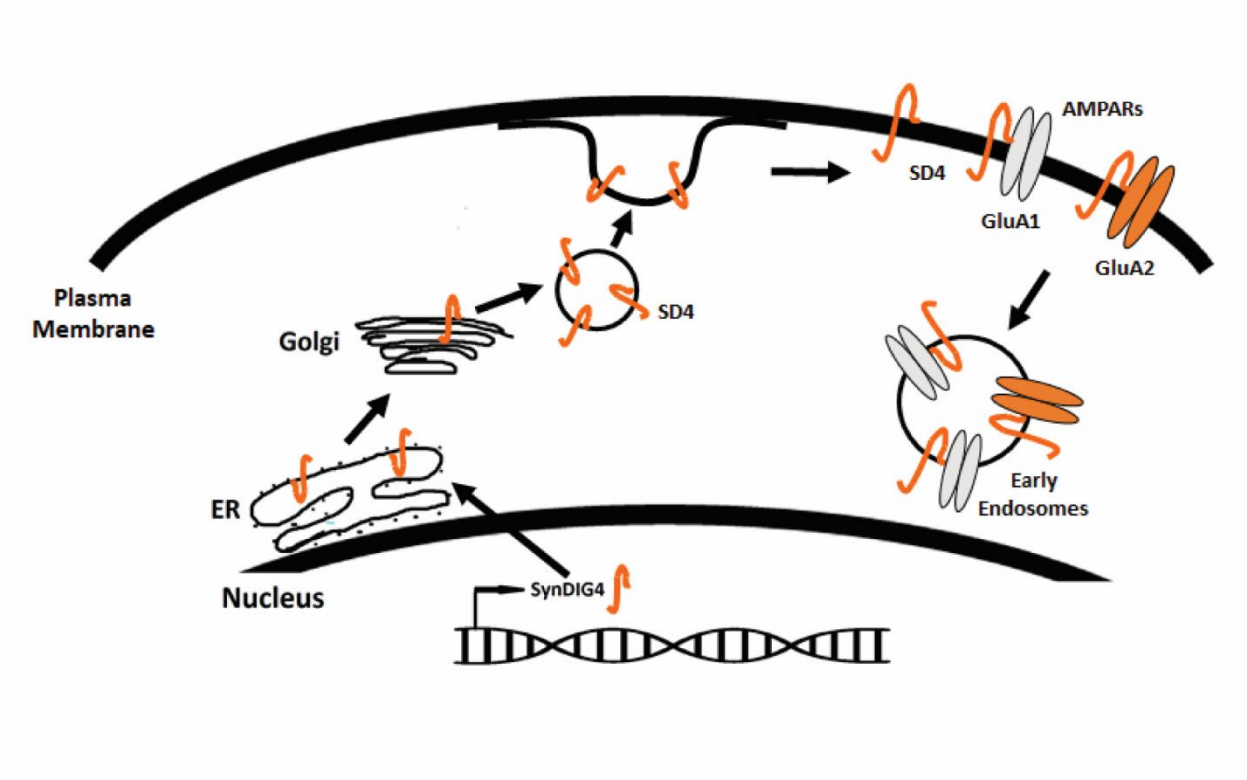
AMPARs
SD4
GluA1
GluA2
Plasma
Membrane
Golgi
SD4
Early
Endosomes
ER
Nucleus
SynDIG4

REFERENCES

1 McAllister, A. K. Dynamic aspects of CNS synapse formation. *Annual review of neuroscience* **30**, 425-450 (2007). https://doi.org:10.1146/annurev.neuro.29.051605.112830

2 Lissin, D. V. *et al.* Activity differentially regulates the surface expression of synaptic AMPA and NMDA glutamate receptors. *Proc Natl Acad Sci U S A* **95**, 7097-7102 (1998). https://doi.org:10.1073/pnas.95.12.7097

3 Scheiffele, P. Cell-cell signaling during synapse formation in the CNS. *Annual review of neuroscience* **26**, 485-508 (2003). https://doi.org:10.1146/annurev.neuro.26.043002.094940

4 Huganir, R. L. & Nicoll, R. A. AMPARs and synaptic plasticity: the last 25 years. *Neuron* **80**, 704-717 (2013). https://doi.org:10.1016/j.neuron.2013.10.025

5 Diaz, E. Regulation of AMPA receptors by transmembrane accessory proteins. *The European journal of neuroscience* **32**, 261-268 (2010). https://doi.org:10.1111/j.1460-9568.2010.07357.x

6 Jackson, A. C. & Nicoll, R. A. The expanding social network of ionotropic glutamate receptors: TARPs and other transmembrane auxiliary subunits. *Neuron* **70**, 178-199 (2011). https://doi.org:10.1016/j.neuron.2011.04.007

7 Jacobi, E. & von Engelhardt, J. Diversity in AMPA receptor complexes in the brain. *Curr Opin Neurobiol* **45**, 32-38 (2017). https://doi.org:10.1016/j.conb.2017.03.001

8 Chen, L. *et al.* Stargazin regulates synaptic targeting of AMPA receptors by two distinct mechanisms. *Nature* **408**, 936-943 (2000). https://doi.org:10.1038/35050030

9 Tomita, S. *et al.* Functional studies and distribution define a family of transmembrane AMPA receptor regulatory proteins. *J Cell Biol* **161**, 805-816 (2003). https://doi.org:10.1083/jcb.200212116

10 Tomita, S. *et al.* Stargazin modulates AMPA receptor gating and trafficking by distinct domains. *Nature* **435**, 1052-1058 (2005). https://doi.org:10.1038/nature03624

11 Ben-Yaacov, A. *et al.* Molecular Mechanism of AMPA Receptor Modulation by TARP/Stargazin. *Neuron* **93**, 1126-1137 e1124 (2017). https://doi.org:10.1016/j.neuron.2017.01.032

12 Schwenk, J. *et al.* Functional proteomics identify cornichon proteins as auxiliary subunits of AMPA receptors. *Science* **323** (2009).

13 von Engelhardt, J. *et al.* CKAMP44: a brain-specific protein attenuating short-term synaptic plasticity in the dentate gyrus. *Science* **327**, 1518-1522 (2010). https://doi.org:10.1126/science.1184178

14 Kalashnikova, E. *et al.* SynDIG1: An activity-regulated, AMPAR-receptor-interacting transmembrane protein that regulates excitatory synapse development. *Neuron* **65** (2010).

15 Lovero, K. L., Blankenship, S. M., Shi, Y. & Nicoll, R. A. SynDIG1 promotes excitatory synaptogenesis independent of AMPA receptor trafficking and biophysical regulation. *PLoS One* **8**, e66171 (2013). https://doi.org:10.1371/journal.pone.0066171

16 Schwenk, J. *et al.* High-resolution proteomics unravel architecture and molecular diversity of native AMPA receptor complexes. *Neuron* **74**, 621-633 (2012). https://doi.org:10.1016/j.neuron.2012.03.034

17 Shanks, N. F. *et al.* Differences in AMPA and kainate receptor interactomes facilitate identification of AMPA receptor auxiliary subunit GSG1L. *Cell Rep* **1**, 590-598 (2012). https://doi.org:10.1016/j.celrep.2012.05.004

18 Kirk, L. M. *et al.* Distribution of the SynDIG4/proline-rich transmembrane protein 1 in rat brain. *J Comp Neurol* **524**, 2266-2280 (2016). https://doi.org:10.1002/cne.23945

19 Matt, L. *et al.* SynDIG4/Prrt1 is required for excitatory synapse development and plasticity underlying cognitive function. *Cell Reports* **22** (2018).

20 Yu, J. *et al.* Hippocampal AMPA receptor assemblies and mechanism of allosteric inhibition. *Nature* **594**, 448-453 (2021). https://doi.org:10.1038/s41586-021-03540-0

21 Almen, M. S., Bringeland, N., Fredriksson, R. & Schioth, H. B. The Dispanins: A Novel Gene Family of Ancient Origin That Contains 14 Human Members. *PLOS One* **7** (2012).

22 Yount, J. S. *et al.* Palmitoylome profiling reveals S-palmitoylation-dependent antiviral activity of IFITM3. *Nat Chem Biol* **6**, 610-614 (2010). https://doi.org:10.1038/nchembio.405

23 Ling, S. *et al.* Combined approaches of EPR and NMR illustrate only one transmembrane helix in the human IFITM3. *Sci Rep* **6**, 24029 (2016). https://doi.org:10.1038/srep24029

24 Martin, E. E., Wleklinski, E., Hoang, H. T. M. & Ahmad, M. Interaction and Subcellular Association of PRRT1/SynDIG4 With AMPA Receptors. *Front Synaptic Neurosci* **13**, 705664 (2021). https://doi.org:10.3389/fnsyn.2021.705664

25 Kay, B. K., Williamson, M. P. & Sudol, M. The importance of being proline: the interaction of proline-rich motifs in signaling proteins with their cognate domains. *Faseb J* **14** (2000).

26 Freund, C., Schmalz, H. G., Sticht, J. & Kuhne, R. Proline-rich sequence recognition domains (PRD): ligands, function and inhibition. *Handb Exp Pharmacol*, 407-429 (2008). https://doi.org:10.1007/978-3-540-72843-6_17

27 Twomey, E. C., Yelshanskaya, M. V., Grassucci, R. A., Frank, J. & Sobolevsky, A. I. Elucidation of AMPA receptor-stargazin complexes by cryo-electron microscopy. *Science* **353**, 83-86 (2016). https://doi.org:10.1126/science.aaf8411

28 Zhao, Y., Chen, S., Yoshioka, C., Baconguis, I. & Gouaux, E. Architecture of fully occupied GluA2 AMPA receptor-TARP complex elucidated by cryo-EM. *Nature* **536**, 108-111 (2016). https://doi.org:10.1038/nature18961

29 Zhang, D., Watson, J. F., Matthews, P. M., Cais, O. & Greger, I. H. Gating and modulation of a hetero-octameric AMPA glutamate receptor. *Nature* **594**, 454-458 (2021). https://doi.org:10.1038/s41586-021-03613-0

30 Babaei, P. NMDA and AMPA receptors dysregulation in Alzheimer's disease. *Eur J Pharmacol* **908**, 174310 (2021). https://doi.org:10.1016/j.ejphar.2021.174310

31 Ge, Y. & Wang, Y. T. GluA1-homomeric AMPA receptor in synaptic plasticity and neurological diseases. *Neuropharmacology* **197**, 108708 (2021). https://doi.org:10.1016/j.neuropharm.2021.108708

32 Kadriu, B. *et al.* Positive AMPA receptor modulation in the treatment of neuropsychiatric disorders: A long and winding road. *Drug Discov Today* **26**, 2816-2838 (2021). https://doi.org:10.1016/j.drudis.2021.07.027

Chapter 3

Surface trafficking and synaptic targeting of GluA1-containing AMPARs is impaired in SynDIG4/PRRT1-knockout hippocampal neurons

Preface:

This chapter represents preliminary data and results that will be included in a future manuscript. All experiments are planned to be replicated by Chun-Wei (Jay) He and will contribute to this manuscript, as well as his future dissertation. In this chapter, I performed all cultures of hippocampal neurons and immunochemistry experiments, as well as data analysis. Hector H. Navarro and Alma Peraza were instrumental in blinding confocal images and performing data analysis.

ABSTRACT

LTP is abolished by single tetanus stimulation of hippocampal slices from SD4-KO animals. We used WT and SD4-KO mice to study SD4 regulation of GluA1-containing AMPARs in hippocampal neurons. We observed a significant increase in co-localization of SD4 with GluA1 after glycine induced LTP. The mean size of GluA1 puncta was significantly increased when stratified, indicating that co-localization with SD4 increases synaptic GluA1 cluster size during LTP. We used WT and SD4 KO mice to study SD4 regulation of GluA1-containing AMPARs in hippocampal neurons. To study GluA1-containing AMPARs during LTP, we used glycine induced chemical LTP on WT and KO neurons. After chemical LTP, WT neurons show a 2-fold increase in synaptic GluA1, while synaptic GluA1 is unchanged in SD4-KO neurons. We rescued this impairment by transfecting KO neurons with WT SD4 to restore the reserve pool of extra-synaptic GluA1, suggesting the effect is a direct result of the loss of SD4. Lastly, we observed a 50% increase in synaptic SD4 density, indicating synaptic targeting of SD4 to synapses during LTP. Given that LTP requires a reserve pool of AMPARs[1], these data are consistent with a model whereby SD4 establishes an extra-synaptic reserve pool of GluA1-containing AMPARs required for LTP.

INTRODUCTION

From birth, our brains begin to grow and form new connections as a result of the innate ability of the central nervous system to adapt and grow in response to stimuli[2-5]. For decades neuroscientists have been studying the mechanisms by which the brain is able to change and adapt in response to experience, a process known as experience-dependent plasticity. Therefore, neuronal plasticity is a crucial aspect of brain function. Furthermore, understanding exactly how plasticity within the brain is carried out may be important for treatment of pathological conditions such as Epilepsy and Alzheimer's disease, where abnormalities in neuronal plasticity have been observed[6]. Characterizing the mechanisms by which neuronal plasticity is regulated will be important for the development of future therapies for such diseases.

Specifically, neuronal communication is carried out through electrochemical signals transmitted through projections from the cell body, called the axon terminals[7]. These axon terminals form connections, or synapses, with the dendrites of other neurons to transfer information. The ability of mature neurons to form synapses remains the traditional method by which neurons are able to communicate within the brain[7]. Furthermore, the number of dendritic spines on the branches of dendrites, which limit the number of synapses that may form, has been directly correlated with cognitive function[8,9]. Specifically, the hippocampus, one of the brain regions identified as a prominent regulator of cognitive functions, has been widely implicated as the main site of learning and memory in both mice and humans[10,11]. Importantly, the ability of the hippocampus to change over time has been regarded as a key characteristic underlying cognitive function, including memory formation[11-13]. Previous studies have shown that changes in synaptic

plasticity are directly correlated with changes in dendritic spine number/density[14]. Therefore, the formation and elimination of individual dendritic spines further underlies synaptic plasticity within the brain.

As the hippocampus is one of the most dynamic regions within the brain, hippocampal neurons were an attractive model for studying spine plasticity and morphogenesis[15,16]. Glutamate receptors predominantly regulate the synaptic communication of excitatory neurons in the brain[35,36]. During synaptic transmission, pre-synaptic axon terminals responsible for export of signaling molecules pair with post-synaptic dendritic spines[17-21]. The pre-synaptic bouton contains hundreds of synaptic vesicles (SVs), which dock at the plasma membrane prior to synaptic activity[17,21,22]. These SVs then fuse with the membrane, allowing the export of cell signaling molecules, such as glutamate, across the synapse. Dendritic spines are densely populated with proteins that include glutamate receptors and ion channels which allow for the binding of molecules during synaptic transmission[18,21,23]. Therefore, signals received from pre-synaptic neurons trigger signaling cascades which dictate neuronal activity.

The goal of this study is to further establish a role of SD4 in regulating GluA1-containing AMPARs in primary hippocampal neurons. We hypothesize that SD4 and surface GluA1 are primarily localized at extra-synaptic sites, while the loss of SD4 results in altered localization and trafficking. Furthermore, we predict a role of SD4 in synaptic trafficking of GluA1. This study indicates that both surface and synaptic trafficking of GluA1 is impaired in SD4-KO neurons at baseline and during glycine induced LTP. Therefore, our results further establish a mechanism for the role of SD4 in regulating hippocampal surface GluA1.

MATERIALS/METHODS

Animals

C57BL/6 mice were bred in house and maintained in the animal facility at UC Davis. Additional Sprawg Dawley rats were obtained from ENVIGO. The use and maintenance of animals were carried out according to the guidelines set forth by UC Davis, the NIH, and AALAC.

Antibodies

The following antibodies were used: mouse IgG2a anti-SynDIG4 [NeuroMab; Cat# 73-409; RRID: AB_2491106; Immunocytochemistry (ICC) 1:200; Immunoblotting (IB) 1:2000]; rat anti-hemagglutinin (HA) (Roche; ICC 1:50; IB 1:1000); Guinea pig anti-vGlut1 (ICC 1:500); Alexa 488-conjugated anti-mouse IgG2a (Molecular Probes; ICC 1:200); Alexa 594-conjugated anti-rat (Jackson ImmunoResearch; ICC 1:200); and Alexa 649-conjugated anti-guinea pig (Jackson ImmunoResearch: ICC 1:500).

Constructs

Full length version of rat SD4 coding sequence was amplified by PCR from pHM6 expression vector[24] and subcloned into pRK5 vector backbone provided by our collaborator Yael Stern-Bach at the Hebrew University of Jerusalem. For surface labeling of SD4, a double tagged FLAG-SD4-HA construct was generated by sequential PCR amplification using megaprimers.

Cell culture

Hippocampal cultures were generated from either P0-P2 mice, or E18 rat embryos. All cultures used the Banker protocol, requiring the culture of an astrocyte feeder layer isolated from rat cortex and grown to 70 – 90% confluency before dissection in astrocyte plating medium (APM) containing 1X MEM, 10% donor horse serum, 0.6% glucose, and 5 mL pen/strep. Prior to dissection, coverslips were etched with 1 M nitric acid and sterilized. Coverslips were then coated with 1 mg/mL poly-L-lysine (PLL) diluted in distilled water and incubated overnight at 37ºC. After incubation, coverslips were washed 3 times with distilled water. Dissection and plating of hippocampal neurons was carried out as previously described. Neurons were first cultured in Neuronal Plating Media (NPM) containing 1X MEM, 10% donor horse serum, 0.45% glucose, 5 mL sodium pyruvate, and 5 mL pen/strep. Astrocyte media is changed during plating using neuronal maintenance media (NMM) containing 1X neurobasal, 10 mL Glutamax, 5 mL sodium pyruvate, and 5 mL pen/strep. After 6 hours neurons are transferred to astrocyte feeder layer. After 4 days the anti-mitotic AraC was added at a final concentration of 5 μM. A half volume change of the NMM was performed every 5 days. Neurons were fixed and stained at DIV 12 – 14 depending on confluency and maturity.

Immunocytochemistry

For primary hippocampal neurons, we surface labeled GluA1 to establish surface localization. For surface labeling of GluA1, neurons were fixed with 4% PFA for 5 minutes at

room temperature. Neurons were then washed 3 times with PBS and stained with anti-GluA1 primary antibody diluted in PBS with 3% BSA for 1.5 hours. Cells were washed with PBS shaking for 5 minutes each and then permeabilized with 0.1% triton for 15 minutes. Neurons were blocked with 10% BSA for 30 minutes. Neurons were then stained for total anti-SynDIG4 and total anti-vGlut1 overnight in 3% BSA at 4ºC. After incubation, coverslips were washed 3 times with PBS and incubated in secondary antibodies for each marker for 1 hour at room temperature. Neurons were then washed 3 times with PBS and mounted on glass coverslips for imaging.

Chemical LTP Induction

Primary hippocampal neurons were cultured to DIV 12 – 14. Neurons were equilibrated in artificial cerebrospinal fluid (aCSF) containing 2 mM magnesium (Mg^{+2}) and 2 mM Calcium (Ca^{+2}) at 37ºC in incubator for 30 minutes. Neurons were washed with PBS and replaced with aCSF containing the treatment buffer, or a DMSO mock treatment control buffer. The aCSF treatment buffer contains 2 mM Ca^{+2}, 200 µM Glycine, 20 µM Bicuculine, and 3 µM Strychnine. Strychnine was diluted in DMSO for storage, so the equivalent volume as added to the control treatment. Glycine and bicuculine were diluted in water, so an additional equivalent volume was also added to the control. Neurons were incubated at 37ºC for 5 minutes for chemical-LTP induction. Coverslips were then transferred to a recovery buffer (aCSF w/ Mg^{+2}; No Drugs) for 20 mins at 37ºC. Coverslips were fixed at 4% for 5 minutes at room temperature prior to surface labeling.

Image Analysis

For quantitative analyses, images were taken using either an Olympus FluoView 1000 or Zeiss LSM510 confocal microscope with a 63x/1.5 NA oil objective with identical settings for laser power, photomultiplier gain, and digital offset. Pinhole (1 AU) and resolution (1024 x 1024 pixels) were constant for all images.

Images were imported into image analysis software (ImageJ) to determine average size of clusters for each condition. Selected cells were cropped from the original pictures and saved, blinded, and subjected to the analysis by an individual not involved in the cell selection and blinding process. The threshold for each independent experiment is determined by averaging the thresholds of at least 25% of images. The average threshold was then applied to all images for analysis. Only clusters within the range of 0.1 – 3.5 μm^2 were measured. After data collection and the unblinding process, the puncta size of all signals was subjected to statistical analysis. For analysis of puncta size based on co-localization with SD4 (stratification analysis), co-localization was defined as overlap of ≥1 pixel. For figure preparation, signals were adjusted for all panels within a figure by using equal linear adjustments of levels in Photoshop (Adobe Systems).

Statistical analyses

Data were collected from at least two independent experiments and a minimum n=10-15 cells per condition per experiment. All graphs and statistical analyses were generated using GraphPad Prism software. Graphs depict the data average and the standard error of the mean (SEM). Statistical

significance was assessed by either unpaired student's t-test or one-way ANOVA. Significance is defined as *$p<0.05$; **$p<0.01$; ***$p<0.001$; ****$p<0.0001$.

RESULTS

A minority of overexpressed SD4 is present on the surface of transfected hippocampal neurons.

To characterize SD4 in neurons, we first cultured WT hippocampal neurons from E16 rat embryos. Hippocampal neurons were cultured to DIV14 and fixed with 4% PFA. As a control, we first labeled hippocampal neurons for surface and total GluA1-containing AMPARs **(Figure 1A)**. Normalized to total, we observed that only about 56% of GluA1 is expressed on the surface of hippocampal neurons when normalized to control. This is consistent with previous results and indicates that our surface labeling protocol was successful. To label surface SD4, we utilized a double tagged FLAG-SD4-HA construct. This construct allows us to label both total and surface SD4, while separating transfected SD4 from endogenous SD4. Immunoblot from COS cell lysates indicate successful expression of both the FLAG and HA tags **(Figure 1C)**. Hippocampal neurons were transfected using calcium phosphate and labeled for total transfected SD4 (anti-FLAG), surface SD4 (anti-HA), and surface GluA1 (anti-GluA1) **(Figure 1D)**. Quantification of the ratio of surface to total SD4 indicates that only about 35% of SD4 is expressed at the surface **(Figure 1E)**. Additionally, we found a trend towards an increase in co-localization of surface GluA1 with surface SD4 compared to co-localization of surface GluA1 with total SD4, however this difference was non-significant **(Figure 1F)**. We conclude that only a small percentage of SD4 is expressed at the surface of WT hippocampal neurons at any given time.

Co-localization of SD4 with surface GluA1 is increased after chemical-LTP.

To test the role of SD4-dependent AMPAR clustering in synaptic plasticity, we utilized primary culture of dissociated rat hippocampal neurons. Neurons were treated with either vehicle (DMSO) or 200 μM glycine in aCSF without magnesium at 37ºC for 10 minutes to induce chemical-LTP. Neurons were then transferred to aCSF recovery buffer for 20 minutes and then live-labeled for surface expressing GluA1-containing AMPARs at 37ºC for 1 hour. Neurons were then fixed, permeabilized, and stained for total SD4, surface GluA1 (sGluA1), and vGlut1 **(Figure 2A)**. The number of sGluA1 puncta per cell increased by 50% after glycine treatment compared to vehicle (vehicle: 907+/-121, n = 12; glycine: 1362+/-142, n = 10; *p*-value = 0.0043), indicating successful chemical-LTP induction. We observed a significant increase in the co-localization of SD4 with sGluA1 after glycine induced LTP **(Figure 2B)**. Additionally, we saw a significant increase of SD4 co-localized with the pre-synaptic marker vGlut1, as well as an increase in co-localization of all three markers after chemical-LTP **(Figure 2B)**. This result indicates that at least a percentage of SD4 redistributes to the synapse during glycine induced chemical-LTP.

Next, we looked at changes in the mean area of GluA1 clusters as a result of chemical-LTP. We stratified these data to determine whether changes in the size of these clusters are dependent on co-localization with SD4. We observed that there was no change in the mean area of GluA1 clusters not colocalized with SD4 after treatment with glycine compared with vehicle **(Figure 2C).** Interestingly, there was a significant increase in the size of GluA1 clusters during vehicle treatment only when GluA1 was co-localized with SD4. Furthermore, we observed a significant increase in the mean area of GluA1 clusters co-localized with SD4 after glycine induced

chemical-LTP **(Figure 2C)**. As a result of these experiments, we conclude that co-localization of SD4 with sGluA1 increases after chemical-LTP, and this co-localization results in an increase in the mean area of GluA1 clusters.

Surface GluA1 distribution is altered in SD4-KO neurons.

To test the necessity of SD4 for the distribution of sGluA1, we cultured hippocampal neurons from either WT or SD4-KO mice. Hippocampal cultures were labeled for total SD4, sGluA1, and vGlut1 **(Figure 3A)**. We observed an increase in the synaptic density of sGluA1 in SD4-KO neurons as well as an increase in the extra-synaptic density of sGluA1 **(Figure 3B)**. These changes in density of sGluA1 were non-significant, however there is a clear trend indicating a difference between WT and KO animals. Further experiments and an increase in the number of neurons for analysis will be necessary to determine significance. Additionally, we looked at the sGluA1 puncta area and observed a significant decrease in extra-synaptic sGluA1, but no significant difference in synaptic sGluA1 in SD4-KO neurons **(Figure 3C)**. Lastly, analysis of the sGluA1 puncta integrated density shows no significant change in synaptic or extra-synaptic sGluA1 integrated density in SD4-KO neurons **(Figure 3D)**.

Proposed mechanism for SD4 role in AMPAR trafficking during LTP.

In wildtype hippocampal neurons, SD4 preferentially co-localizes with GluA1-containing AMPARs at extra-synaptic sites **(Figure 4)**. During LTP, the total number of SD4 does not change,

while surface GluA1 is increased. Additionally, the number of synaptic SD4 and GluA1 puncta are increased, indicating that at least a small number of SD4 puncta traffic to the synapse with GluA1 during LTP. In SD4-KO neurons, the number of baseline extra-synaptic surface GluA1 puncta is significantly increased at non-synaptic localizations. After LTP, the synaptic trafficking of surface GluA1-containing AMPARs is impaired, which may impact the synaptic targeting of GluA1. Therefore, we conclude that SD4 is important for maintaining extra-synaptic surface GluA1-containing AMPARs, while the absence of SD4 results in an increased extra-synaptic pool at baseline, but decreased synaptic trafficking of GluA1 necessary for LTP.

DISCUSSION

From these experiments, we observed an increased cluster size of GluA1 that overlaps with SD4 in primary hippocampal neurons upon chemical-LTP, suggesting that this clustering activity is a mechanism underlying strengthening of synapses during synaptic plasticity. It is important to note that our experiments utilize stratified data, therefore, we are able to identify SD4 co-localized with surface GluA1 at extra-synaptic and synaptic localizations. As most studies look at total surface GluA1, we can separate total surface GluA1 into these sub-categories to get a better picture of differences in co-localization of SD4 and surface GluA1 at baseline and after LTP. We propose that SD4 establishes a reserve pool of extra-synaptic surface AMPARs through bidirectional clustering of SD4 and AMPARs necessary for synaptic potentiation.

A recent study demonstrated overlap of SD4 with early endosomes in hippocampal neurons[25], consistent with its role in clustering AMPARs that have been internalized. Interestingly, our data show that cluster size of GluA1 that overlaps with SD4 is also increased, but only at extra-synaptic sites at both baseline and in primary hippocampal neurons upon chemical-LTP. After considering the importance of endocytosis for sGluA1-SD4 co-localization, our current model states that SD4-induced clustering of AMPARs occurs intracellularly after endocytosis to establish a reserve pool of intracellular extra-synaptic AMPARs. The number of extra-synaptic receptors available for synaptic trafficking must be carefully regulated, which may be the cause of the increase in number of sGluA1 receptors at extra-synaptic pools. sGluA1 can then be deployed to the synapse during LTP. However, in SD4-KO hippocampal neurons show deficits in synaptic trafficking during LTP, even though the number of available extra-synaptic sGluA1 has increased.

Therefore, we conclude that SD4 regulates the number of available sGluA1 at extra-synaptic pools, and that a loss of SD4 results in impaired synaptic trafficking of these receptors.

In addition, others have shown that SD4-KO mice are deficient for LTD[26]; thus, the intracellular clustering of AMPARs could also be employed during LTD as a mechanism to restrict the surface accumulation of AMPARs perhaps upon differential regulation. Additional experiments beyond the scope of this study are needed to investigate the effects of SD4 on AMPAR trafficking in neurons during synaptic plasticity.

Our results demonstrate the effects of SD4 on clustering both GluA1 and GluA2 in heterologous cells. Although SD4 induces clustering of GluA1- and GluA2-AMPARs in heterologous COS cells, in SD4-KO neurons we observed a significant reduction in both extra-synaptic GluA1 and extra-synaptic GluA12 puncta density[27,28]. As GluA1/2 heteromers constitute 95% of AMPARs at an extra-synaptic AMPAR pool under baseline conditions[29]. This may suggest that SD4 is required to regulate an extra-synaptic pool of GluA1 and GluA2, while an absence of SD4 leads to a build-up of surface extra-synaptic AMPARs. Certain effects of SD4 were specific for GluA1. For example, puncta size and intensity of both extra-synaptic and synaptic GluA1 (but not GluA2) were slightly reduced in SD4 KO neurons[27], indicating an additional role for SD4 in regulating GluA1. These results fit our proposed model where in SD4-KO neurons, the loss of SD4 leads to an increase in extra-synaptic surface GluA1 and an overall decrease in trafficking and number of synaptic GluA1 receptors.

GluA1 homomers account for most, if not all, calcium-permeable AMPARs (CP-AMPARs) in the hippocampus, which are largely absent at PSDs under basal conditions; however, under certain conditions, CP-AMPARs become transiently detectable at postsynaptic sites

including the induction of LTP[30] and LTD[31]. Thus, it is tempting to speculate that SD4 might establish reserve pools of GluA1 homomers that are transiently targeted to synapses during synaptic plasticity.

Previous studies have shown a decrease in surface GluA1 and GluA2 after a loss of other auxiliary factors[1,32]. Interestingly, in SD4-KO neurons, we observed a significant increase in surface AMPARS at extra-synaptic sites which leads to decreases in synaptic GluA1 and deficits in LTP[1,33]. From this study, we observed a significant increase in extra-synaptic pools of GluA1-containing AMPARs in SD4-KO animals. Furthermore, there is a decrease in synaptic GluA1, a decrease in co-localization of SD4 and GluA1, and inhibition of LTP[33]. Again, it is important to note that these previous studies look at total surface GluA1, while our data is stratified into synaptic and extra-synaptic puncta. One potential caveat of these experiments could be that since synaptic GluA1 is decreased, the effects on LTP could just be effects of a lack of GluA1 to begin with. Additional experiments using an acute KD of SD4 may be necessary to investigate this possibility. Furthermore, the study by Granger et al. showed the importance of the extra-synaptic pool of AMPARS[1]. They observed that if you knockout all hippocampal AMPARs and replace them with Kainate receptors, LTP is rescued. Therefore, the type of receptor is not necessarily important, but the mechanisms or auxiliary factors (i.e. SD4) by which these extra-synaptic and synaptic receptors are regulated, maintained, and trafficked is crucial. These results fit with my observations whereby SD4-KO results in a build-up and increased number of surface GluA1 at extra-synaptic pools[28]. Lastly, previous studies have shown that SD4 has a direct effect on the gating properties of GluA1 when co-expressed in *Xenopus* oocytes, indicating a direct

interaction[28,34]. However, it is still possible that there may be a tertiary binding partner in neuronal systems. In addition to my results, these data provide strong evidence that SD4 functions as a true auxiliary factor which modulates both the trafficking and biophysical properties of GluA1- and GluA2-containing AMPARs.

Figure 1. A minority of overexpressed SD4 is present on the surface of transfected hippocampal neurons.

(A) Representative confocal images of WT rat hippocampal neurons and selected dendritic stretches DIV14. **(B)** Quantification of surface GluA1 puncta normalized to total GluA1 punctate represents the relative number of GluA1 puncta expressed on the surface of hippocampal dendrites. **(C)** Representative immunoblot shows expression of the double tagged FLAG-SD4-HA construct and specificity of the FLAG and HA antibodies. **(D)** Representative confocal images of WT rat hippocampal neurons transfected with a double tagged FLAG-SD4-HA construct. Neurons were stained for anti-FLAG (total SD4), anti-HA (surface SD4), and anti-GluA1 (total GluA1). **(E)** Quantification of the number of surface SD4 puncta normalized to total SD4 puncta. **(F)** Quantification of either total SD4 or surface SD4 co-localized with total GluA1. N=15 cells per condition. Data represented as mean +/- SEM; n.s., non-significant; t-test. Scale bar = 5 μm.

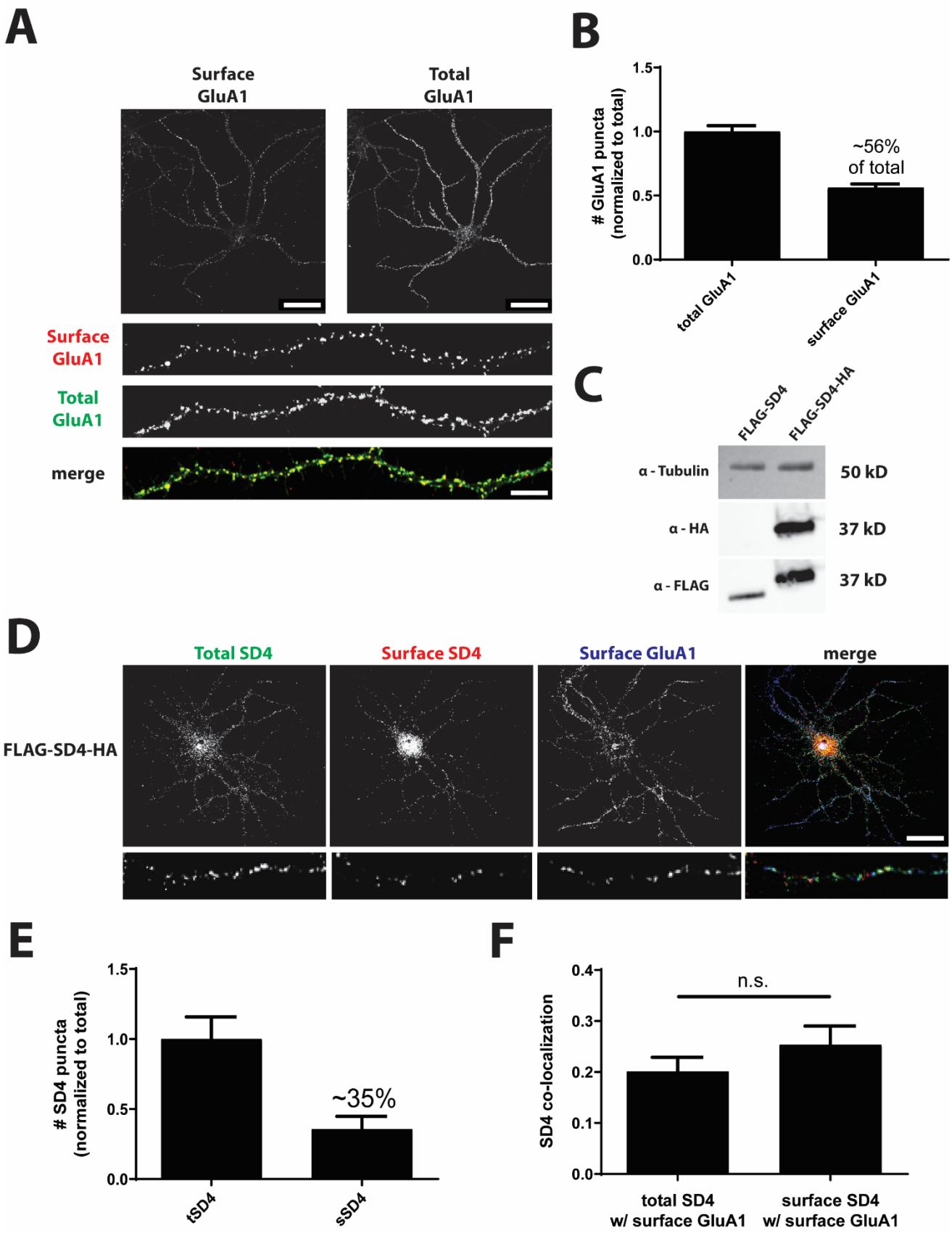
A
Surface GluA1
Total GluA1
Surface GluA1
Total GluA1
merge
B
GluA1 puncta (normalized to total)
1.5
1.0
0.5
0.0
~56% of total
total GluA1
surface GluA1
C
FLAG-SD4
FLAG-SD4-HA
α - Tubulin
50 kD
α - HA
37 kD
α - FLAG
37 kD
D
Total SD4
Surface SD4
Surface GluA1
merge
FLAG-SD4-HA
E
SD4 puncta (normalized to total)
1.5
1.0
0.5
0.0
~35%
tSD4
sSD4
F
SD4 co-localization
0.4
0.3
0.2
0.1
0.0
n.s.
total SD4 w/ surface GluA1
surface SD4 w/ surface GluA1

Figure 2. Co-localization of SD4 with surface GluA1 is increased after chemical-LTP.

(A) Representative confocal images of dendritic stretches from primary rat hippocampal neurons DIV13 with replicate experiments. Neurons were treated with either a mock DMSO vehicle control, or 200 μM glycine in aCSF w/o magnesium at 37ºC for 10 minutes. Neurons were transferred to aCSF recovery buffer (no drugs) for 20 minutes and then live-labeled for surface expressing GluA1-containing AMPARs at 37ºC for 1 hour. Neurons were then fixed, permeabilized, and stained for total SD4, surface GluA1, and vGlut1. **(B)** Quantification of co-localization between SD4, GluA1, and vGlut1. Overlap with pre-synaptic vGlut1 indicates a synaptic localization, while no overlap indicates extra-synaptic. **(C)** Quantification of mean area of GluA1 clusters either co-localized or non-colocalized with SD4 after treatment with vehicle or glycine. n=15 cells per condition. Data represented as mean +/- SEM; n.s., non-significant; *p<0.05; ***p<0.001; ****p<0.0001; one-way ANOVA; Scale bar = 5 μm.

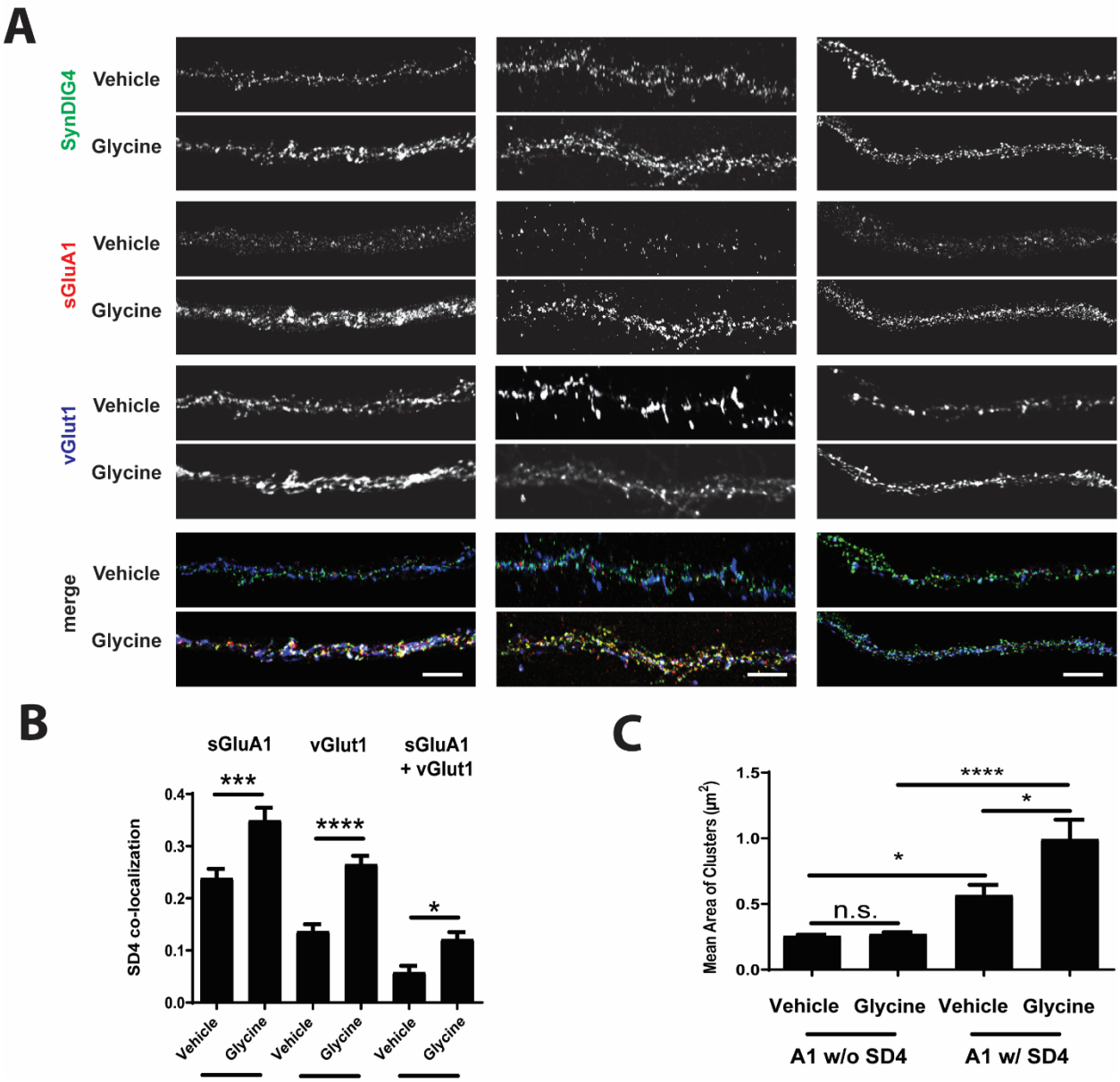
A
SynDIG4
sGluA1
vGlut1
merge
Vehicle
Glycine
B
sGluA1
vGlut1
sGluA1
+ vGlut1
***
****
*
SD4 co-localization
0.4
0.3
0.2
0.1
0.0
Vehicle
Glycine
C
Mean Area of Clusters (μm²)
1.5
1.0
0.5
0.0
****
*
n.s.
A1 w/o SD4
A1 w/ SD4

Figure 3. Surface GluA1 distribution is altered in SD4-KO neurons.

(A) Representative confocal images of dendritic stretches from either wildtype (WT), or SD4-knockout (KO) mouse hippocampal neurons DIV14. Neurons were first live labeled for surface GluA1. **(B-D)** Graphs depict puncta density **(B),** area **(C)**, and integrated density (I.D.) **(D)** of synaptic (defined as overlap with vGlut1) and extra-synaptic sGluA1 (no overlap with vGlut1). Data represented as mean +/- SEM; n.s., non-significant; **p<0.01; one-way ANOVA **(C, D)**. Scale bar = 5 μm.

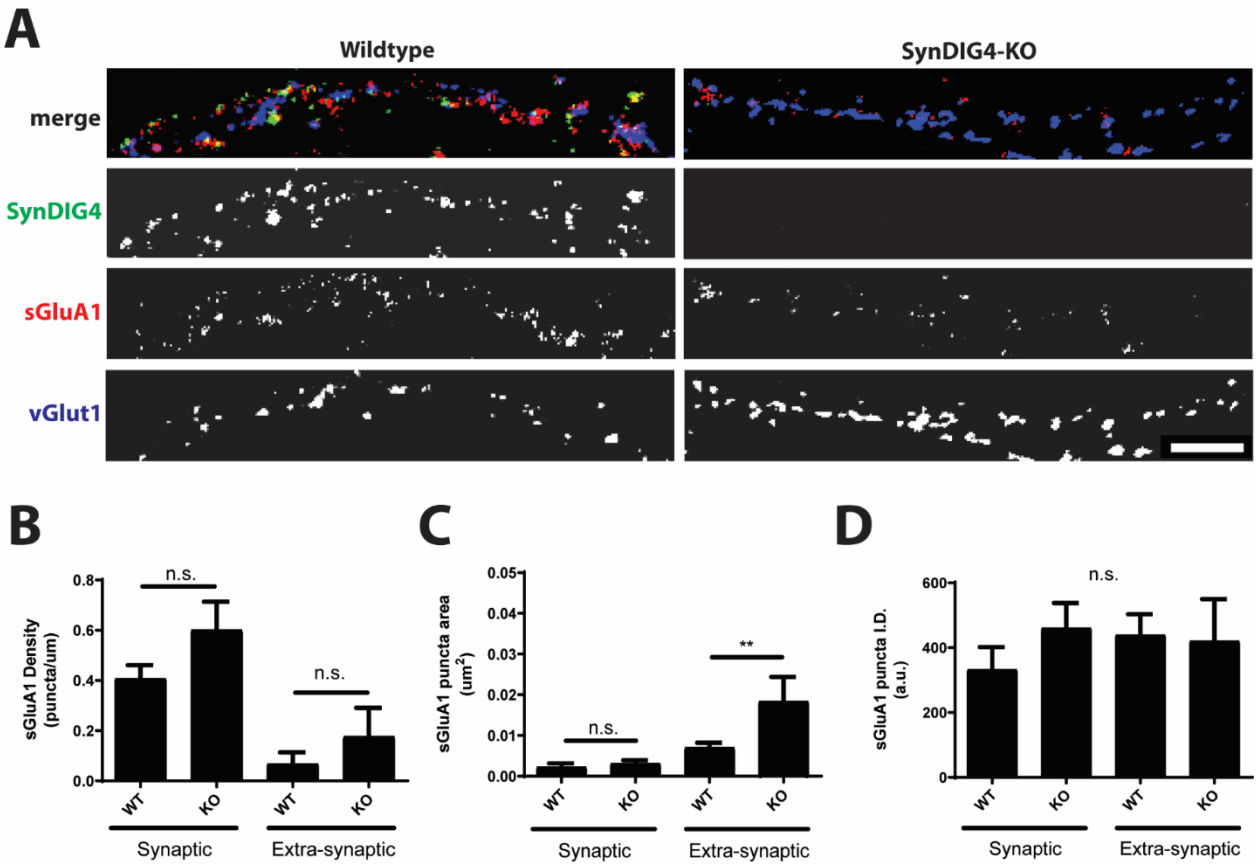
A
Wildtype
SynDIG4-KO
merge
SynDIG4
sGluA1
vGlut1
B
sGluA1 Density (puncta/um)
n.s.
n.s.
WT
KO
WT
KO
Synaptic
Extra-synaptic
C
sGluA1 puncta area (um2)
n.s.
**
WT
KO
WT
KO
Synaptic
Extra-synaptic
D
sGluA1 puncta I.D. (a.u.)
n.s.
WT
KO
WT
KO
Synaptic
Extra-synaptic

Figure 4. Proposed mechanism for SD4 role in AMPAR trafficking during LTP.

Basal levels of extra-synaptic surface GluA1 are increased in SD4-KO neurons compared to WT. LTP induction of WT and SD4-KO neurons indicates SD4 may be necessary for surface trafficking of GluA1-containing AMPARs. SD4-KO neurons also result in a loss of surface GluA1 trafficking to pools of extra-synaptic GluA1-containing AMPARs.

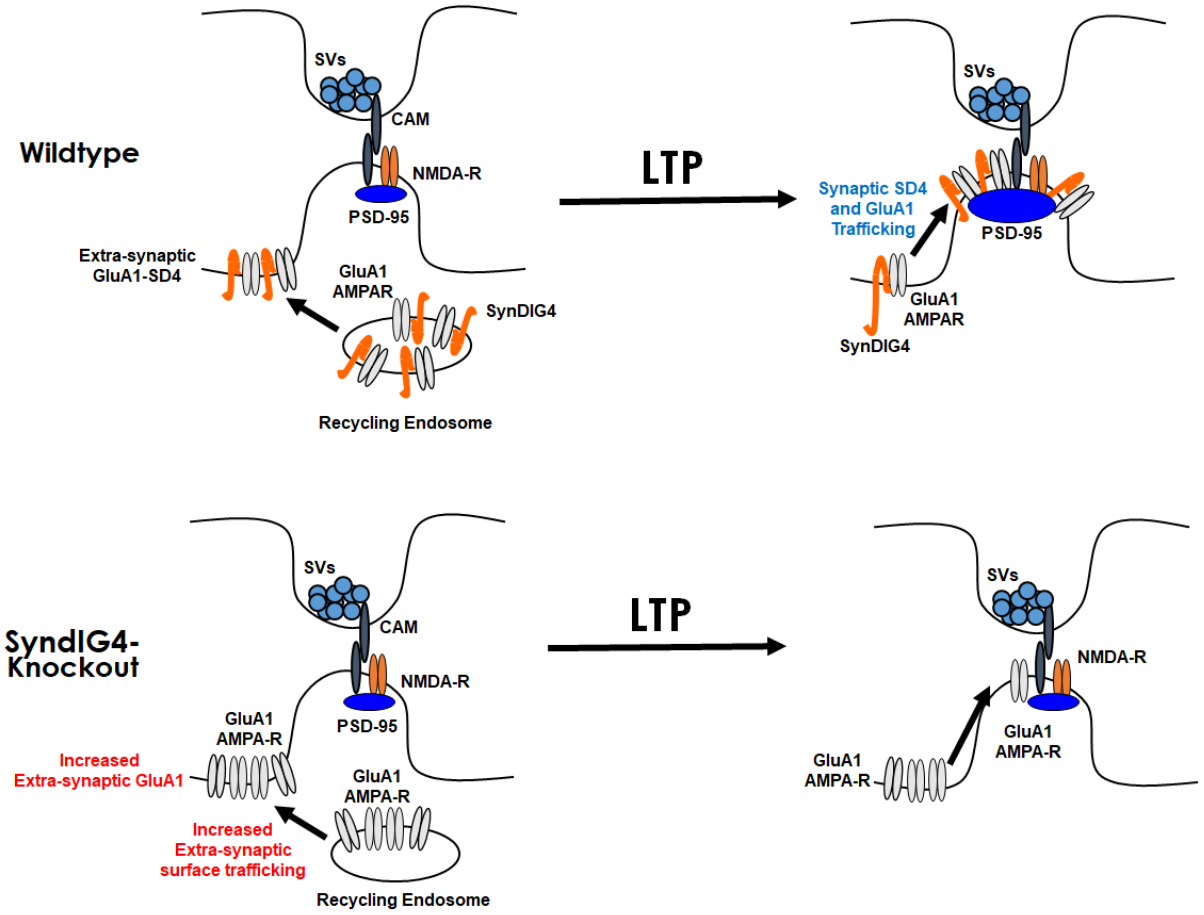
Wildtype
SVs
CAM
NMDA-R
PSD-95
Extra-synaptic
GluA1-SD4
GluA1
AMPAR
SynDIG4
Recycling Endosome
LTP
SVs
Synaptic SD4
and GluA1
Trafficking
PSD-95
GluA1
AMPAR
SynDIG4
SyndIG4-
Knockout
SVs
CAM
NMDA-R
PSD-95
GluA1
AMPA-R
Increased
Extra-synaptic GluA1
GluA1
AMPA-R
Increased
Extra-synaptic
surface trafficking
Recycling Endosome
LTP
SVs
NMDA-R
GluA1
AMPA-R
GluA1
AMPA-R

REFERENCES

1 Granger, A. J., Shi, Y., Lu, W., Cerpas, M. & Nicoll, R. A. LTP requires a reserve pool of glutamate receptors independent of subunit type. *Nature* **493**, 495-500 (2013). https://doi.org:10.1038/nature11775

2 Anthony Holtmaat, L. w., Graham W. Knott, Egbert Welker, and Karel Svoboda. Experience-dependent and cell-type-specific spine growth in the neocortex. *Nature* **441** (2006).

3 Balazs Lendvai, E. A. S., Brian Chen, and Karel Svoboda. Experience-dependent plasticity of dendritic spines in the developing rat barrel cortex in vivo. *Nature* **404** (2000).

4 Bonhoeffer, R. Y. a. T. Morphological changes in dendritic spines associated with long-term synaptic plasticity. *Annu. Rev. Neurosci.* **24** (2001).

5 Zito, A. H. a. K. A thorny question the role of spine morphogenesis in adaptive plasticity. *The MIT Press* (2011).

6 John C. Fiala, J. S., and Kristen M. Harris. Dendritic spine pathology: cause or consequence of neurological disorders? *Brain Research Reviews* **39** (2002).

7 Cohen-Cory, S. The developing synapse: construction and modulation of synaptic structures and circuits. *Science* **298**, 770-776 (2002).

8 Adlard PA, S. A., Gunawan L, Bray L, Hare D, Lear J, Doble P, Bush Al, Finkelstein Dl, and Cherny RA. A novel approach to rapidly prevent age-related cognitive decline. *Aging Cell* **13**, 351-359 (2014).

9 L J Garey, W. Y. O., T S Patel, M Kanani, A Davis, A M Mortimer, T R E Barnes, and S R Hirsch. Reduced dendritic spine density on cerebral cortical pyramidal neurons in schizophrenia. *J Neurol Neurosurg Psychiatry* **65**, 446-453 (1998).

10 Jessberger, K. C. V. a. S. Functional neurogenesis in the adult hippocampus: then and now. *Frontiers in Neuroscience* **8** (2014).

11 Peter S. Eriksson, E. P., Thomas Bjork-Eriksson, Ann-Marie Alborn, Claes Nordborg, Daniel A. Peterson, and Fred H. Gage. Neurogenesis in the adult human hippocampus. *Nature Medicine* **4**, 1313 - 1317 (1998).

12 H. Georg Kuhn, H. D.-A., and Fred H. Gage. Neurogenesis in the Dentate Gyrus of the Adult Rat: Age-Related Decrease of Neuronal Progenitor Proliferation. *The Journal of Neuroscience* **16**, 2027 - 2033 (1996).

13 Mora, F. Successful brain aging: plasticity, environmental enrichment, and lifestyle. *Dialogues in Clinical Neuroscience* **15**, 45 - 52 (2013).

14 S. J. Martin, P. D. G., and R. G. M. Morris. Synaptic plasticity and memory: an evaluation of the hypothesis. *Annu. Rev. Neurosci.* **23**, 649-711 (2000).

15 Bonhoeffer, F. E. a. T. Dendritic spine changes associated with hippocampal long-term synaptic plasticity. *Nature* (1999).

16 M. Maletic-Savatic, R. M., and K. Svoboda. Rapid dendritic morphogenesis in CA1 hippocampal dendrites induced by synaptic activity. *Science* **283** (1999).

17 Diaz, E. SynDIG1 regulation of excitatory synapse maturation. *J Physiol* **590**, 33-38 (2012). https://doi.org:10.1113/jphysiol.2011.213884

18 Bats, C., Groc, L. & Choquet, D. The Interaction between Stargazin and PSD-95 Regulates AMPA Receptor Surface Trafficking. *Neuron* **53** (2007).

19 Diaz, E. SynDIG1 regulation of synaptic AMPA receptor targeting. *Communicative & integrative biology* **3**, 347-349 (2010). https://doi.org:10.4161/cib.3.4.11765

20 Diaz, E. Dynamic expression of SynDIG1 mRNA in cerebellar Purkinje neurons. *Current Neurobiology* **1** (2010).

21 Evgenia Kalashnikova, R. A. L. I. K., Gustavo A. Barisone, Bonnie Li, Tatuto Ishimaru, James S. Trimmer, Durga P. Mohapatra, and Elva Diaz. SynDIG1: an activity-regulated AMPA receptor-interacting transmembrane protein that regulates excitatory synapse development. *Neuron* **65** (2010).

22 Guillermo M. Elias, L. F., Valentin Stein, Seth G. Grant, David S. Bredt, and Roger A. Nicoll. Synapse-Specific and Developmentally regulated Targeting of AMPA Receptors by a Family of MAGUK Scaffolding Proteins. *Neuron* **52** (2006).

23 Diaz, E. From microarrays to mechanisms of brain development and function. *Biochem Biophys Res Commun* **385**, 129-131 (2009). https://doi.org:10.1016/j.bbrc.2009.05.057

24 Kirk, L. M. *et al.* Distribution of the SynDIG4/proline-rich transmembrane protein 1 in rat brain. *J Comp Neurol* **524**, 2266-2280 (2016). https://doi.org:10.1002/cne.23945

25 Martin, E. E., Wleklinski, E., Hoang, H. T. M. & Ahmad, M. Interaction and Subcellular Association of PRRT1/SynDIG4 With AMPA Receptors. *Front Synaptic Neurosci* **13**, 705664 (2021). https://doi.org:10.3389/fnsyn.2021.705664

26 Troyano-Rodriguez, E., Mann, S., Ullah, R. & Ahmad, M. PRRT1 regulates basal and plasticity-induced AMPA receptor trafficking. *Mol Cell Neurosci* **98**, 155-163 (2019). https://doi.org:10.1016/j.mcn.2019.06.008

27 Matt, L. *et al.* SynDIG4/Prrt1 is required for excitatory synapse development and plasticity underlying cognitive function. *Cell Reports* **22** (2018).

28 Plambeck, K. E., He, C. W., Navarro, H. H. & Diaz, E. Mutually Dependent Clustering of SynDIG4/PRRT1 and AMPA Receptor Subunits GluA1 and GluA2 in Heterologous Cells and Primary Neurons. *Front Mol Neurosci* **15**, 788620 (2022). https://doi.org:10.3389/fnmol.2022.788620

29 Lu, W. *et al.* Subunit composition of synaptic AMPA receptors revealed by a single-cell genetic approach. *Neuron* **62**, 254-268 (2009). https://doi.org:10.1016/j.neuron.2009.02.027

30 Plant, K. *et al.* Transient incorporation of native GluR2-lacking AMPA receptors during hippocampal long-term potentiation. *Nat Neurosci* **9**, 602-604 (2006). https://doi.org:10.1038/nn1678

31 Sanderson, J. L., Gorski, J. A. & Dell'Acqua, M. L. NMDA Receptor-Dependent LTD Requires Transient Synaptic Incorporation of Ca(2)(+)-Permeable AMPARs Mediated by AKAP150-Anchored PKA and Calcineurin. *Neuron* **89**, 1000-1015 (2016). https://doi.org:10.1016/j.neuron.2016.01.043

32 Bissen, D., Foss, F. & Acker-Palmer, A. AMPA receptors and their minions: auxiliary proteins in AMPA receptor trafficking. *Cell Mol Life Sci* **76**, 2133-2169 (2019). https://doi.org:10.1007/s00018-019-03068-7

33 Matt, L. *et al.* SynDIG4/Prrt1 is required for excitatory synapse development and plasticity underlying cognitive function. *Cell Reports* (2018).

34 Ben-Yaacov, A. *et al.* Molecular Mechanism of AMPA Receptor Modulation by TARP/Stargazin. *Neuron* **93**, 1126-1137 e1124 (2017). https://doi.org:10.1016/j.neuron.2017.01.032

Chapter 4:

Conclusions and Future Directions

Summary and Conclusions

The purpose of this study is to further characterize the AMPAR auxiliary protein SynDIG4/Prrt1 and its role in binding and trafficking of GluA1- or GluA2-containing AMPARS during LTP. In this study, we first confirmed the ability of SD4 to cluster GluA1- and GluA2-containing AMPARs in heterologous COS cells. We then aimed to further identify a specific domain of SynDIG4 necessary for clustering of AMPARs. Therefore, I generated GluA1 and GluA2 AMPARs using the kainate receptor GluK2. From this study, we concluded that the N-terminus of GluA1 and GluA2 are dispensable for binding with SD4, while the TM and CT domains are sufficient for clustering. Furthermore, we observed that clustering of AMPARs by SD4 is dependent on endocytosis of SD4 and AMPARs, further indicating that SD4 may play a role in trafficking of AMPARS to and from the plasma membrane, as well as the PSD, during LTP. Further experiments will be required to identify the specific mechanism of SD4 during endocytosis

Next, we sought to answer the question of what happens to SD4 localization before and after LTP. We observed that the synaptic localization of SD4 is increased after chemically induced LTP. Additionally, we observed the loss of SD4 affects localization and trafficking of GluA1 whereby extra-synaptic sGluA1-SD4 cluster size and co-localization is increased, but LTP is

impaired. This could present a possible caveat in our interpretations whereby trafficking is not an essential role of SD4 and is primarily responsible for maintaining AMPARs at extra-synaptic pools. Therefore, deficits in clustering and LTP could simply be the result of a decrease in the number of readily available extra-synaptic AMPARs at the plasma membrane. One last caveat may be how to accurately identify whether SD4-KO animals are increasing endocytosis or reducing exocytosis of GluA1/A2 AMPARs. One method may be to use the dynasore reagent to inhibit endocytosis and identify changes in endocytosis events. My data further indicates the overall importance of endocytosis/exocytosis for SD4 activity and AMPAR trafficking to the PSD[1]. Endocytosis to occur I observed significant clustering of GluA1 and GluA2 AMPAR subunits by SD4 at 37ºC, the required temperature for endocytosis. Endocytosis and clustering is eliminated at 4ºC, indicating the requirement of endocytosis for clustering of GluA1 or GluA2 by SD4[1].

Future Directions

Based on my collected data, we require several additional experiments to further elucidate the role of SD4 in AMPAR trafficking and gating during LTP. Using co-immunoprecipitation, we can further substantiate the finding that SD4 binds to sGluA1 or total GluA1, or further attempt to identify any tertiary binding factor in both heterologous cells and dissociated hippocampal neurons. I predict that co-expression of SD4 with GluA1 will result in a clustering phenotype as depicted in Figure 3. Additionally, using co-IP experiments will produce a positive GluA1 signal

after SD4 is pulled out of the crude lysates. From the dissociated neurons, I expect to see a preferential localization of SD4 with GluA1 at extra-synaptic sites as previously seen in the literature4. These data taken together would indicate the presence of a SD4/GluA1 complex, and potential interaction. Furthermore, I would conclude that this interaction is necessary for the extrasynaptic localization of GluA1.

It has not been definitively established that SD4 interacts directly with GluA1. My preliminary results could be the result of a tertiary interaction through some intermediate AMPAR auxiliary protein. Therefore, it may be necessary to use both purified SD4 and GluA1 in the co-IP assay to further establish a definitive interaction between SD4 and GluA1. As with the previously described clustering assay, heterologous COS cells will be co-expressed with GluA1 and either the WT control or chimeric constructs. I will use co-IP with WT and chimeric SD4 to confirm interaction. Lastly, I will confirm that the identified domain imparts co-localization of chimeric SD4 with GluA1 at extrasynaptic sites in dissociated neurons in vitro. SD4-KO neurons will be cultured and transfected with either WTSD4, WT-IFITM3, and each of the chimeras. Neurons will then be fixed, stained for HA, GluA1, and vGlut1 and imaged by confocal microscopy for analysis of co-localization.

Other auxiliary factors such as Stargazin have been shown to modulate AMPARs through distinct and separate protein domains. Therefore, it is possible that the TM and NT of SD4 may also have distinct functions. It is possible that the chimeric constructs could become less stable, resulting in deficits in expression. To circumvent this issue, I may need to study conserved amino

acid residues across other species. This could allow me to identify narrow down the important protein domains or identify previously unknown protein motifs (SH3 motif, etc.)[2], which could increase stability of the chimeras. Additionally, it would be of interest to generate the reverse chimeras to test sufficiency of these domains. Lastly, due to resolution constraints, it may be necessary to use additional techniques such as super-resolution or TIRF microscopy to definitively assess changes in protein localization.

Previous studies using chemical LTP have shown an increase in surface GluA1 due to glycine treatment. It remains unclear whether SD4 will remain localized to extra-synaptic sites after stimulation in WT mice. If chem-LTP results in release of GluA1 from SD4, then I expect to see a reduction in extra-synaptic co-localization of GluA1 with SD4, as well as a reduction of GluA1 signal in the extra-synaptic fraction after stimulation, indicating a loss of interaction. However, if interaction of GluA1 with SD4 remains after chem-LTP, then I expect to see an increase in synaptic localization of the SD4/GluA1 complex, as well as an enrichment of SD4 and GluA1 in the synaptic fractions after stimulation. Potential caveat could be that increases in SD4/GluA1 localization could be solely due to increases in surface GluA1 due to chem-LTP. It will be important to additionally confirm changes in SD4 localization by co-staining SD4 with PSD95 and vGlut1 synapses during LTP.

As mentioned previously, it is possible that the NT and TM of SD4 have separate functions. As a result, I may find that one domain is necessary for localization and interaction with GluA1, while the other is necessary for trafficking and LTP. Therefore, it is possible that the loss of the necessary SD4 domains could result in a loss of extra-synaptic GluA1 regardless of LTP induction.

Therefore, it will be important to further establish total versus surface GluA1 to understand where GluA1 is localized during LTP in the absence of SD4. Additionally, it is possible that the maintenance of pools of GluA1 is not unique to SD4, or that interaction between GluA1 and SD4 is mediated through a tertiary binding protein. If a loss of SD4 does not result in deficits in surface GluA1 due to chemical LTP stimulus, I will investigate the involvement of additional AMPAR auxiliary factors. For example, it has previously been observed that GluR4 clusters with the auxiliar subunit Stargazin, but only in the presence of PSD-95[3]. This suggests that the PDZ-binding site of Stargazin is required to bind GluA4, and then anchor GluA4 to PSD-95 to form synaptic clusters[3]. Does clustering of GluA1/A2 occur by SD4 through binding to Tarp-γ8 and being anchored by binding of Tarp-γ8 to PDZ binding site on PSD95? SD4 has previously been found in complex with Tarp-γ8[4,5]. We would try a similar experiment to assess clustering of GluA1/2 by SD4 through confocal imaging of GluA1/A2 expressed with SD4, or both Tarp-γ8 and SD4 both GluA4 and Tarp-γ8 in heterologous COS cells and neuronal hippocampal cultures.

Additionally, we could use live-imaging of heterologous COS cells and cultured hippocampal neurons expressing a SEP-tagged GluA1 receptors. SEP is a super ecliptic phluorin which only produces GFP under neutral pH conditions. Therefore, it has the ability to detect changes in pH and produce fluorescence, making it ideal for dectecting endocytosis and exocytosis events. We would first test SEP-GluA1 in COS cells to observe that GFP is expressing while insertion and removal is detected by changes in fluorescence. Therefore, we would culture hippocampal neurons from SD4-WT and SD4-KO expressing SEP-GluA1 with each of the SD4/IFITM3 chimeras and observe changes before and after chem-LTP to identify important SD4

protein domains. However, one caveat may be a failure of SEP-GluA1 insertion or a failure to increase the rate of endocytosis events. Therefore, we may additionally look at changes in the motility/diffusion rates of SEP-GluA1 after chem-LTP.

Another study used super-resolution imaging to visualize extra-synaptic pools of GluA1 closest to the PSD[6]. They observed that AMPAR nanodomains are tightly correlated with synaptic vesicle release where AMPAR complexes must be present directly across from the pre-synaptic vesicle release sites[6]. This results in pools of perisynaptic GluA1, representing surface GluA1 that is present within the synaptic PSD, but not at vesicle release sites. Therefore, we could use super-resolution imaging or single particle tracking to further identify SD4 localization and co-localization with GluA1 by further observing SD4 at synaptic and perisynaptic sites during LTP.

Through a collaborative project with the lab of Dr.Yael Stern-Bach, we observed that the biophysical properties of GluA1- and GluA2-containing AMPARs were altered when co-expressed with SD4 in *Xenopus* oocytes[7]. These changes include increases in latency and receptor activation, while the rate of desensitization is decreased. Changes in the gating properties of GluA1/A2 AMPARs were amplified further when co-expressed with Tarp-γ8[7]. Additionally, another group found that Stargazin binds, traffics, and alters the biophysical properties of AMPARs through two distinct protein domains[8]. Utilizing chimeras generated from replacing specific Stargazin domains with those from Tarp-γ5, they identified two different protein domains responsible for trafficking and gating of GluA1[8,9]. Therefore, we would replicate these gating experiments expressing GluA1 with the SD4/IFITM3 chimeras to see whether distinct protein domains may be identified for protein trafficking and gating. Lastly, specific point mutations

within GluA2 have been found to affect the activity of CNIHs and TARPs[10]. Therefore, we can make similar mutations within important protein domains of GluA1, GluA2, and SD4, and repeat clustering and biophysical experiments to further identify smaller binding sites necessary for trafficking and gating of AMPARs by SD4.

Previous collaborative studies from the Diaz lab have demonstrated a role for SD4 in functional LTP using SD4-KO mice[7]. Stimulation of hippocampal slices from SD4-KO mice showed no increase in stable EPSPs indicating impaired LTP[7]. Therefore, SD4 is important for functional LTP. Functional LTP is often correlated with structural enhancements in dendritic spines. During structural LTP (sLTP), AMPARs are actively recruited to synapses, resulting in a stable increase in spine size. It has been observed that GluA1-containing AMPARs are necessary for sLTP. Additionally, our lab has found enhancements in sLTP in the absence of the related protein SD1, which we interpret as a lack of synapse maturation since young spines exhibit greater structural plasticity. It is unclear whether SD4 is also important for GluA1-dependent sLTP.

To establish whether SD4 is necessary for GluA1-dependent sLTP, we will use two-photon glutamate uncaging to stimulate individual dendritic spines in WT and SD4-KO mice. Two-photon glutamate uncaging is used to stimulate individual spines through the focal release of glutamate, resulting in the structural enhancement of the stimulated post-synaptic spine. I will first extract the brains of mice at postnatal day 7. The hippocampus will then be isolated, sectioned, and plated on a matrigel. I will use a biolistic particle delivery system, or gene gun, to co-transfect live hippocampal slices with a GFP-expressing DNA construct to visualize CA1 hippocampal neurons by two-photon microscopy. Neurons will be visualized while in solution

containing aCSF and caged MNI-glutamate. MNI is a light sensitive photoprotective molecule used to make caged ligand molecules. When fused with glutamate, it is inactive until stimulated by the appropriate wavelength. Candidate regions of interest (ROI) will be identified in GFP-expressing neurons to be used for glutamate uncaging. A 720 nM laser will be used to locally uncage MNI-glutamate, resulting in stimulation of glutamate receptors at the ROI in WT or SD4-KO mice. After stimulation, I will be able to assess deficits in LTP-associated spine enlargement in SD4-KO neurons. To rescue deficits in sLTP, I will express GFP, WT-SD4 and each of the SD4/IFITM3 chimeras in slice culture. Glutamate uncaging will be used to stimulate dendritic spines in neurons as previously described. stimulated spines will be measured for changes in spine volume.

If SD4 is necessary for GluA1-dependent sLTP, then the stimulation of spines in the KO mice should exhibit deficits in structural spine enhancements. Overexpression of WT-SD4 should rescue these deficits on uncaging-induced spine enlargement, while neurons expressing GFP alone will still exhibit impairments in long-term spine enlargement. Furthermore, if either the NT or TM domain is necessary for structural LTP, I expect to see impairments in the chimera where that domain has been replaced.

It is possible that the SD4-KO mice will not exhibit deficits in GluA1-dependent sLTP. Behavioral studies using SD4-KO mice have demonstrated severe deficits in hippocampal dependent learning and memory. Taken with the functional LTP studies (Figure 2), these data suggest that SD4 is important for hippocampal plasticity, so it is likely this would translate into

structural LTP. As the mechanism of SD4-mediated sLTP is not yet known, it is unclear whether results from chem-LTP stimulation will correlate with changes in sLTP. Therefore, results from these experiments remain mutually exclusive.

REFERENCES

1 Plambeck, K. E., He, C. W., Navarro, H. H. & Diaz, E. Mutually Dependent Clustering of SynDIG4/PRRT1 and AMPA Receptor Subunits GluA1 and GluA2 in Heterologous Cells and Primary Neurons. *Front Mol Neurosci* **15**, 788620 (2022). https://doi.org:10.3389/fnmol.2022.788620

2 Kay, B. K., Williamson, M. P. & Sudol, P. The importance of being proline: the interaction of proline-rich motifs in signaling proteins with their cognate domains. *Faseb J* **14**, 231-241 (2000).

3 Chen, L. *et al.* Stargazin regulates synaptic targeting of AMPA receptors by two distinct mechanisms. *Nature* **408**, 936-943 (2000). https://doi.org:10.1038/35050030

4 Rouach, N. *et al.* TARP gamma-8 controls hippocampal AMPA receptor number, distribution and synaptic plasticity. *Nat Neurosci* **8**, 1525-1533 (2005). https://doi.org:10.1038/nn1551

5 Schwenk, J. *et al.* High-resolution proteomics unravel architecture and molecular diversity of native AMPA receptor complexes. *Neuron* **74**, 621-633 (2012). https://doi.org:10.1016/j.neuron.2012.03.034

6 Chen, H., Tang, A. H. & Blanpied, T. A. Subsynaptic spatial organization as a regulator of synaptic strength and plasticity. *Curr Opin Neurobiol* **51**, 147-153 (2018). https://doi.org:10.1016/j.conb.2018.05.004

7 Matt, L. *et al.* SynDIG4/Prrt1 is required for excitatory synapse development and plasticity underlying cognitive function. *Cell Reports* (2018).

8 Tomita, S. *et al.* Stargazin modulates AMPA receptor gating and trafficking by distinct domains. *Nature* **435**, 1052-1058 (2005). https://doi.org:10.1038/nature03624

9 Ben-Yaacov, A. *et al.* Molecular Mechanism of AMPA Receptor Modulation by TARP/Stargazin. *Neuron* **93**, 1126-1137 e1124 (2017). https://doi.org:10.1016/j.neuron.2017.01.032

10 Dawe, G. B. *et al.* Distinct Structural Pathways Coordinate the Activation of AMPA Receptor-Auxiliary Subunit Complexes. *Neuron* **89**, 1264-1276 (2016). https://doi.org:10.1016/j.neuron.2016.01.038

Appendix:

Lab Protocols

Detailed protocols have been included as an appendix to provide information on all experiments and to aid in future studies.

COS/HEK Cell Live Labeling Protocol

Day 1:

1. Coat coverslips with Poly-L-Lysine (PLL); 25 ug/mL in 0.1 M Borate Buffer, pH 8.5. Incubate coverslips at 37C for minimum 1 hr. Wash 3x with ddH20.
2. Seed cells at desired concentration. Incubate for 24hrs.

Day 2:

3. Transfect cells and incubate for another 24 – 48 hrs.

Day 3:

4. Incubate plates on ice in 4C room for 10 mins.
5. Prepare primary antibody in TCR hood (cold growth media, 800 uL per well, additionally add BSA if you get high background).
6. Wash cells one time with cold 1x PBS.
7. Incubate coverslips with 800 uL media plus primary antibody for 10 minutes.
8. Prepare secondary antibody media in TCR hood.
9. Wash coverslips three times with 1x PBS (no interval).
10. Incubate with secondary antibody solution for 10 minutes (for fluorescent antibodies, be sure to cover plates).
11. Prepare 4% PFA.
12. Wash three times with 1x PBS.
13. Fix plates with 4% PFA for 10 minutes at 4C.
14. Wash coverslips three times with 1x PBS for 5 minutes each.
15. Plates can be stored at 4^{o}C or continue to additional staining for total protein.

Next Steps (Total Protein):

16. Incubate in 0.1% Triton X-100 for 15 minutes while shaking.

17. Block w/ 5% milk (in 1x PBS) for 30 minutes while shaking. Alternatively, can block with 5 – 10% BSA (IgG free).

18. Prepare primary antibody in 5% milk (or 3% BSA). For six well coverslips, use 100 uL per coverslip.

19. Invert coverslips onto antibody on parafilm in foil or covered chamber and incubate at room temperature for 1.5 hours.

20. Wash three times with 1x PBS for 10 minutes each.

21. Prepare secondary antibody in 5% milk (or 3% BSA).

22. Invert coverslips onto antibody and incubate at room temperature for 1 hour.

23. Wash three times with 1x PBS for 10 minutes. Additionally, can include DAPI at this step if desired.

24. Mount on slides with Fluoromount G (southern biotech), or other fluorescence protecting mounting medium.

25. Allow to dry overnight and then seal with nail polish.

Defined Media Primary Neuronal Culture

This protocol can be used for both mice and rats but is commonly used for mouse cultures. Any modifications for mouse cultures will be denoted in red.

Day 1

The day before dissection, coat nitric acid sterilized coverslips with 1 mg/mL of poly-L-lysine, incubate overnight at 37°C.

**Coat coverslips on day pups are born (P0).

Day 2

1. Wash coverslips 3x with distilled water and place wax dots on coverslips
   a. Transfer coverslips to 6-well plates (at least four; 24 coverslips total) in biosafety cabinet.
   b. For sterility, turn on Bunsen burner and place near hot plate. Sterilize bench area with 70% ethanol.
   c. Begin boiling water in small beaker on hot plate at your bench.
   d. Melt wax pellets by placing pellets into a smaller beaker.
   e. Place this beaker into the water on hot plate as it begins to boil.
   f. Bring coverslips to bench. Using 200 uL pipet, carefully add wax dots to the corners of each coverslip.

2. Transfer plates to bio-safety cabinet to dry

3. Genotype mice.
   a. Use a sharpie to number each pup on the belly.
   b. Snip a small piece of the tail and transfer to individually numbered tubes.
   c. Digest tail snips to extract DNA and perform genotyping by following the Diaz Lab genotyping protocol.

d. Separate wildtype animals from knockout animals and proceed to dissection.

4. Perform hippocampal dissection and plating (see following protocol for details).

Day 6: (4DIV)

5. Add AraC (10 mM stock; 5 uM final concentration) per well directly to culture medium (1:2000 dilution from stock in -20ºC, i.e. 2.5 uL AraC to 5 mL NBC).

Day 7: (5DIV), **Day 12**: (10DIV), **Day 17**: (15DIV), **Day 21**: (20DIV)

6. Remove 700 µL of media and replace with 1 mL fresh NBC.

Hippocampal Dissection and Plating

1. Before dissection, sterilize tools at 250°C for 15 minutes.

2. Decapitate P0-P2 pups, and remove brains from skull, placing in dissection buffer on ice.

3. After removing all brains, remove the hippocampi from each brain being careful to remove the meninges, and transfer to a 15mL conical tube on ice.

4. Transfer hippocampi to new 15 mL conical tube containing 5 mL of HBSS and 100 µL of 2.5% Trypsin (Gibco).

*** Add 100 µL papain (Wellingsworth) to 5 mL HBSS. Warm in 37°C water bath to aid in dissolving. Filter sterilize before use. ***

5. Incubate hippocampi in 37°C water bath for 12 or 15 minutes, inverting gently every few minutes.

6. After incubation, add 5mL of NPM.

7. Centrifuge for 5 min at 1000 rpm and carefully remove the supernatant.

8. Resuspend pellet in 3 mL of NPM and dissociate cells by pipetting up and down with a 1mL pipette 3x or 5x, followed by trituration with a fire polished long stem pipette until most chunks of tissue have been dissociated. For best results with mouse neurons do not triturate with glass pipette more than 12x. If there are tissue chunks remaining, let them settle to the bottom of the conical tube and then remove them.

9. Add NPM to a final concentration of 5-10 mLs.

10. Use a hemocytometer to determine cell density (45 uL of cell suspension plus 5 uL of trypan blue). Trypan blue will stain dead cells blue. Do not include dead cells in your count. For mouse neurons, 80% of your cells should be viable at this stage.

11. Dilute cells to 25,000/ mL (75,000 cells/ mL) with NPM in a separate container (make sure to account for pipetting error). Add 2 mLs per well, over the poly-L-lysine coated coverslips. This will give a final cell density of 50,000 (150,000) cells per well.

12. Place dishes in incubator for 5-6 hrs.

13. Replace media with NBC.

Media Formulations:

Dissection Buffer:

- 500 mL HBSS (remove 10 mL)
- 5 mL HEPES
- 5 mL Sodium Pyruvate

Neuronal Plating Media (NPM):

- 500 mL MEM (remove 68 mL)
- 10% Donor horse serum (50mL)
- 0.45% glucose (7.5 mL of 30% stock in DI water)
- 5 mL Sodium Pyruvate
- 5 mL Penicillin/ Streptomycin

Neurobasal complete (NBC):

- 500 mL Neurobasal (remove 27 mL)
- 5 mL HEPES
- 5 mL Sodium Pyruvate
- 5 mL Penicillin/ Streptomycin
- 1.5 mL L-glutamine

****Filter sterilize****

- Add 10 mL B-27 after filter sterilizing

Additional Solutions:

Poly-L-Lysine Solution (PLL):

PLL stocks are at 200 mg/mL located in the -20C fridge.

For 25 ug/mL:

- Dilute stock at 1:8,000 in 0.1 M Borate Buffer, i.e. add 6.25 uL PLL to 50 mL 0.1M Borate Buffer

For 1 mg/mL:

- Dilute stock at 1:200 in 0.1 M Borate Buffer, i.e. add 50 uL PLL to 10 mL 0.1 M Borate Buffer

0.1 M Borate Buffer:

- 900 mL milli-Q water
- 17.2 g sodium tetra-borate
- 3.1 g boric acid
- Adjust pH to 8.5
- Bring up to 1 L with milli-Q water
- Filter Sterilize

1M Nitric Acid:

- Add 64 mL 70% w/w 15.8 N nitric acid to 250 mL H_20.
- Bring up to 1000 mL.

Banker Style Primary Mouse Hippocampal Culture

Wildtype and SynDIG4-knockout

Outline:

Note: For mouse cultures, astrocyte feeder layer must be timed with birth of mouse pups. Mouse dissection must occur at P0-P2.

For astrocyte feeder layer:

Day 1: Coat plates with poly-L-lysine (PLL) for astrocytes.

Day 2: Plate astrocytes.

Day 5: Change astrocyte plating media (APM). Continue to change APM every 3 days until pups are born.

Hippocampal neuron culture:

Day 0: Perform nitric acid sterilization and etching of coverslips.

Day 1: The day before dissection, coat nitric acid sterilized/etched coverslips with 1 mg/mL of poly-L-lysine (PLL). Replace APM media on astrocytes with 5 mL NBC.

Day 2 (DIV 0): Place wax dots on coverslips for primary neurons. Genotype mice. Perform hippocampal dissection and plating

Day 6 (DIV 4): Add 5 μM AraC to each well.

Day 7: (5DIV), **Day 12**: (10DIV), **Day 17**: (15DIV), **Day 21**: (20DIV)

- Perform half media change every 5 days by removing 2.5 mL old media and replacing with 3 mL fresh NBC.

Sequence of events and detailed procedures:

Setting up astrocyte feeder layer:

Day 1:

1. Coat 6-well plates with 25 μg/mL of poly-L-lysine (PLL) in 0.1 M Borate buffer. Incubate overnight in $C0_2$ incubator at 37°C.

Day 2:

1. Wash 6-well plates 3x with Milli-Q water. Keep in last wash until astrocytes are ready to be plated.
2. Revive frozen astrocytes by thawing quickly in water bath. 1 mL of frozen astrocytes (1 vial) will be enough for two 6-well plates.
3. Transfer thawed astrocytes into Astrocyte Plating Media (APM), and plate 2 mL of suspended astrocytes per well.
4. Place in $C0_2$ incubator. Monitor cells after 2 days, confluency should be around 20%.

Day 5:

1. Change astrocyte plating media (APM). Continue to change APM every 3 days until pups are born. Astrocytes should be at least 70% confluent on day of hippocampal dissection and plating.

Hippocampal Neuron Culture:

Day 0:

1. Perform nitric acid sterilization and etching of glass coverslips
    a. Place coverslips in ceramic racks and place racks in glass container.
    b. Wash coverslips 1x with Milli-Q water to remove any dust/particles.
    c. Fill container with 1M Nitric Acid (coverslips should be completely submerged.
    d. Place glass container on shaker at RT at low speed overnight.
    e. Remove Nitric Acid and save for future use (can be used up to three times).
    f. Rinse glass container and coverslips 3x with Milli-Q water (quick rinses).
    g. Fill container with Milli-Q water so coverslips are submerged and place on shaker at low speed 3x for 20 minutes each. Ethanol rinse to aid drying.
    h. Remove excess liquid by tapping ceramic racks on Kim-wipes.
    i. Wrap in foil and autoclave on Cycle 8 (Wrapped at 250C).

Day 1:

1. Replace APM media with 5 mL Neurobasal Complete (NBC).
2. Coat etched/sterilized coverslips (with wax dots) with 1 mg/mL of PLL in 0.1M Borate buffer. Use 350 µL solution per well and bubble on top of coverslips using a 1 mL pipet. Incubate in the $C0_2$ incubator overnight.

Day 2 (DIV 0):

1. Wash coverslips 3x with sterile Milli-Q water.
2. Place wax dots on coverslips.
    a. Transfer coverslips to 6-well plates (at least four; 24 coverslips total) in biosafety cabinet.

b. For sterility, turn on Bunsen burner and place near hot plate. Sterilize bench area with 70% ethanol.
c. Begin boiling water in small beaker on hot plate at your bench.
d. Melt wax pellets by placing pellets into a smaller beaker.
e. Place this beaker into the water on hot plate as it begins to boil.
f. Bring coverslips to bench. Using 200 uL pipet, carefully add wax dots to the corners of each coverslip.

3. Allow to dry in bio-safety cabinet while preparing for dissection.
4. Add 2 mL NPM per well and place in CO_2 incubator at 37C.

5. Genotype mice.
   a. Use a sharpie to number each pup on the belly.
   b. Snip a small piece of the tail and transfer to individually numbered tubes.
   c. Digest tail snips to extract DNA and perform genotyping by following the Diaz Lab genotyping protocol.
   d. Separate wildtype animals from knockout animals and proceed to dissection.

6. Perform Hippocampal Dissection and plating.
   a. Before dissection, sterilize tools at 250C for 15 minutes (dry bath in dissection room).
   b. Euthanize E18-E19 pregnant rat with carbon dioxide. Ensure complete euthanasia by cervical dislocation.
   c. Spray abdomen with 70% ethanol.
   d. Cut through skin and remove the uterus to a petri dish.
   e. Remove fetuses from the uterus, decapitate, and put heads in dissection buffer on ice.
   f. Remove the hippocampi from each brain being careful to remove all meninges, and transfer to a 15 mL conical tube on ice.

g. Transfer wildtype and SynDIG4-knockout tissue to separate 15 mL tubes.
h. Add 100 µL papain (Wellingsworth) to each tube with 5 mL dissection media. Warm in 37°C water bath to aid in dissolving. Filter sterilize before use.
i. Incubate hippocampi in 37C water bath for 15 min, inverting gently every few minutes.
j. After incubation, add 5 mL of NPM.
k. Centrifuge for 5 min at 1000 rpm and carefully remove the supernatant.
l. Resuspend pellet in 3 mL of NPM and dissociate cells by pipetting up and down with a 1 mL pipette 5x, followed by trituration 10x with a fire polished long stem pipette until most chunks of tissue have been dissociated.
m. Add NPM to a final volume of 5mL.
n. Use a hemacytometer to determine cell density (45 uL of cell suspension plus 5 uL of trypan blue). Trypan blue will stain dead cells blue. Do not include dead cells in your count.
o. Dilute cells to 60,000 cells per mL of NPM (make sure to account for pipetting error). Add 2 mL of cells to each well containing PLL coated coverslips. This will give a final cell density of 120,000 cells per well and a total volume of 2 mL per well.
p. Place dishes in incubator for 5 – 6 hours.
q. Transfer coverslips, wax dot side down, to the plates containing astrocyte feeder layers.
r. Place in $C0_2$ incubator.
s. Perform a half media change every 5 days by removing 2.5 mL old media and adding 3 mL fresh NBC.

Day 6 (4 DIV):

1. Add AraC (10 mM stock; 5 uM final concentration) per well directly to culture medium (1:2000 dilution from stock in -20ºC, i.e. 2.5 uL AraC to 5 mL NBC).

Day 7 (5 DIV) …Day 12 (10 DIV), etc.:

1. Half media change. Remove 2.5 mL of media and replace with 3 mL fresh NBC. Perform half media change every 5 days.
2. Fix and stain neurons at 14 DIV, or appropriate age, depending on development and confluency.

**This protocol can also be used for cortical cultures. However, cortical tissue must be mechanically "chopped" with forceps into smaller pieces before digestion. Cortical neurons will also mature more quickly than hippocampal neurons. **

Media Formulations:

Dissection Buffer:

- 500 mL HBSS (remove 10 mL)
- 5 mL HEPES
- 5 mL Sodium pyruvate

Astrocyte Plating Media (APM):

- 500 mL 1X MEM (remove 65 mL)
- 10% Donor horse serum (50 mL)
- 0.6% Glucose (10 mL of 30% glucose stock in Milli-Q water)
- 5 mL Penicillin/Streptomycin

Neuronal Plating Media (NPM):

- 500 mL 1X MEM (remove 68 mL)
- 10% Donor horse serum (50 mL)
- 0.45% glucose (7.5 mL of 30% glucose stock in Milli-Q water)
- 5 mL Sodium pyruvate
- 5 mL Penicillin/Streptomycin

Neurobasal complete (NBC):

- 500 mL Neurobasal (remove 27 mL)
- 5 mL Hepes
- 5 mL Sodium Pyruvate
- 5 mL Penicillin/ Streptomycin
- 1.5 mL L-glutamine

****Filter sterilize****

- Add 10 mL B-27 after filter sterilizing

<u>Additional Solutions:</u>

Poly-L-Lysine Solution (PLL):

PLL stocks are at 200 mg/uL located in the -20C fridge.

For 25 ug/uL:

- Dilute stock at 1:8,000 in 0.1 M Borate Buffer, i.e. add 6.25 uL PLL to 50 mL 0.1M Borate Buffer

For 1 mg/uL:

- Dilute stock at 1:200 in 0.1 M Borate Buffer, i.e. add 50 uL PLL to 10 mL 0.1 M Borate Buffer

0.1 M Borate Buffer

- 900 mL milli-Q water
- 17.2 g sodium tetra-borate
- 3.1 g boric acid
- Adjust pH to 8.5
- Bring up to 1 L with milli-Q water
- Filter Sterilize

1M Nitric Acid:

- Add 64 mL 70% w/w 15.8 N nitric acid to 250 mL H_20.
- Bring up to 1000 mL.

Banker Style Primary Rat Hippocampal Culture

Outline:

Day 1 (Monday): Coat plates with poly-L-lysine (PLL) for astrocytes. Order E16 timed pregnant rat through TRACS/ATS (Animal Tracking System)

1. Strain: SD
2. Gestation requirements: E16
3. Vendors: ENVIGO or Charles River
4. Vivarium: TRACS/GBSF 636

Day 2 (Tuesday): Plate astrocytes.

Day 5 (Friday): Change astrocyte plating media (APM).

Day 8 (Monday): Change APM. Perform nitric acid sterilization and etching of coverslips.

Day 9 (Tuesday): Place wax dots on coverslips for primary neurons.

Day 10 (Wednesday): Replace APM media on astrocytes with NMM. Coat coverslips with PLL for neurons.

Day 11 (Thursday): Perform hippocampal dissection and plating.

Day 15 (Monday): Add AraC to each well of neurons for a final concentration of 5 μM.

Day 16 (Tuesday – 5 DIV) … Day 21 (Sunday – 10 DIV), etc.: Half media change. Fix and stain neurons at ~14 DIV, or alternative appropriate date.

Sequence of events and detailed procedures:

Day 1 (Monday):

1. Coat 6-well plates with 25 µg/µL of poly-L-lysine (PLL) in 0.1 M Borate buffer. Incubate overnight in $C0_2$ incubator at 37ºC.
2. Order an E16 timed pregnant rat to arrive the following week (next Tuesday).
    a. Strain: SD
    b. Gestation requirements: E16
    c. Vendors: ENVIGO or Charles River
    d. Vivarium: TRACS/GBSF 636

Day 2 (Tuesday):

1. Wash 6-well plates 3x with Milli-Q water. Keep in last wash until astrocytes are ready to be plated.
2. Revive frozen astrocytes by thawing quickly in water bath. 1 mL of frozen astrocytes (1 vial) will be enough for two 6-well plates.
3. Transfer thawed astrocytes into Astrocyte Plating Media (APM), and plate 2 mL of suspended astrocytes per well.
4. Place in $C0_2$ incubator. Monitor cells after 2 days, confluency should be around 20%.

Day 5 (Friday):

1. Change APM media for astrocytes.

Day 8 (Monday):

1. Change APM media for astrocytes.

2. Perform nitric acid sterilization and etching of glass coverslips
    a. Place coverslips in ceramic racks and place racks in glass container.
    b. Wash coverslips 1x with Milli-Q water to remove any dust/particles.
    c. Fill container with 1M Nitric Acid (coverslips should be completely submerged).
    d. Place glass container on shaker at RT at low speed overnight.
    e. Remove Nitric Acid and save for future use (can be used up to three times).
    f. Rinse glass container and coverslips 3x with Milli-Q water (quick rinses). Container with Milli-Q water so coverslips are submerged and place on shaker at low speed 3x for 20 minutes each. Ethanol rinse to aid drying.
    g. Remove excess liquid by tapping ceramic racks on Kim-wipes.
    h. Wrap in foil and autoclave on Cycle 8 (wrapped at 250 ºC).

Day 9 (Tuesday):

1. Place wax dots on coverslips.
    a. Transfer coverslips to 6-well plates (at least four; 24 coverslips total) in biosafety cabinet.
    b. For sterility, turn on Bunsen burner and place near hot plate. Sterilize bench area with 70% ethanol.
    c. Begin boiling water in small beaker on hot plate at your bench.
    d. Melt wax pellets by placing pellets into a smaller beaker.
    e. Place this beaker into the water on hot plate as it begins to boil.
    f. Bring coverslips to bench. Using 200 uL pipet, carefully add wax dots to the corners of each coverslip.

2. Allow to dry in bio-safety cabinet overnight.

Day 10 (Wednesday):

1. Replace APM media with 5 mL Neuronal Maintenance Media (NMM).
2. Coat etched/sterilized coverslips (with wax dots) with 1 mg/mL of PLL in 0.1M Borate buffer. Use 350 µL solution per well and bubble on top of coverslips using a 1 mL pipet. Incubate in the $C0_2$ incubator overnight.

Day 11 (Thursday):

1. Wash coverslips 3x with Milli-Q water.
2. Add 2 mL NPM per well and place in CO_2 incubator at 37C.
3. Perform Hippocampal Dissection and plating.
    a. Before dissection, sterilize tools at 250C for 15 minutes (dry bath in dissection room).
    b. Euthanize E18-E19 pregnant rat with carbon dioxide. Ensure complete euthanasia by cervical dislocation.
    c. Spray abdomen with 70% ethanol.
    d. Cut through skin and remove the uterus to a petri dish.
    e. Remove fetuses from the uterus, decapitate, and put heads in dissection buffer on ice.
    f. Remove the hippocampi from each brain being careful to remove all meninges, and transfer to a 15 mL conical tube on ice.
    g. Add 4.5 mL of dissection buffer and 0.5 mL of 2.5% Trypsin (Gibco).
    h. Incubate hippocampi in 37C water bath for 12 min, inverting gently every few minutes.
    i. After incubation, add 5 mL of NPM.
    j. Centrifuge for 5 min at 1000 rpm and carefully remove the supernatant.

k. Resuspend pellet in 3 mL of NPM and dissociate cells by pipetting up and down with a 1 mL pipette 3x, followed by trituration x10 with a fire polished long stem pipette until most chunks of tissue have been dissociated.
l. Add NPM to a final volume of 5mL.
m. Use a hemacytometer to determine cell density (45 uL of cell suspension plus 5 uL of trypan blue). Trypan blue will stain dead cells blue. Do not include dead cells in your count.
n. Dilute cells to 50,000 cells per mL of NPM (make sure to account for pipetting error). Add 1 mL of cells to each well containing PLL coated coverslips. This will give a final cell density of 50,000 cells per well and a total volume of 3 mL per well.
o. Place dishes in incubator for 4 – 6 hours.
p. Transfer coverslips, wax dot side down, to the plates containing astrocyte feeder layers.
q. Place in $C0_2$ incubator.
r. Perform a half media change every 5 days by removing 2.5 mL old media and adding 3 mL fresh NMM.

Day 15 (Monday) – 4 DIV:

1. Add AraC per well directly to culture medium. Final concentration: 5 uM (1:2000 dilution from stock in -20^{o}C, i.e. 2.5 uL AraC to 5 mL NMM).

Day 16 (Tuesday – 5 DIV) … Day 21 (Sunday – 10 DIV), etc.:

1. Half media change. Remove 2.5 mL of media and replace with 3 mL fresh NMM. Perform half media change every 5 days.

2. Fix and stain neurons at 14 DIV, or appropriate age, depending on development and confluency.

** This protocol can also be used for cortical cultures. However, cortical tissue must be mechanically "chopped" with forceps into smaller pieces before digestion. Cortical neurons will also mature more quickly than hippocampal neurons. **

Media Formulations:

Dissection Media:

- 500 mL HBSS
- 5 mL HEPES
- 5 mL Sodium pyruvate

Astrocyte Plating Media (APM)

- 500 mL 1X MEM (remove 65 mL)
- 10% Donor horse serum (50 mL)
- 0.6% Glucose (10 mL of 30% glucose stock in Milli-Q water)
- 5 mL Penicillin/Streptomycin

Neuronal Plating Media (NPM)

- 500 mL 1X MEM (remove 68 mL)
- 10% Donor horse serum (50 mL)
- 0.45% glucose (7.5 mL of 30% glucose stock in Milli-Q water)
- 5 mL Sodium pyruvate
- 5 mL Penicillin/Streptomycin

Neuronal Maintenance Media (NMM)

- 500 mL Neurobasal (remove 25 mL)
- 10 mL B-27
- 5 mL Glutamax
- 5 mL Sodium Pyruvate
- 5 mL Penicillin/Streptomycin

Additional Solutions:

Poly-L-Lysine Solution (PLL)

PLL stocks are at 200 mg/uL located in the -20C fridge.

For 25 ug/uL:

- Dilute stock at 1:8,000 in 0.1 M Borate Buffer, i.e. add 6.25 uL PLL to 50 mL 0.1M Borate Buffer

For 1 mg/uL:

- Dilute stock at 1:200 in 0.1 M Borate Buffer, i.e. add 50 uL PLL to 10 mL 0.1 M Borate Buffer

0.1 M Borate Buffer

- 900 mL milli-Q water
- 17.2 g sodium tetra-borate
- 3.1 g boric acid
- Adjust pH to 8.5
- Bring up to 1 L with milli-Q water
- Filter Sterilize

1M Nitric Acid:

- Add 64 mL 70% w/w 15.8 N nitric acid to 250 mL H_20.
- Bring up to 1000 mL.

ACSF recipe

Fresh ACSF should be made every two weeks. Discard any old ACSF in the fridge.

1. For 1 liter of ACSF, to MilliQ water (950ml) add the following:
    - 7.422g Sodium Chloride (M.W. 58.44)
    - 2.100g Sodium Bicarbonate (M.W. 84.01)
    - 0.173g Monobasic Sodium Phosphate (M.W. 137.99)
    - 0.187g Potassium Chloride (M.W. 74.56)
    - 4.505g Glucose (M.W. 180.20)

2. Increase the volume to 1L with MilliQ water.
3. Bubble with carbogen until saturated (approx. 15 mins).
4. Check pH. Should be between 7.10 and 7.20.
5. Check osmolarity. Should be between 310 and 315.
6. Rinse bubbler with diH_20.

When using ACSF, take 200ml of the above solution and add magnesium and calcium:

Magnesium Chloride (M.W. 203.31)

	100ml	**200ml***	500ml	1L
0.1mmol	0.00102g	0.00408g	0.0102g	0.0204g
1mmol*	0.0204g	**0.0408g***	0.102g	0.204g
4mmol	0.0816g	0.1632g	0.408g	0.816g

Add Calcium Chloride (use the 1M solution on the shelf).

	100ml	**200ml***	500ml	1L
2mmol*	200µl	**400µl***	1ml	2ml
3mmol	300µl	600µl	1.5ml	3ml
4mmol	400µl	800µl	2ml	4ml

*Most common concentrations are in **bold**.

Primary Astrocyte Cultures

Astrocyte Plating Media (APM)

- 500 mL MEM (remove 65 mL)
- 10% Donor horse serum (50 mL)
- 0.6% Glucose (10 mL of 30% stock in DI water)
- 5 mL Penicillin/Streptomycin

1. Order time-pregnant rat at E16 (about 1 week before dissection). Rat should give birth around E20-E21.
2. Coat 30 ten cm dishes with 25 ug/mL poly-L-lysine and make new APM.
3. On day of dissection, wash plates 3x with sterile H20 and leave in hood for plating.
4. Pick P0 or P1 pups (at least 12).
5. Sacrifice pups. Decapitate. Place heads in 10 cm dish with dissection buffer (HBSS/HEPES/Na-Pyruvate)
    - Dissection buffer: 500 mL HBSS, 5 mL HEPES, 5 mL Na-Pyruvate
6. Remove brains from head and place in new dish with dissection buffer
7. Under microscope, carefully remove the meninges from brains to expose cortex
8. Secure brain by placing forceps at 45^{o} angle through upper portion of the cortex. Remove small square chunk of tissue with forceps.
9. Repeat for other brain hemisphere.
10. Remove any remaining blood vessels and transfer tissue to new dish with dropper.
11. After tissue has been extracted from all brains, use forceps to break up chunks of isolated tissue.

12. Transfer all tissue to 50 mL conical tube and fill to 12 mL with dissection buffer.
13. Add 1.5 mL of 2.5% Trypsin.
14. Incubate at 37C for 15 mins. Invert tube every 2 mins.
15. After incubation, add equal volume of astrocyte plating medium (APM).
16. Centrifuge at 1000 rpm for 5 mins.
17. Carefully remove supernatant (do not use suction).
18. Resuspend pellet in 5 mL APM.
19. Dissociate cells by pipetting up and down with a Pasteur pipet, and then with a fire polished pipet.
20. Leave suspension so tissue chunks settle to bottom.
21. Collect supernatant carefully and transfer to clean collection bottle (500 mL).
22. Bring up to final volume of 300 mL APM.
23. Add 10 mL to each PLL coated dish.
24. Change media every 3 days.
25. Freeze cultures at ~80% confluency (7 – 14 days).

Chemical LTP Induction of Primary Hippocampal Neurons

1. Use cultured primary neurons at DIV 12 – 14 depending on confluency and maturity.

2. Equilibrate neurons in artificial cerebrospinal fluid (aCSF) with magnesium (Mg^{+2}) at 37ºC in incubator for 30 minutes.

3. Wash Cells 1x with PBS.

4. Replace aCSF buffer with either treatment or DMSO mock ctrl. **Important: Treatment and Ctrl buffer must be Mg^{+2} free.**

    a. aCSF Treatment Buffer
    b. 200 µM Glycine; Stock = 1 M
    c. 20 µM Bicuculine; Stock = 20 mM
    d. 3 µM Strychnine; Stock = 1 mM
    e. 2 mM Calcium

5. Incubate at 37ºC for 5 minutes.

6. Transfer coverslips to recovery buffer (aCSF w/ Mg^{+2}; No Drugs) for 20 mins at 37ºC.

7. Fix with 4% PFA for 5 minutes at room temperature.

8. Wash 3x with PBS. Shaking, 5 minutes each.

9. Store at 4ºC in PBS.

Surface labeling of Primary Hippocampal Neurons

1. Wash cells 1X with PBS briefly

2. Brief fixation: 4% PFA/4% Sucrose/PBS for 5 min at RT

3. Wash 3X with PBS for 10 mins each

4. Blocking: 10% BSA in PBS for 30 min

5. Incubate with GluA1 antibody at RT for 1 hour
a. (Neuromab IgG1 anti-GluA1; 1:50)

6. Wash 3X with PBS for 10 mins each

7. Permeabilization: 0.1% Triton X-100 in PBS for 15 mins at RT

** After permeabilization, you can proceed to normal immunostaining for internal proteins **

The above protocol uses a brief fixation prior to surface labeling. This could potentially result in slight permeabilization of the membrane, resulting in antibody leaking into the cell. However, this should be minimal, and this protocol is used widely in the literature.

A second surface staining protocol may be used where the cells are slowly cooled to 4ºC. This would be a truer surface labeling; however, it is commonly observed that this results in increased cell death and abnormal morphology. The protocol is as follows:

1. Place coverslips at RT until the media temperature reaches RT
2. Transfer coverslips to 4C cold room or ice
3. Incubate with GluA1 antibody at 4C for 20 mins, shaking
4. Wash 3X with PBS, briefly
5. Fix with 4% PFA/4% Sucrose/PBS for 10 mins at RT
6. Wash 3X with PBS for 10 mins each
7. Proceed to immunostaining for internal proteins

ImageJ Analysis of Dendritic Stretches

1. File > Open > Select Image for Analysis
2. Image > Color > Make Composite
3. Image > Color > Split Channels
4. Determine threshold for 25% of all images. This must be done separately for each channel. Save threshold values in an excel file.
    a. Select channel for thresholding
    b. Image > Duplicate
    c. Place both channels next to each other
    d. Select channel for thresholding
    e. Image > Adjust > Threshold
    f. Threshold window should say ‘Default’ and B&W. Select ‘Dark Background.’
    g. Use the color image to adjust the top threshold value so that the black and white image is representative of the color image. Bottom threshold value will remain unchanged.
5. Close all images.
6. Once the threshold has been determined for 25% of images, take the average threshold of each channel.
7. Open the three-channel script in notepad or other text editor.
8. Input threshold values and save the script. Each channel has a space to input the threshold values.

9. Select 2-3 dendritic stretches from each image.

    a. File > Open > Select Image for Analysis
    b. Image > Color > Make Composite
    c. Click on ‘Polygon Selections’ tool.
    d. Select dendrite with polygon tool.
    e. Edit > Clear Outside
    f. File > Save As > TIFF file (to new folder)
    g. Repeat for all Images and Dendritic Stretches

10. Once all dendrites for all images have been selected, close all images.
11. File > Open > Select Dendrite Image for Analysis
12. Select either ‘Segmented Line’ or ‘Freehand Line’ tool.
13. Trace the length of the dendrite.
14. Analyze > Measure
15. Record the dendritic length in excel. This will be necessary to determine puncta density. Additionally, make sure unit of length is set to micron. (Analyze > Set Scale)
16. Close results.
17. Plugins > Macros > Run > Select script with thresholds from earlier.
18. Record the summary results in excel for each dendrite.

ImageJ Protocol for Manual Analysis of Puncta Clusters

in Heterologous Cells

1. File > Open > Select Image for Analysis
2. Image > Color > Make Composite
3. Image > Color > Split Channels
4. Determine threshold for 25% of all images. This must be done separately for each channel. Save threshold values in an excel file.

    a. Select channel for thresholding
    b. Image > Duplicate
    c. Place both channels next to each other
    d. Select channel for thresholding
    e. Image > Threshold
    f. Threshold window should say 'Default' and B&W. Select 'Dark Background.'
    g. Use the color image to adjust the top threshold value so that the black and white image is representative of the color image. Bottom threshold value will remain unchanged.

5. Close all images.
6. Once the threshold has been determined for 25% of images, take the average threshold of each channel.
7. Open the two-channel script in notepad or other text editor.

8. Input threshold values and save the script. Each channel has a space to input the threshold values for SD4 and the receptor.
9. File > Open > Select Image for Analysis
10. Identify a representative secondary or tertiary dendritic stretch.
11. Using the freehand selection tool, select the dendrite of interest.
12. Edit > Clear Outside
13. Save image as a TIF file to a new folder.
14. Right click on the line tool and select freehand line.
15. Trace the representative dendritic stretch linearly down the middle of the dendrite.
16. Analyze > Measure. Record the length of the dendritic stretch.
17. Plugins > Macros > Open. Select script for analysis and save all results.
18. Divide the number of puncta by the length to obtain puncta density.

END OF DOCUMENT